Shell formation and microstructure of the ocean quahog *Arctica islandica*:
Does ocean acidification matter?

Dissertation zur Erlangung des Grades eines Doktors der Naturwissenschaften
-Dr.rer.nat.-

Fachbereich 2 Biologie/Chemie
Universität Bremen

Vorgelegt von
Kristina Stemmer

Bremen
Februar 2013

Shell formation and microstructure of the ocean quahog *Arctica islandica*:
Does ocean acidification matter?

Schalenbau und Mikrostruktur der Islandmuschel *Arctica islandica*: Beeinflusst durch Ozeanversauerung?

Vorgelegt von
Kristina Stemmer

Bremen
Februar 2013

Prüfungsausschuss:

1. Gutachter: Prof. Dr. Thomas Brey (Funktionelle Ökologie, Alfred-Wegener-Institut Helmholtz-Zentrum für Polar- und Meeresforschung, Bremerhaven)

2. Gutachter: PD Dr. Barbara Niehoff (Funktionelle Ökologie, Alfred-Wegener-Institut Helmholtz-Zentrum für Polar- und Meeresforschung, Bremerhaven)

1. Prüfer: Dr. Dirk de Beer (Microsensor Gruppe, Max-Planck-Institut für Marine Mikrobiologie, Bremen)

2. Prüfer: Prof. Dr. Kai Bischof (Marine Botanik, Universität Bremen)

Staunen ist der Samen des Wissens (Francis Bacon)

Table of Contents

Abbreviations and Acronyms

ANOVA: Analysis of Variance

arag = aragonite

A_T = total alkalinity

ATP = adenosine triphosphate

BCECF = 2',7'-bis-(2-carboxyethyl)-5-(and-6)-carboxyfluorescein

BIOACID = Biological Impact of Ocean Acidification

BMBF = Bundesministerium für Bildung und Forschung

bp = base pair

C = carbon

Ca^{2+} = calcium-ion

$CaCO_3$ = calcium carbonate

COI = cytochrome c oxidase subunit I

CO_2 = carbon dioxide

CO_3^{2-} = carbonate-ion

CRM = Confocal Raman Microscopy

C_T = total dissolved inorganic carbon

DIC = dissolved inorganic carbon

dog = direction of growth

EPF = extrapallial fluid

EPS = extrapallial space

Gbn # = GenBank accession number

H^+ = hydrogen-ion

HCO_3^- = bicarbonate-ion

H_2CO_3 = carbonic acid

IPCC = Intergovernmental Panel on Climate Change

ISL = inner shell layer

K*sp = stoichiometric solubility product

$\log_{10}$ = common logarithm

LSG = line of strongest growth

MRD = metabolic rate depression

mtDNA = mitochondrial DNA (desoxyribonucleic acid)

NADH = nicotinamide adenine dinucleotide

OA = Ocean Acidification

OME = outer mantle epithelium

Ω = Omega, saturation state

oOSL = outer outer shell layer

OSL = outer shell layer

$p\text{CO}_2$ = partial pressure of carbon dioxide

PCR = polymerase chain reaction

pH_{NBS} = pH calibrated with Nist Buffer Standard

Pif97, Pif80 = aragonite specific protein complex

ppmv = parts per million by volume

psu = practical salinity units

SD = standard deviation

SRP54 = Signal Recognition Partical 54 gene

Σ = Sigma, summation operator

TA = total alkalinity

Synopsis

Synopsis

Carbon dioxide concentration (pCO_2) in the ocean is steadily increasing causing a drop of pH, consequently turning the surface seawater more acidic. Due to possible adaptation mechanisms some marine organisms can cope better with high pCO_2 and low pH than others. The ocean quahog *Arctica islandica* is widely distributed in the North Atlantic region. Populations of this species are also well established in the high fluctuating environment of the Kiel Bight in the Western Baltic Sea and show high tolerance to environmental parameters like salinity, temperature and low oxygen levels. In my thesis I am interested in the performance of *A. islandica* from Kiel Bight to build and maintain its shell in a high pCO_2 environment and the general aspects of bivalve shell properties as well as the site of calcification within the bivalve as a prerequisite for a mechanistic understanding of the biomineralization process.

Thus, in my thesis I focused on the following main subjects:
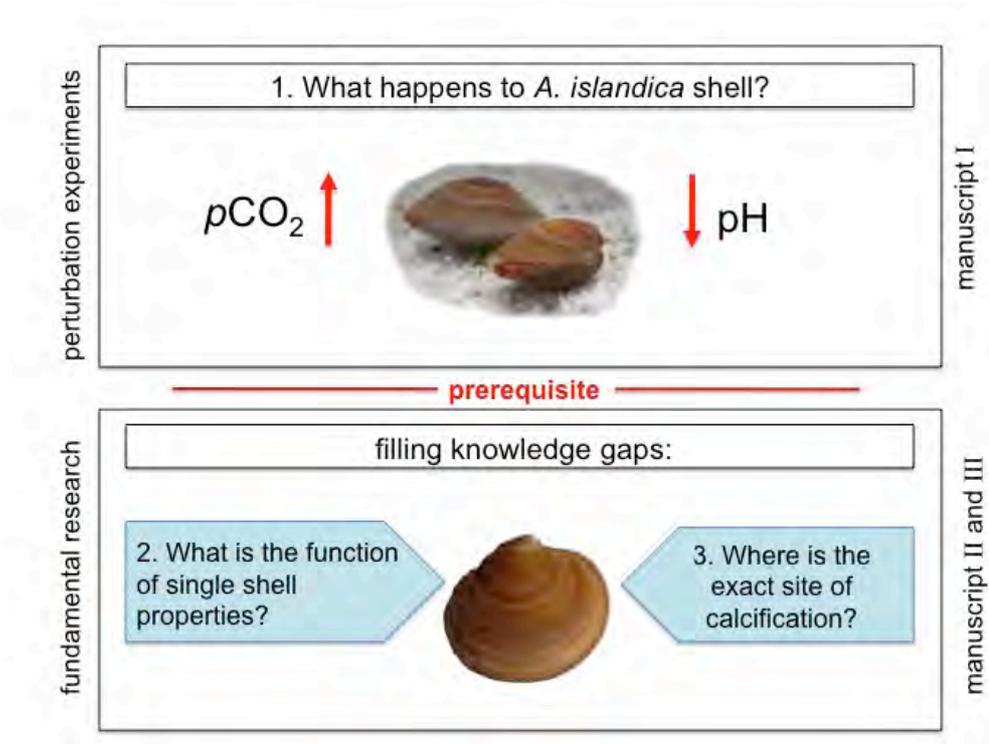
In the first study (**manuscript I**) *A. islandica* from the Kiel Bight was exposed to three different pCO_2 levels (380 ppm - ambient, 760 ppm - double from today and 1120 ppm - four times higher than pre-industrial) over 90 days to evaluate whether shell growth and shell structure are affected. No changes in growth and shell microstructure were observed suggesting pre-adaptation to a wider range of pCO_2 levels due to naturally fluctuating pCO_2 levels within the Kiel Bight area. Furthermore, the use of certain shell-proxies was verified. Shell proxies are measurable parameters (e.g. trace elements or isotopic ratios) closely related to environmental conditions during shell formation and some can be affected by shell-growth and structure and were thus suggested to contain no pCO_2 related bias.

Our knowledge on shell components and detailed processes involved in biomineralization of calcareous skeletons that may explain higher resistances against elevated pCO_2 is very limited. Organic molecules play a significant role in formation and maintenance of the shell. A fundamental knowledge of these components is necessary to understand if and why some marine calcifiers can compensate high pCO_2. The following two approaches were dedicated to i) single organic shell components and ii) the actual site where the shell is produced.

The focus of **manuscript II** is on pigment polyenes, polyunsaturated organic molecules that often occur in coloured parts of mollusc shells. Biogenic carbonates like the bivalve shell consist of inorganic and organic compounds making them unique materials with different qualities compared to inorganically precipitated minerals. So far, not much is known about single shell compounds, their origin or their function. Using Confocal Raman Microscopy I identified pigment polyenes in *A. islandica* shells from four geographically different regions. Polyenes displayed the same molecular structure suggesting no habitat related origin. Spatial distribution of polyenes within *A. islandica* shell cross-sections from the Kiel Bight showed that polyenes are integrated within calcium carbonate granules. They are also not homogeneously distributed within the shell, but they mostly occur in the outer shell layer visible as intra-annual growth lines. This suggests, that pigment polyenes might play a role in the biomineralization process.

Manuscript III focuses on the extrapallial fluid (EPF) of *A. islandica* and whether or not calcification is possible in this microenvironment. The EPF is located in a compartment between inner shell surface, secreting outer mantle epithelium (OME), and is enclosed by the organic periostracum around the mantle margin. We used *in situ* microscopy to identify pH

gradients within the EPF between inner shell surface and the OME. A gradual inversion was measured when pH around the OME increased from under pH 7 to above 9 suggesting active proton pumping. Simultaneous pH and calcium microsensor measurements showed remarkable short-term dynamics that were synchronous most of the time suggesting also active proton pumping. The bulk of the EPF rarely reaches calcium carbonate saturation and thus cannot be the site of calcification. However, the pH values at the OME surface can increase the saturation state between 15-20 fold. When the OME is in close contact with the inner shell surface forming a microsite, ion pumping could drive calcification.

This thesis summarizes that i) *A. islandica* from Kiel Bight populations is resistant and most likely pre-adapted towards elevated pCO_2 over a short period of time (90 days) and contributes to the fundamental understanding of ii) single organic shell-compounds identified as pigment polyenes, that are not habitat related and may contribute to shell formation and that iii) the calcification process itself is not happening inside the bulk EPF but rather within a supersaturated microsite created by active ion pumping by the OME.
Understanding the biomineralization process and all components involved is crucial and thus the next challenge in order to estimate the robustness of *A. islandica* and other marine calcifiers in a high pCO_2 world.

As supplementary material (S1 and S2) I provide two studies as a contribution to ocean acidification research on other marine taxa: S1) The actively swimming king scallop, *Pecten maximus*, was investigated for its clapping performance under elevated pCO_2 and S2) a diversity study on soft corals, marine invertebrates that exhibit minute calcareous spicules, which formation may be also hampered by future ocean acidification.

Zusammenfassung

Der ansteigende Kohlestoffdioxid-Gehalt (pCO$_2$) der Meere reduziert den pH. Versauerung von Oberflächenwasser ist die Folge. Manche Meeresorganismen verhalten sich hohem pCO$_2$ Gehalt toleranter als andere. Die Muschel *Arctica islandica* ist im Nord Atlantik weit verbreitet. Populationen dieser Art haben sich auch in der Kieler Bucht in der Ostsee etabliert und zeigen eine hohe Toleranz gegenüber Umweltschwankungen wie Salinität, Temperatur und Sauerstoff-Gehalt. Ziel meiner Arbeit war es, zum einen anhand kontrollierter Laborversuche den Effekt steigenden pCO$_2$-Gehaltes auf die Schalenstruktur von *A. islandica* zu untersuchen um potentielle Anpassungen der Muschel an sich ändernden pCO$_2$-Gehalt aufzudecken und zum anderen generelle Aspekte der Muschelschale und deren Aufbau zu untersuchen um mögliche Veränderungen oder Anpassungen besser zu verstehen.

In meiner Dissertation war ich besonders an den folgenden Fragen interessiert:
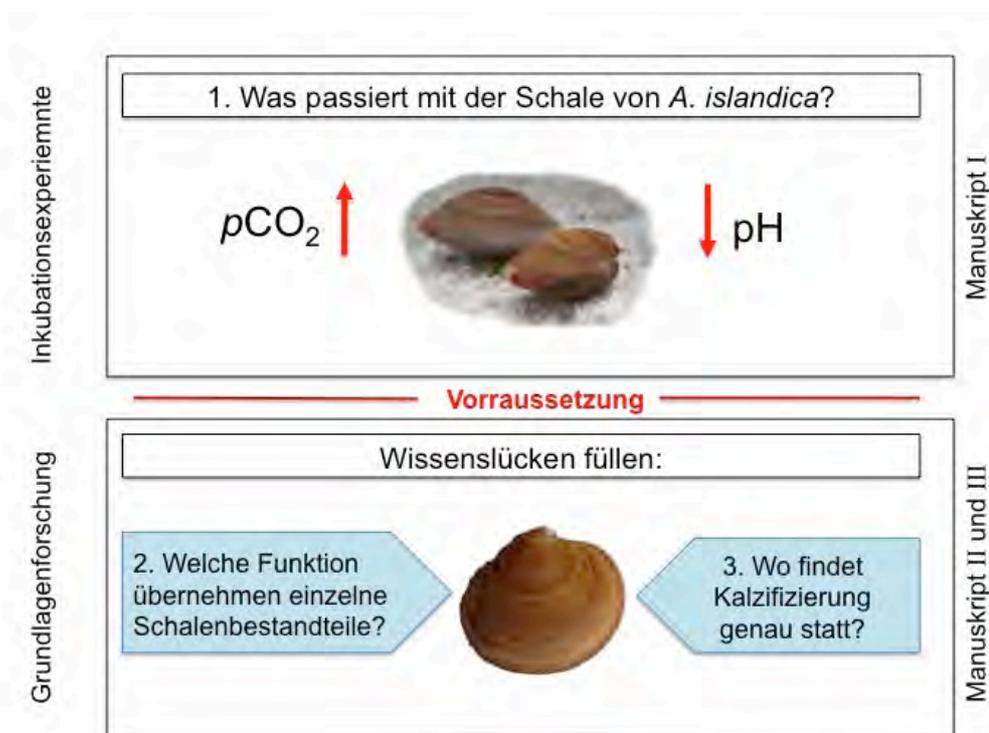
In der ersten Studie (Manuskript I) wurde *A. islandica* aus der Kieler Bucht in einem Laborexperiment für 90 Tage, drei unterschiedlichen pCO_2-Konzentrationen ausgesetzt (Einheit = parts per million) (380 ppm - heute, 760 ppm – doppelt so hoch, und 1120 ppm – vierfach so hoch verglichen zu vorindustriellen Konzentrationen) um den Einfluss auf Schalenzuwachs und Schalenmikrostruktur zu untersuchen. Es wurden keine Veränderungen festgestellt, weder beim Schalenwachstum noch bei der Mikrostruktur. Die Ergebnisse weisen auf eine Preadaption hin, vermutlich induziert durch natürliche pCO_2 Schwankungen in der Kieler Bucht. Gleichzeitig wurden indirekt die Nutzung von Schalenproxies verifiziert (indirekte Anzeiger der Umgebungsparameter während des Schalenbaus, z.B. elementare Zusammensetzung oder Isotopen Verhältnis) von denen manche durch Schalenwachstum und –struktur verändert werden und demnach nicht durch erhöhte pCO_2-Konzentrationen verfälscht werden (zumindest für Muscheln aus dieser Region).

Bisher wissen wir zu wenig über einzelne Schalenkomponenten und detaillierte Prozesse, die in Zusammenhang mit der Biomineralisation von Kalkschalern stehen, um mögliche Resistenzen gegen erhöhte pCO_2 Bedingungen aufzudecken und verstehen zu können. Organische Moleküle in der Muschelschale z.B. spielen eine Rolle während des Schalenaufbaus und grundsätzliche Kenntnisse über diese Komponenten können unser Verständnis für die Sensitivität von Kalkschalern erweitern. Hinzu können Einsichten in den Schalenaufbau Erklärungen geben, warum manche Kalkschaler erhöhte pCO_2 Konzentartionen besser kompensieren können als andere. Die folgenden zwei Arbeitsabschnitte meiner Thesis befassten sich mit i) einzelnen organischen Schalenkomponenten und ii) dem eigentlichen Ort der Kalzifizierung.

Der Fokus des zweiten Manuskripts (II) liegt auf polyenen Pigmenten, mehrfach ungesättigte organische Moleküle, die häufig in farbigen Schalenteilen von Mollusken vorkommen. Biogene Karbonate, wie die der Muschelschale, sind Verbundstoffe mit inorganischem und organischem Anteil. Diese Mischung macht Biominerale zu einzigartigen Materialien mit speziellen Eigenschaften und unterscheidet diese von anorganischen Mineralien. Bisher ist jedoch relativ wenig über einzelne Schalenkomponenten, deren Entstehen und deren Funktion bekannt. Konfokale Raman Mikroskopie ermöglichte die Detektion von polyenen Pigmenten in der Schale von *A. islandica* und die Identifizierung des exakt gleichen Moleküls in Schalen von vier unterschiedlichen Regionen, welche demnach als nicht-Habitat-spezifisch eingestuft wird. Die räumliche Verteilung von polyenen Pigmenten wurde in Schalen aus der Kieler

Bucht bemessen. Im Schalenquerschnitt zeigte sich eine inhomogene Verteilung. Die meisten Polyene wurden in der äußeren Schalenschicht gefunden und in einem linearen Muster, die eine intra-annuelle Auflösung von Wachstumslinien vermuten lässt. Der letztere Fund wirft die Frage auf, ob diese Polyene eine Funktion im Biomineralisationsprozess übernehmen.

Die dritte Studie meiner Thesis (Manuskript III) fokussiert auf die Extrapallialflüssigkeit (EPF) von *A. islandica* und die Möglichkeit der Kalzifizierung in diesem Mikrohabitat. Die EPF befindet sich in einem Kompartiment zwischen Schale, sekretierendem äußeren Mantelepithel (OME) und wird abgeschlossen durch das organische Periostracum. *In Situ* Mikroskopie identifizierte pH Gradienten im EPF, zwischen der inneren Schalenfläche und dem OME. Dieser pH Gradient veränderte sich graduell, induziert durch mögliche Ionen-Pumpen am OME, von 7 auf über 9. Gleichzeitige pH- und Calcium- Messungen mit Mikrosensoren zeigten außerordentliche, synchron verlaufende, Kurzzeit-Dynamiken, die ein aktives Pumpen von Ionen vermuten lässt. Der niedrige Sättigungsgrad im Großteil des EPFs macht das Ausfällen von Kalziumkarbonat kaum möglich. Jedoch kann das OME durch Ionen-Pumpen den pH um das 15-20 fache erhöhen, was eine Übersättigung und demnach eine Ausfällung induzieren kann sobald ein kleineres Mikrokompartiment geschaffen ist, z.B. durch engeren Kontakt des OME mit der inneren Schalenfläche.

Zusammenfassend habe ich in meiner Thesis gezeigt, dass i) *A. islandica* aus der Kieler Bucht kurzzeitig resistent und höchst wahrscheinlich pre-adaptiert an erhöhte pCO$_2$ Bedingungen ist und ein grundlegendes Verständnis der Schale sowie des Schalenaufbaus Voraussetzungen für das Verständnis von Adaptionsmechanismen ist, ii) einzelne organische Komponenten in Form von polyenen Pigmenten in der Schale von *A. islandica* vorkommen und diese weitere Funktionen für den Schalenaufbau mit sich bringen können und iii) der Kalzifizierungsprozess nicht im EPF an sich stattfinden kann aber durch ein Mikrokompartiment und das Pumpen von Ionen induziert durch das OME gefördert werden kann.

Ein grundlegendes Verständnis für den Biomineralisationsprozess, dem Kalzifizierungsort und den treibenden Kräften der organischen Moleküle stellt eine Herausforderung dar aber ist Vorraussetzung für weitere Analysen an möglichen Veränderungen oder Resistenzen von Kalkschalern in saueren Meeren.

Als Zusatzinformation zur Erforschung von Auswirkungen der Ozeanversauerung habe ich dieser Thesis zwei weitere Studien angehängt. S1) Die Schalenklappleistung der aktiv schwimmende Kammmuschel, *Pecten maximus*, wurde unter erhöhtem pCO$_2$ untersucht um den Einfluss auf die Fitness der Muschel zu evaluieren. S2) Diese Studie fokussiert die Diversität von Weichkorallen, ein ganz anderes Taxon von marinen Invertebraten welche aber kleinste Kalknadeln bzw. –plättchen besitzen die durch die Ozeanversauerung genauso Schaden nehmen können wie andere Kalkschaler.

1. General introduction

1. 1 What is ocean acidification?

Increasing atmospheric carbon dioxide (CO_2) causes global warming and the lately addressed problem of ocean acidification (Caldeira & Wickett 2003; Doney 2009; Feely et al. 2004; Solomon et al. 2007). The ocean surface waters stay in constant equilibrium with the atmosphere and absorb over a third of the atmospheric CO_2 (Sabine et al. 2004). That alters the seawater carbonate chemistry with a reduction of pH and the ocean turns more acidic (Box 1) (Zeebe & Wolf-Gladrow 2001) (Figure 1). Within the next decades the impact of ocean acidification (together with ocean warming) is expected to affect marine organisms directly by influencing the physiology and performance of the single organism and indirectly through changes in food web structure and thus the whole marine ecosystem. Emerging knowledge indicates that sensitivity to elevated CO_2 levels differs between animal taxa (Doney 2009; Ries et al. 2009; Thomsen & Melzner 2010). Marine calcifiers are expected to show changes in growth rates, structure and elemental compositions (of their shells and skeletons) (Bijma et al. 1999; Riebesell et al. 2000; Ries 2005).

The surface ocean pH has fallen by about 0.1 units from pre-industrial to recent values and modellers predict another drop of $0.3 - 0.4$ units by the end of the century (Orr et al. 2005).
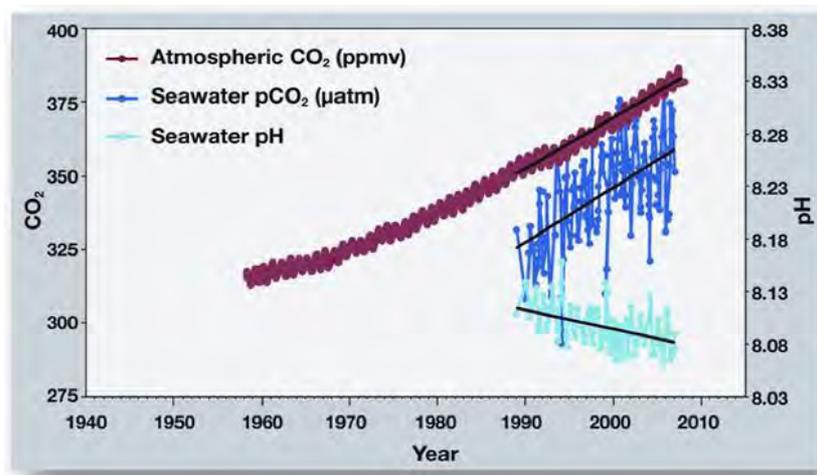

Figure 1: Simultaneous increase in atmospheric and dissolved ocean CO_2, and decrease of ocean pH (increase in acidity). (websource: www.indymedia.org.uk after Doney et al. 2009)

Box 1: Seawater cabonate chemistry

When CO_2 dissolves in seawater several chemical reactions occur:

$$CO_{2(atm)} \leftrightarrow CO_{2(aq)} + H_2O \leftrightarrow H_2CO_3 \leftrightarrow HCO_3^- + H^+ \leftrightarrow CO_3^{2-} + H^+$$

Aqueous CO_2 ($CO_{2(aq)}$) forms the unstable carbonic acid (H_2CO_3) that dissociates directly in bicarbonate (HCO_3^-) ions. A small fraction dissociates further in carbonate ions (CO_3^{2-}). Both reactions produce protons (H^+) that influence the pH, i.e. the negative logarithm of proton concentration or activity pH = -$\log_{10}$ (H^+) (Zeebe & Wolf-Gladrow 2001).

$\Sigma CO_2 = CO_{2(aq)} + HCO_3^- + CO_3^{2-}$ = dissolved inorganic carbon (DIC). The small fraction of H_2CO_3 (carbonic acid) is merged with $CO_{2(aq)}$.

Total alkalinity (TA or A_T) = $HCO_3^- + CO_3^{2-}$ = proton acceptors describing the buffer capacity of seawater (simplified description of carbonate alkalinity, for more details see Zeebe and Wolf-Gladrow 2001).

When $CO_{2(aq)}$ is reduced by CO_3^{2-}, the produced HCO_3^- ions will again dissociate in CO_3^{2-} with excess of H^+. Both ions are then out of balance and the increase of protons leads to a consumption of CO_3^{2-} and ocean acidification takes place with a drop of pH and the decrease of CO_3^{2-}. Thus it is obvious, that the buffer capacity of the ocean is limited depending on the amount of CO_3^{2-} present (Figure 2).
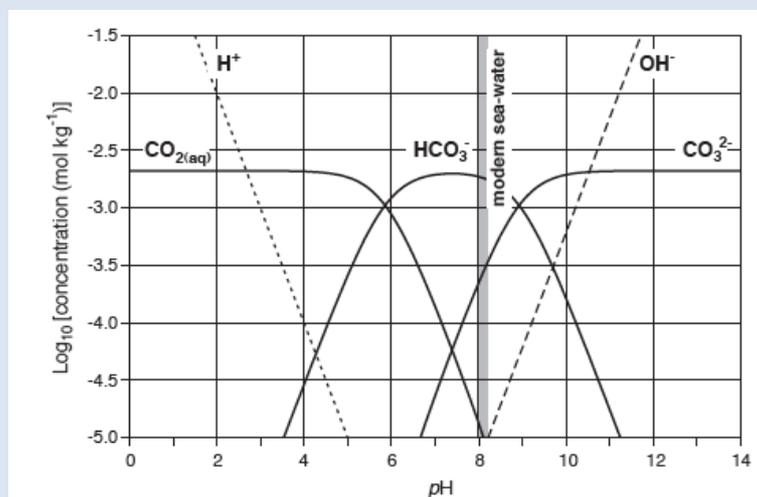

Figure 2: Bjerrum Plot (Ridgwell & Zeebe 2005). The ambient ocean pH is around 8.1 with carbon species being distributed with mainly bicarbonate (~90%), carbonate (~10%) and $CO_{2(aq)}$ (< 1%; combined with the tiny fraction of H_2CO_3).

1.2 Why are marine calcifiers affected?

Calcification is a fundamental building block within the biomineralization process to form biogenic carbonate, i.e. shells and skeletons (e.g. minute spicules, coral skeletons, mollusk shells), following the reaction:

$$Ca^{2+} + HCO_3^- \leftrightarrow CaCO_3 + H^+$$
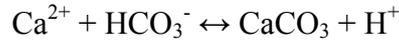
Calcification reduces DIC concentration and produces protons, thus contributes to acidification of the ambient solution (e.g. (Kleypas et al. 2006).

However, calcification depends on the $CaCO_3$ saturation state (Ω) of the ambient solution and $CaCO_3$ structures can dissolve under unfavorable conditions (Gazeau et al. 2007; Langdon et al. 2000; Lischka et al. 2011; Riebesell et al. 2000).

The $CaCO_3$ saturation state is the ion product of calcium and carbonate ions at the ambient temperature, salinity and pressure divided by the stoichiometric solubility product (K^*sp) of the calcium carbonate polymorph (e.g. calcite or aragonite) for those conditions (Kleypas et al. 2006):

$$\Omega = \frac{[Ca^{2+}][CO_3^{2-}]}{K^* sp}$$

Solutions are supersaturated when $\Omega > 1$ and $CaCO_3$ can precipitate, whereas undersaturated conditions with $\Omega < 1$ resemble low CO_3^{2-} concentrations and $CaCO_3$ minerals dissolve. Aragonite is the more soluble $CaCO_3$ phase, which has implications for organisms constructing aragonitic shells and skeletons in projected future oceans (Figure 3).
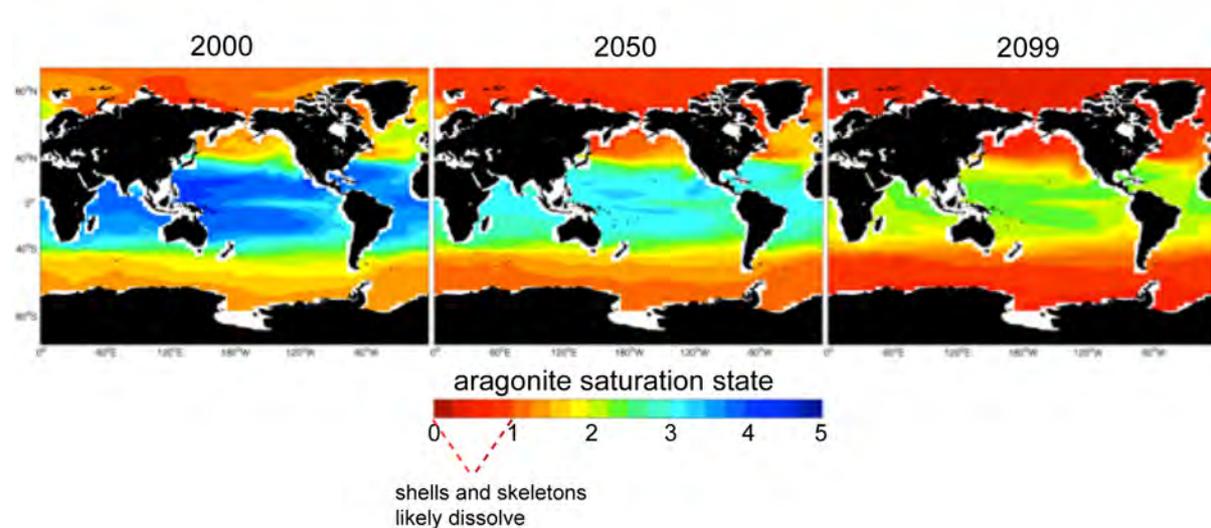

Figure 3: Present state and future predictions of aragonite saturation state of the world oceans (Feely et al. 2009)

1.3 What are biogenic carbonates?

Numerous marine organisms form calcareous shells and skeletons that received much attention in the past decade in the fields of i) medicine and bionic, ii) biogeochemistry and environmental reconstruction and iii) their vulnerability due to ocean acidification (Bijma et al. 1999; Riebesell et al. 2000; Ries et al. 2009; Wanamaker et al. 2008b). Especially, widespread upon marine invertebrates a variety in structures and colors occur from minute sclerites within soft coral tissue, over diverse distinctly formed and colored shells of different mollusk species to massive skeletons of hard corals, some acting as bio-engineers by providing a biogenic carbonate framework for a whole ecosystem (e.g. coral reefs, mussel beds).

The biological process by which organisms form minerals is called biomineralization with the widely accepted concept of crystallization within an extra-epithelial enclosed liquid-filled compartment (Adkins et al. 2003; Jacob et al. 2008; Saleuddin & Petit 1983). Studies on biominerlization represent calcifying extracellular fluids located between a mineralizing epithelium and the growing surface of the calcareous shell or skeleton. For corals the basal ectoderm of the coral polyps and the sub-ectodermal fluid are often illustrated (Adkins et al. 2003; Allemand et al. 2004). In mollusks the outer mantle epithelium and the extrapallial fluid are widely discussed in biomineralization concepts (Cuif et al. 2012; Jacob et al. 2008; Saleuddin & Petit 1983; Wheeler 1992; Wilbur 1983). However, for calcium carbonate precipitation the calcifying fluid has to be highly ion-saturated (Al-Horani et al. 2003; Bissett et al. 2008; Ludwig et al. 2005; McConnaughey & Falk 1991) and ion-transportation mechanisms are recently discussed (e.g. intracellular with ion-pumps or channels, paracellular diffusion) (Carre et al. 2006; Tambutte et al. 2012).

Advanced analytical approaches verified the biological control over biomineralization in several taxa, including molluska, exercised by assembling organic compounds in form of an organic matrix prior to the mineral formation itself (Lowenstam 1981; Weiner & Dove 2003). Several organic molecules secreted by the mineralizing epithelium are potentially involved in this process and deciphering biochemical compositions and functions of some molecules (Samata 2004 for review) triggered new models of organic-matrix mediated biomineralization within a controlled liquid-filled compartment (Levi-Kalisman et al. 2001; Nudelman et al. 2006; Weiss 2010).

Hence biogenic carbonates are complex composites of inorganic and organic compounds (Crenshaw 1972; Gregoire 1960) and it is obvious that these detailed structures and unique architectures do not precipitate equally to inorganically precipitated calcium carbonate (Figure 4) (Cuif et al. 2012).
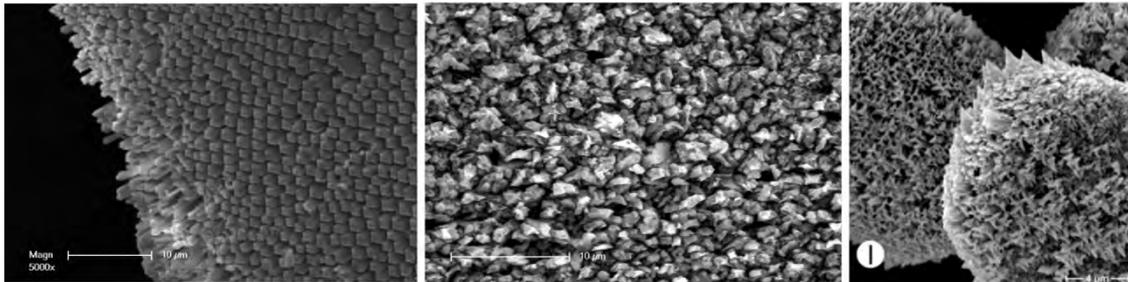
Figure 4: Biogenic carbonates. Scanning electron microscope pictures of A) calcite prisms of *Mytilus edulis* shell; B) aragonitic granules of *Arctica islandica* shell; C) aragonitic sclerites of xeniid soft coral (Stemmer et al. 2012).

Valuable information is stored within marine carbonate skeletons and shells, relating skeletal properties (e.g. elemental composition, isotopic fractionation) to the surrounding environmental condition during the time the biomineral was formed. These measurable parameters are called proxies and were first discovered in 1950 when H.C. Urey reported the "geological thermometer" (Urey et al. 1951). During following decades data was accumulated on the composition of biogenic carbonates and proxies within.

For mollusk shells the fossil record goes back to the Cambrian, 500 my ago (Stix & Abbott 1991), when the first $CaCO_3$ shells were excreted presumably induced by the $CaCO_3$ oversaturated ocean and due to elimination of calcium ions that are toxic to cells (Knoll 2003). Bivalve shells, like *Arctica islandica* which are long lived with ages > 350 yrs, are widely used as bioarchives due to valuable annual growth lines enabling reconstruction of environmental information from the surrounding at time of shell formation (Krause-Nehring et al. 2012; Schoene et al. 2011; Thebault et al. 2009; Wanamaker et al. 2008a). One of the major challenges in biomineralization research is the mechanistic understanding of processes dictating characteristic features (i.e. size, polymorphism, geometry, elemental composition) of the calcareous shell.

1.4 What makes *Arctica islandica* so interesting?

The target specimen for most of my studies was the bivalve *Arctica islandica* (Linnaeus, 1767). *A. islandica* is interesting for several reasons, e.g. i) its economical and ecological value, ii) its wide distribution in the North Atlantic region iii) its renowned longevity iv) its shell as a tool for environmental reconstructions. Good background information on *A. islandica* shells in sclerochronology and biogeochemistry made *A. islandica* also a very suitable candidate for my investigations.

Major Facts

A. islandica is the sole-surviving remnant of the once diverse Arcticidae (Newton 1891; Nicol 1951) that has its roots in the early Cretaceous (~135 – 65 mya) (Casey 1952; Lutz et al. 1982) and is known under several names like "ocean quahog", "bivalved Methuselah" or "tree of the sea" (Schoene et al. 2005; Witbaard et al. 1994). The bivalve is widely distributed on the continental shelves on both sides of the North Atlantic Ocean (Dahlgren et al. 2000; Nicol 1951).

The burrowing bivalve *A. islandica* inhabits the first layers of fine sediments at a depth range of 10 - 280 m (Kennish & Lutz 1995). *A. islandica* is a suspension feeder using its short siphons that are extended above the sediment to provide food and oxygen uptake due to seawater filtration (Figure 5). It is a high saline and low temperature species that exhibits a thermal tolerance window between 0 and 19 °C (Hiebenthal et al. 2012; Witbaard et al. 1994) with an optimum growth between 6 and 10 °C (Mann 1982; Philipp et al. 2012) tolerating a salinity range of 20 -35 PSU (Basova et al. 2012). *A. islandica* from different regions show different shell growth and growth experiments by Kraus et al. (1992) suggest a rather environmental influence in size variations. Shell growth is controlled by at least one environmental parameter, e.g. temperature, salinity or food supply (Epple et al. 2006; Schoene et al. 2005).

Figure 5: Exposed young *Arctica islandica* specimen with a yellowish brown periostracum and actively filtrating. The inhale- (left) and exhale- (right) siphons are wide expanded. Water filling the mantle cavity inside presses the outer mantle margin outward and between the two valves.

The bivalve gained much attention in the 21st century when its longevity was discovered (Thompson et al. 1980) and became a model object in aging research (Philipp et al. 2012; Ridgway et al. 2010). *A. islandica* is now recognized as the oldest known non-colonial animal (Ridgway & Richardson 2011) with the oldest individuals found around Iceland with 374 years (Schoene et al. 2005) and 405 years (Wanamaker et al. 2008b). The maximum life span of *A. islandica* differs between geographically separated populations (Basova et al. 2012). Extremely old animals occur around Iceland (Schoene et al. 2005; Wanamaker et al. 2008b) while life spans of ~150 years and only ~40 years were found within populations from the North Sea (Epple et al. 2006; Witbaard & Klein 1994), and in populations from the brackish waters of the Western Baltic Sea (Begum et al. 2010), respectively.

Despite high environmental variations (oxygen, salinity, temperature, pCO$_2$) in Kiel Bight (Hiebenthal et al. 2012; Melzner et al. 2012; Thomsen et al. 2010), *A. islandica* populations established well in this region but with significantly lowered life span. The species dominates the benthic fauna with respect to biomass and production in the Kiel Bight (Brey et al. 1990) and Mecklenburg Bight (Zettler et al. 2001) below the halocline at ~15 m. *A. islandica* has the ability to tolerate low oxygen concentrations and was identified as an oxyconforming species that can regulate its metabolic rate to the environmental oxygen level, entering a metabolic depression when oxygen is depleted and accelerating metabolism when oxygen is available (Abele et al. 2010; Oeschger 1990). The metabolic depressed state can be self-induced by burrowing into the sediment and closing of the shell creating an internal

hypoxic environment with completely anoxic conditions for several days (Strahl et al. 2011). This may possibly contribute to the mechanism of slow physiological aging. The energy saving effect of metabolic rate depression may not affect Baltic Sea *A. islandica* that are chronically exposed to high environmental variability (Philipp et al. 2012). Extreme conditions rather may have pre-adapted animals from these populations making them more robust at the expense of life span.

Arctica islandica shell

Bivalve shells fulfill multiple functions e.g. protection, locomotion, rigidity, hanging device for muscles or as digging device. The exoskeleton of *A. islandica*, like many other bivalve shells, is composed of two valves hinged together by a ligament and covered by a thick organic layer, the periostracum. Over ten morphological types of shell structure have been discriminated from bivalve shells (Kobayashi & Samata 2006). The shell of *A. islandica* is rather simple structured with a homogenous constitution of calcium carbonate granules, with a solely aragonitic phase. Within shell cross sections three layers are distinguishable to greater or lesser extend (i.e. depending on region), with the prismatic outer shell layer, which is separated from the inner layer by a thin myostracum (Kennedy et al. 1969; Witbaard et al. 1997). The outer layer extends the shell via incremental growth along the outer shell margin whereas the inner shell layer is responsible for thickening of the shell. How the shell is formed in particular became a large research field in the past decades. The inner and outer shell layers derive from two separated compartments divided by the pallial line where the mantle tissue is attached to the inner shell surface. The organic phase of the shell consists of water-insoluble chitin and the soluble organic matrix (Addadi et al. 2003; Belcher et al. 1996; Weiner & Traub 1980). *A. islandica* contains approximately 99.54 wt % $CaCO_3$ as well as water-soluble organic matrix, and only 0.46 wt % water-insoluble organic matrix (Schone et al. 2010). Possible mechanisms of bivalve shell formation will be discussed further below. Major parts of the bivalve shell are shown in Figure 6.
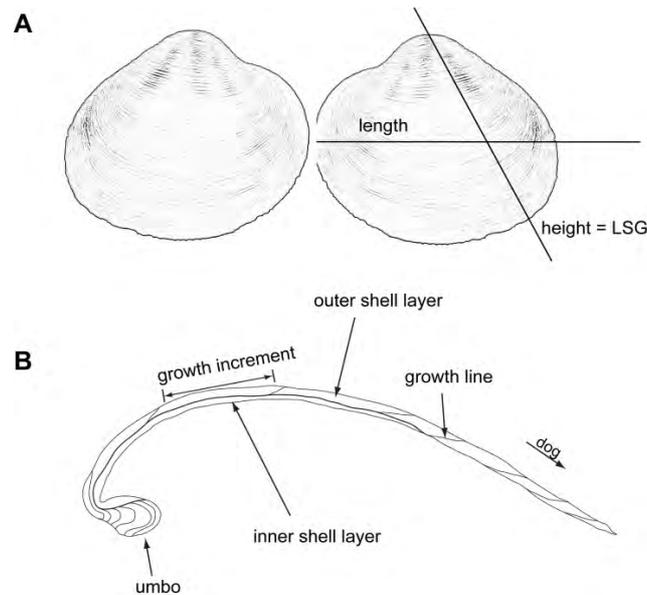
Figure 6: Sketches of *A. islandica* shell. A) Right and left valve showing the line of strongest growth (LSG) and measure of the valve length. B) Shell cross-section with major shell parts. The umbo is the oldest part of the shell; the inner shell is divided from the outer shell by a thin myostracum. Shell increments and growth lines form the latter. dog = direction of growth.

Fossilized and recent shells of *A. islandica* are increasingly used for environmental reconstruction (e.g. Krause-Nehring et al. 2012; Schoene et al. 2005). The growth increments are subdivided by organic rich growth lines similar to tree rings that form when growth decreases during winter or even stops (Jones 1980; Thompson et al. 1980; Witbaard et al. 1994). Annual growth lines function as a tool to determine the age of the shell when date of death is known. Formation of intra-annual or even daily growth lines was described by Schone et al. (2005). Like several other bivalves, *A. islandica* records changes of ambient seawater parameters, in particular temperature, food, salinity and pollution during shell formation. These measureable parameters called proxies can be used for environmental reconstruction when calibrated. *A. islandica* has been used several times as "bioarchive" and appears to appropriately integrate several proxies within its shell (e.g. Butler et al. 2011; Dunca et al. 2009; Schoene et al. 2011; Wanamaker et al. 2011). However, reliable data from these shell-proxies require a detailed understanding of factors influencing crystal formation, elemental uptake and isotopic ratios of the shell material (e.g. Schoene et al. 2011).

1.5 Bivalve shell formation

The secreting organ for the shell is the outer mantle epithelium (OME). At the outer mantle margin, the mantle enfolds and forms the periostracal groove from where the organic cuticle periostracum is getting secreted (Figure 7). Constituents for the organic matrix that may initiate nucleation and control crystal growth are also secreted from specialized mantle cells and gained much attention due to the many varying functions of e.g. proteins, glycoproteins, chitin, silk fibroin and amino acids in relation to shell formation (Addadi et al. 2006; Nudelman et al. 2006; Samata 2004).

The OME, the inner shell surface and the periostracum enclose an inner compartment called the extrapallial space (EPS) (Figure 7). Divided into an inner and an outer section by the pallial line it is filled with the inner and the outer extrapallial fluid (EPF), respectively (Wheeler 1992; Wilbur 1983). The microenvironment in which the biomineral is getting precipitated has to be $CaCO_3$ supersaturated, tightly controlling the biomineralization process (Crenshaw 1980; Weiner & Dove 2003) and it is not yet clear if the EPF is that site where biomineralization can occur.
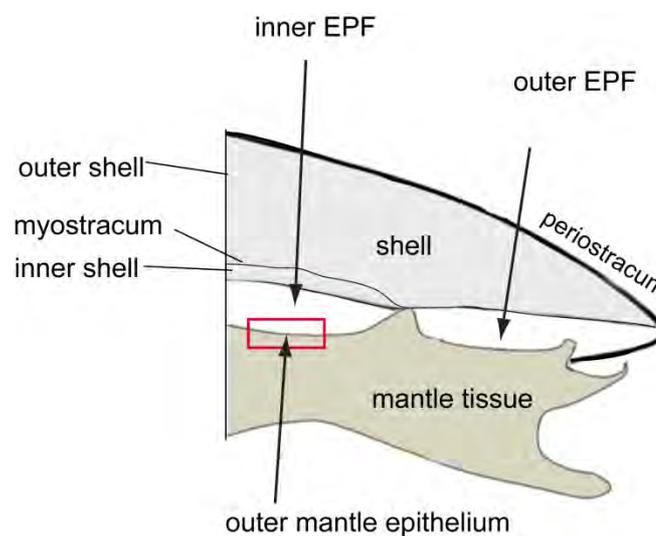
**Figure 7**: Simplified sketch showing a shell cross-section with attached mantle tissue (modified after McConnaughey et al. 2008). The extrapallial space is divided by the attachment of the outer mantle epithelium and thus filled with an inner and an outer extrapallial fluid (EPF). The periostracum is secreted by the outer mantle fold, encloses the outer EPF and covers the outer shell (followed by myostracum and inner shell layer).

The detailed understanding of biomineralization of $CaCO_3$ bivalve shells is complex and still lacking. Several models of shell formation were presented in the past decade (Addadi et al. 2006; Levi-Kalisman et al. 2001; Nudelman et al. 2007) proposing structured and gel-like domains, hydrophobic and hydrophilic surfaces, spatial differentiation and functionalized domains on the organic matrix surface and also the participation of amorphous precursor phase for mature crystals (Addadi et al. 2003). Weiss (2010) combined previous calcification models together with the new discovery of an aragonite-specific protein complex named Pif97 and Pif80 (Suzuki et al. 2009). Here, the OME cells need to function as a dynamic chitinous membrane that mechanically gets in close contact with the inner shell and forms new shell material together with Pif complex and aragonitic crystal lattice. To avoid local acidification and to balance mineralization gradients, the author suggests Ca^{2+}/H^+ shuttles are. The precipitation of aragonite by Pif-complex only on the one side of the OME on the nanoscale could then draw in more DIC e.g. via CO_2 diffusion (Weiss 2010). Biominerlization models combine the information gained so far and simultaneously illustrate the many gaps in our knowledge of single processes and components. Only interdisciplinary approaches may enable a mechanistic understanding of the shell formation process.

References

Abele, D., Kruppe, M., Philipp, E. E. R. & Brey, T. 2010 Mantle cavity water oxygen partial pressure (Po(2)) in marine molluscs aligns with lifestyle. *Canadian Journal of Fisheries and Aquatic Sciences* 67, 977-986.

Addadi, L., Joester, D., Nudelman, F. & Weiner, S. 2006 Mollusk shell formation: A source of new concepts for understanding biomineralization processes. *Chemistry-a European Journal* 12, 981-987.

Addadi, L., Raz, S. & Weiner, S. 2003 Taking advantage of disorder: Amorphous calcium carbonate and its roles in biomineralization. *Advanced Materials* 15, 959-970.

Adkins, J. F., Boyle, E. A., Curry, W. B. & Lutringer, A. 2003 Stable isotopes in deep-sea corals and a new mechanism for "vital effects". *Geochimica Et Cosmochimica Acta* 67, 1129-1143.

Al-Horani, F. A., Al-Moghrabi, S. M. & de Beer, D. 2003 The mechanism of calcification and its relation to photosynthesis and respiration in the scleractinian coral *Galaxea fascicularis*. *Marine Biology* 142, 419-426.

Allemand, D., Ferrier-Pages, C., Furla, P., Houlbreque, F., Puverel, S., Reynaud, S., Tambutte, E., Tambutte, S. & Zoccola, D. 2004 Biomineralisation in reef-building corals: from molecular mechanisms to environmental control. *Comptes Rendus Palevol* 3, 453-467.

Basova, L., Begum, S., Strahl, J., Sukhotin, A., Brey, T., Philipp, E. & Abele, D. 2012 Age-dependent patterns of antioxidants in *Arctica islandica* from six regionally separate populations with different lifespans. *Aquatic Biology* 14, 141-152.

Begum, S., Basova, L., Heilmayer, O., Philipp, E. E. R., Abele, D. & Brey, T. 2010 Growth and energy budget models of the bivalve *Arctica islandica* at six different sites in the Northeast Atlantic realm *Journal of Shellfish Research* 29, 107-115.

Belcher, A. M., Wu, X. H., Christensen, R. J., Hansma, P. K., Stucky, G. D. & Morse, D. E. 1996 Control of crystal phase switching and orientation by soluble mollusc-shell proteins. *Nature* 381, 56-58.

Bijma, J., Spero, H. & Lea, D. 1999 Reassessing foraminiferal stable isotope geochemistry: impact of the oceanic carbonate system (experimental results). *In Use of Proxies in Paleoceanography: Examples from the South Atlantic, ed. G Fischer, G Wefer, pp. 489–512. Springer-Verlag*.

Bissett, A., de Beer, D., Schoon, R., Shiraishi, F., Reimer, A. & Arp, G. 2008 Microbial mediation of stromatolite formation in karst-water creeks. *Limnology and Oceanography* 53, 1159-1168.

Brey, T., Arntz, W. E., Pauly, D. & Rumohr, H. 1990 *Arctica - (Cyprina) - islandica* in Kiel Bay (Western Baltic) - growth, production and ecological significance *Journal of Experimental Marine Biology and Ecology* 136, 217-235.

Butler, P. G., Wanamaker, A. D., Jr., Scourse, J. D., Richardson, C. A. & Reynolds, D. J. 2011 Long-term stability of delta C-13 with respect to biological age in the aragonite shell of mature specimens of the bivalve mollusk *Arctica islandica*. *Palaeogeography Palaeoclimatology Palaeoecology* 302, 21-30.

Caldeira, K. & Wickett, M. E. 2003 Anthropogenic carbon and ocean pH. *Nature* 425, 365-365.

Carre, M., Bentaleb, I., Bruguier, O., Ordinola, E., Barrett, N. T. & Fontugne, M. 2006 Calcification rate influence on trace element concentrations in aragonitic bivalve shells: Evidences and mechanisms. *Geochimica Et Cosmochimica Acta* 70, 4906-4920.

Casey, R. 1952 Some genera and subgenera, mainly new, of Mesozoic heterodont lamellibranchs. *Proc Malacol Soc London* 29, 121-176.

Crenshaw, M. A. 1972 The soluble matrix from *Mercenaria mercenaria* shell. *Biomineralization Res Rep* 6, 6.

Crenshaw, M. A. 1980 Mechanisms of shell formation and dissolution. *Topics in Geobiology* 1, 115-132.

Cuif, J. P., Dauphin, Y., Nehrke, G., Nouet, J. & Perez-Huerta, A. 2012 Layered growth and crystallization in calcareous biominerals: Impact of structural and chemical evidence on two major concepts in invertebrate biomineralization studies. *Minerals* 2, 11-39.

Dahlgren, T. G., Weinberg, J. R. & Halanych, K. M. 2000 Phylogeography of the ocean quahog (*Arctica islandica*): influences of paleoclimate on genetic diversity and species range. *Marine Biology* 137, 487-495.

Doney, S. C. F. V. F. R. K. J. 2009 Ocean Acidification: the other CO_2 Problem. *Annual Review of Marine Science* 1, 169 - 92.

Dunca, E., Mutvei, H., Goransson, P., Morth, C.-M., Schoene, B. R., Whitehouse, M. J., Elfman, M. & Baden, S. P. 2009 Using ocean quahog (*Arctica islandica*) shells to reconstruct palaeoenvironment in A-resund, Kattegat and Skagerrak, Sweden. *International Journal of Earth Sciences* 98, 3-17.

Epple, V. M., Brey, T., Witbaard, R., Kuhnert, H. & Paetzold, J. 2006 Sclerochronological records of Arctica islandica from the inner German Bight. *Holocene* 16, 763-769.

Feely, R. A., Sabine, C. L., Lee, K., Berelson, W., Kleypas, J., Fabry, V. J. & Millero, F. J. 2004 Impact of anthropogenic CO2 on the CaCO3 system in the oceans. *Science* 305, 362-366.

Gazeau, F., Quiblier, C., Jansen, J. M., Gattuso, J.-P., Middelburg, J. J. & Heip, C. H. R. 2007 Impact of elevated CO2 on shellfish calcification. *Geophysical Research Letters* 34.

Gregoire, C. 1960 Further studies on structure of the organic components in mother-of-pearl, especially in Pelecypods (Part 1.). *Bull Inst Sci nat belg* 36, 1-22.

Hiebenthal, C., Philipp, E., Eisenhauer, A. & Wahl, M. 2012 Effects of seawater pCO2 and temperature on shell growth, shell stability, condition and cellular stress of Western Baltic Sea *Mytilus edulis* (L.) and *Arctica islandica* (L.). *Marine Biology*.

Jacob, D. E., Soldati, A. L., Wirth, R., Huth, J., Wehrmeister, U. & Hofmeister, W. 2008 Nanostructure, composition and mechanisms of bivalve shell growth. *Geochimica Et Cosmochimica Acta* 72, 5401-5415.

Jones, D. S. 1980 Annual cycle of shell growth increment formation in 2 continental-shelf bivalves and its paleoecologic significance *Paleobiology* 6, 331-340.

Kennedy, W. J., Taylor, J. D. & Hall, A. 1969 Environmental and biological controls on bivalve shell mineralogy *Biological Reviews of the Cambridge Philosophical Society* 44, 499-&.

Kennish, M. J. & Lutz, R. A. 1995 Assessment of the ocean quahog, *Arctica islandica* (Linneaus, 1767), in the New Jersey Fishery *Journal of Shellfish Research* 14, 45-52.

Kleypas, J., Feely, R., Fabry, V., C, C. L., Sabine, C. & Robbins, L. 2006 Impacts of ocean acidification on coral reefs and other marine calcifiers: a guide for future research. *88 pp. Report of a workshop sponsored by NSF, NOAA, and the U.S. Geological Survey. St. Petersburg, Florida*.

Knoll, A. H. 2003 Biomineralization and evolutionary history. In *Biomineralization*, vol. 54, pp. 329-356.

Kobayashi, I. & Samata, T. 2006 Bivalve shell structure and organic matrix. *Materials Science & Engineering C-Biomimetic and Supramolecular Systems* 26, 692-698.

Kraus, M. G., Beal, B. F., Chapman, S. R. & McMartin, L. 1992 A comparison of growth rates in Arctica islandica (Linnaeus, 1767) between field and laboratory populations. *Journal of Shellfish Research* 11, 289-294.

Krause-Nehring, J., Brey, T. & Thorrold, S. R. 2012 Centennial records of lead contamination in northern Atlantic bivalves (*Arctica islandica*). *Marine Pollution Bulletin* 64, 233-240.

Langdon, C., Takahashi, T., Sweeney, C., Chipman, D., Goddard, J., Marubini, F., Aceves, H., Barnett, H. & Atkinson, M. J. 2000 Effect of calcium carbonate saturation state on the calcification rate of an experimental coral reef. *Global Biogeochemical Cycles* 14, 639-654.

Levi-Kalisman, Y., Falini, G., Addadi, L. & Weiner, S. 2001 Structure of the nacreous organic matrix of a bivalve mollusk shell examined in the hydrated state using Cryo-TEM. *Journal of Structural Biology* 135, 8-17.

Lischka, S., Buedenbender, J., Boxhammer, T. & Riebesell, U. 2011 Impact of ocean acidification and elevated temperatures on early juveniles of the polar shelled pteropod *Limacina helicina*: mortality, shell degradation, and shell growth. *Biogeosciences* 8, 919-932.

Lowenstam, H. A. 1981 Minerals formed by organisms *Science* 211, 1126-1131.

Ludwig, R., Al-Horani, F. A., de Beer, D. & Jonkers, H. M. 2005 Photosynthesis-controlled calcification in a hypersaline microbial mat. *Limnology and Oceanography* 50, 1836-1843.

Lutz, R. A., Mann, R., Goodsell, J. G. & Castagna, M. 1982 Larval and early post-larval developments of Arctica islandica. *Journal of the Marine Biological Association of the United Kingdom* 62, 745-769.

Mann, R. 1982 The seasonal cycle of gonadal development in Arctica islandica from the southern New England shelf. *U S Fish and Wildlife Service Fishery Bulletin* 80, 315-326.

McConnaughey, T. A. & Falk, R. H. 1991 Calcium-Proton exchange during algal calcification *Biological Bulletin* 180, 185-195.

Melzner, F., Thomsen, J., Koeve, W., Oschlies, A., Gutowska, M. A., Bange, H., Hansen, H. P. & Körtzinger, A. 2012 Future ocean acidification will be amplified by hypoxia in coastal habitats. *Marine Biology*.

Newton, R. B. 1891 Systematic List of the F. E. Edwards Collection of British Oligocene and Eocene Mollusca in the British Museum (Natural History), &c. In *Systematic List of the F. E. Edwards Collection of British Oligocene and Eocene Mollusca in the British Museum*, pp. xxviii & 365 pp.-xxviii & 365 pp.

Nicol, D. 1951 Recent species of the veneroid pelecypod Arctica. *Jour Washington Acad Sci* 41, 102-106.

Nudelman, F., Chen, H. H., Goldberg, H. A., Weiner, S. & Addadi, L. 2007 Spiers memorial lecture: Lessons from biomineralization: comparing the growth strategies of mollusc shell prismatic and nacreous layers in *Atrina rigida*. *Faraday Discussions* 136, 9-25.

Nudelman, F., Gotliv, B. A., Addadi, L. & Weiner, S. 2006 Mollusk shell formation: Mapping the distribution of organic matrix components underlying a single aragonitic tablet in nacre. *Journal of Structural Biology* 153, 176-187.

Oeschger, R. 1990 Long-term anaerobiosis in sublittoral marine invertebrates from the Western Baltic Sea - *Halicryptus spinulosus* (Priapulida), *Astarte borealis* and *Arctica islandica* (Bivalvia) *Marine Ecology Progress Series* 59, 133-143.

Orr, J. C., Fabry, V. J., Aumont, O., Bopp, L., Doney, S. C., Feely, R. A., Gnanadesikan, A., Gruber, N., Ishida, A., Joos, F., Key, R. M., Lindsay, K., Maier-Reimer, E., Matear, R., Monfray, P., Mouchet, A., Najjar, R. G., Plattner, G. K., Rodgers, K. B., Sabine, C. L., Sarmiento, J. L., Schlitzer, R., Slater, R. D., Totterdell, I. J., Weirig, M. F., Yamanaka, Y. & Yool, A. 2005 Anthropogenic ocean acidification over the twenty-first century and its impact on calcifying organisms. *Nature* 437, 681-686.

Philipp, E. E. R., Wessels, W., Gruber, H., Strahl, J., Wagner, A. E., Ernst, I. M. A., Rimbach, G., Kraemer, L., Schreiber, S., Abele, D. & Rosenstiel, P. 2012 Gene Expression and Physiological Changes of Different Populations of the Long-Lived Bivalve *Arctica islandica* under Low Oxygen Conditions. *Plos One* 7.

Ridgway, I. D. & Richardson, C. A. 2011 Arctica islandica: the longest lived non colonial animal known to science. *Reviews in Fish Biology and Fisheries* 21, 297-310.

Ridgway, I. D., Richardson, C. A. & Austad, S. N. 2010 Maximum Shell Size, Growth Rate, and Maturation Age Correlate With Longevity in Bivalve Molluscs. *Journals of Gerontology Series a-Biological Sciences and Medical Sciences* 66, 183-190.

Ridgwell, A. & Zeebe, R. E. 2005 The role of the global carbonate cycle in the regulation and evolution of the Earth system. *Earth and Planetary Science Letters* 234, 299-315.

Riebesell, U., Zondervan, I., Rost, B., Tortell, P. D., Zeebe, R. E. & Morel, F. M. M. 2000 Reduced calcification of marine plankton in response to increased atmospheric CO2. *Nature* 407, 364-367.

Ries, J. B. 2005 Aragonite production in calcite seas: effect of seawater Mg/Ca ratio on the calcification and growth of the calcareous alga *Penicillus capitatus*. *Paleobiology* 31, 445-458.

Ries, J. B., Cohen, A. L. & McCorkle, D. C. 2009 Marine calcifiers exhibit mixed responses to CO2-induced ocean acidification. *Geology* 37, 1131-1134.

Sabine, C. L., Feely, R. A., Gruber, N., Key, R. M., Lee, K., Bullister, J. L., Wanninkhof, R., Wong, C. S., Wallace, D. W. R., Tilbrook, B., Millero, F. J., Peng, T. H., Kozyr, A., Ono, T. & Rios, A. F. 2004 The oceanic sink for anthropogenic CO2. *Science* 305, 367-371.

Saleuddin, A. & Petit, H. 1983 The mode of formation and the structure of the periostracum. *In The Mollusca; Saleuddin, A.S.M., Wilbur, K.M., Eds.; Academic Press: New York, NY, USA* volume 4 pp. 199–234.

Samata, T. 2004 Recent advances in studies on nacreous layer biomineralization, molecular and cellular aspects. *Thalassas* 20, 25-44.

Schoene, B. R., Fiebig, J., Pfeiffer, M., Gless, R., Hickson, J., Johnson, A. L. A., Dreyer, W. & Oschmann, W. 2005 Climate records from a bivalved Methuselah (*Arctica islandica*, Mollusca; Iceland). *Palaeogeography Palaeoclimatology Palaeoecology* 228, 130-148.

Schoene, B. R., Radermacher, P., Zhang, Z. & Jacob, D. E. 2011 Crystal fabrics and element impurities (Sr/Ca, Mg/Ca, and Ba/Ca) in shells of *Arctica islandica* - implications for paleoclimate reconstructions. *Palaeogeography Palaeoclimatology Palaeoecology* DOI:10.1016/j.palaeo.2011.05.013.

Schoene, B. R., Wanamaker, A. D., Jr., Fiebig, J., Thebault, J. & Kreutz, K. 2011 Annually resolved delta C-13(shell) chronologies of long-lived bivalve mollusks (*Arctica islandica*) reveal oceanic carbon dynamics in the temperate North Atlantic during recent centuries. *Palaeogeography Palaeoclimatology Palaeoecology* 302, 31-42.

Schone, B. R., Houk, S. D., Castro, A. D. F., Fiebig, J., Oschmann, W., Kroncke, I., Dreyer, W. & Gosselck, F. 2005 Daily growth rates in shells of *Arctica islandica*: Assessing sub-seasonal environmental controls on a long-lived bivalve mollusk. *Palaios* 20, 78-92.

Schone, B. R., Zhang, Z., Jacob, D., Gillikin, D. P., Tutken, T., Garbe-Schonberg, D., McConnaughey, T. & Soldati, A. 2010 Effect of organic matrices on the determination of the trace element chemistry (Mg, Sr, Mg/Ca, Sr/Ca) of aragonitic bivalve shells (*Arctica islandica*)-Comparison of ICP-OES and LA-ICP-MS data. *Geochemical Journal* 44, 23-37.

Solomon, S., Qin, D., Manning, M., Chen, Z. & Marquis, M. 2007 Climate Change 2007: The Physical Science Basis: Contribution of Working Group I to the Fourth Assessment Report of the Intergovernmental Panel on Climate Change. *New York: Cambridge Univ. Press*.

Stemmer, K., Burghardt, I., Mayer, C., Reinicke, G. B., Wägele, H., Tollrian, R. & Leese, F. 2012 Morphological and genetic analyses of xeniid soft coral diversity (Octocorallia; Alcyonacea). *Organisms Diversity & Evolution* DOI 10.1007/s13127-012-0119-x.

Stix, H. a. M. & Abbott, R. T. 1991 The Shell: Five Hundred Million Years of Inspired Design. *Bdd Promotional Book CoISBN 978-0792447160*.

Strahl, J., Brey, T., Philipp, E. E. R., Thorarinsdottir, G., Fischer, N., Wessels, W. & Abele, D. 2011 Physiological responses to self-induced burrowing and metabolic rate depression in the ocean quahog Arctica islandica. *Journal of Experimental Biology* 214, 4223-4233.

Suzuki, M., Saruwatari, K., Kogure, T., Yamamoto, Y., Nishimura, T., Kato, T. & Nagasawa, H. 2009 An Acidic Matrix Protein, Pif, Is a Key Macromolecule for Nacre Formation. *Science* 325, 1388-1390.

Tambutte, E., Tambutte, S., Segonds, N., Zoccola, D., Venn, A., Erez, J. & Allemand, D. 2012 Calcein labelling and electrophysiology: insights on coral tissue permeability and calcification. *Proceedings of the Royal Society B-Biological Sciences* 279, 19-27.

Thebault, J., Schoene, B. R., Hallmann, N., Barth, M. & Nunn, E. V. 2009 Investigation of Li/Ca variations in aragonitic shells of the ocean quahog *Arctica islandica*, northeast Iceland. *Geochemistry Geophysics Geosystems* 10.

Thompson, I., Jones, D. S. & Dreibelbis, D. 1980 Annual internal growth banding and and life-history of the ocean quahog *Arctica islandica* (Mollusca, Bivalvia) *Marine Biology* 57, 25-34.

Thomsen, J., Gutowska, M. A., Saphoerster, J., Heinemann, A., Truebenbach, K., Fietzke, J., Hiebenthal, C., Eisenhauer, A., Koertzinger, A., Wahl, M. & Melzner, F. 2010 Calcifying invertebrates succeed in a naturally CO2-rich coastal habitat but are threatened by high levels of future acidification. *Biogeosciences* 7, 3879-3891.

Thomsen, J. & Melzner, F. 2010 Moderate seawater acidification does not elicit long-term metabolic depression in the blue mussel *Mytilus edulis*. *Marine Biology* 157, 2667-2676.

Urey, H. C., Lowenstam, H. A., Epstein, S. & McKinney, C. R. 1951 Measurement of paleotemperatures and temperatures of the Upper Cretaceous of England. Denmark, and the southeastern United States. *Bull Geol Soc Amer* 62, 399-416.

Wanamaker, A. D., Jr., Heinemeier, J., Scourse, J. D., Richardson, C. A., Butler, P. G., Eiriksson, J. & Knudsen, K. L. 2008a Very long-lived mollusks confirm 17th century ad tephra-based radiocarbon reservoir ages for North Icelandic shelf waters *Radiocarbon* 50, 399-412.

Wanamaker, A. D., Jr., Kreutz, K. J., Schoene, B. R. & Introne, D. S. 2011 Gulf of Maine shells reveal changes in seawater temperature seasonality during the Medieval Climate Anomaly and the Little Ice Age. *Palaeogeography Palaeoclimatology Palaeoecology* 302, 43-51.

Wanamaker, A. D., Jr., Kreutz, K. J., Schoene, B. R., Pettigrew, N., Borns, H. W., Introne, D. S., Belknap, D., Maasch, K. A. & Feindel, S. 2008b Coupled North Atlantic slope water forcing on Gulf of Maine temperatures over the past millennium. *Climate Dynamics* 31, 183-194.

Weiner, S. & Dove, P. 2003 An Overview on Biomineralization Processes and the Problem of the Vital Effect.

Weiner, S. & Traub, W. 1980 X-ray-diffraction study of the insoluble organic matrix of mollusk shells *Febs Letters* 111, 311-316.

Weiss, I. M. 2010 Jewels in the Pearl. *Chembiochem* 11, 297-300.

Wheeler, A. P. 1992 Mechanisms of molluscan shell formation. In *Calcification in biological systems.*, pp. 179-216.

Wilbur, K. M. 1983 Shell formation. In *The Mollusca. Volume 4. Physiology. Part 1.*, pp. 253-287.

Witbaard, R., Franken, R. & Visser, B. 1997 Growth of juvenile *Arctica islandica* under experimental conditions. *Helgolander Meeresuntersuchungen* 51, 417-431.

Witbaard, R., Jenness, M. I., Vanderborg, K. & Ganssen, G. 1994 Verification of annual growth increments in *Arctica islandica* from the North Sea by means of oxygen and carbon isotopes *Netherlands Journal of Sea Research* 33, 91-101.

Witbaard, R. & Klein, R. 1994 Long-term trends on the effects of the southern North Sea beamtrawl fishery on the bivalve mollusk *Arctica islandica* (Mollusca, Bivalvia) *Ices Journal of Marine Science* 51, 99-105.

Zeebe, R. & Wolf-Gladrow, D. 2001 CO2 in Seawater: Equilibrium, Kinetics, Isotopes. *Elsevier Oceanography Series, 65, pp. 346, Amsterdam*.

Zettler, M. L., Bonsch, R. & Gosselck, F. 2001 Distribution, abundance and some population characteristics of the ocean quahog, *Arctica islandica* (Linnaeus, 1767), in the Mecklenburg Bight (Baltic Sea). *Journal of Shellfish Research* 20, 161-169.

2. Aims and objectives

2. Aims and Objectives

The aim of this thesis is to identify affects of high pCO$_2$ on *Arctica islandica* shell growth and structure to identify possible adaption of this species towards elevated pCO$_2$ and as a prerequisite to fill fundamental knowledge gaps regarding the shell's composition and the biomineralization process.

Manuscript I:

Elevated CO$_2$ levels do not affect shell structure of the bivalve *Arctica islandica* from the Western Baltic

Some of the biochemical proxies (i.e. measureable parameters within the shell that relate to environmental parameters at time of formation) used for environmental reconstruction change with growth and crystal structure of the bivalve shell. I wanted to verify those proxies for a wider range of environmental conditions and investigated the impact of elevated pCO$_2$ on shell properties of *Arctica islandica* shell grown in a controlled perturbation experiment.

Manuscripts II and III:

To understand where and when to look precisely for changes within the bivalve shell caused by changing seawater parameters and to gain more information about possible adaptations of single species, I further i) questioned specific organic components of the biomineral itself (manuscript II) and ii) investigated the extrapallial fluid that is located between the shell and the mantle tissue and questioned its possible role in the biomineralization process (manuscript III).

Manuscript II:

Polyenes in the shell of *Arctica islandica* and their relation to the provenance of the shell: a confocal Raman microscopy study

Pigment polyenes are widely found in coloured parts of mollusk shells. Polyenes are organic compounds containing conjugated linear carbon-carbon single and double bonds building a polyenic chain. The origin and function of polyenes from mollusc shells is still unknown. Using Confocal Raman Microscopy, the spectral position related to the vibrational modes of the C-C single and C=C double bonds can be determined. I questioned the origin of polyenes within *A. islandica* shell by comparing shells from different regions. I further analysed the

distribution of polyenes within shell cross-sections to gain more information about their nature and functions and questioned their role in the shell-formation process.

Manuscript III:

In situ measurements of pH, Ca^{2+} and DIC dynamics within the extrapallial fluid of the North Atlantic bivalve *Arctica islandica*

It is generally assumed that the bivalve shell is mineralized from the extrapallial fluid (EPF) located between the outer mantle epithelium (OME) and the inner shell surface. I questioned how far the EPF is involved in the biomineralization process of *A. islandica* and performed *in situ* measurements of pH, calcium and dissolved organic carbon (DIC) dynamics within the EPF using pH microscopy and pH and Ca^{2+} microsensors.

S1 and **S2** are included within this thesis as further contributions and supplementary material.

S1:

Impact of ocean acidification on escape performance of the king scallop, Pecten maximus, from Norway

This study focuses on the clapping performance of the actively swimming king scallop, *Pecten maximus*, under elevated $p\mathrm{CO_2}$ to evaluate $p\mathrm{CO_2}$-induced energetic trade-offs that reduce locomotion, growth and/or stress resistance.

S2:

Morphological and genetic analyses of xeniid soft coral diversity (Octocorallia; Alcyonacea)

The paper describes the genetic and morphological based difficulties in identifying soft corals species. Concerning the problem to form calcium carbonate structures caused by ocean acidification, soft corals have not been considered often if at all in ocean acidification research. However, minute calcium carbonate spicules form within soft coral tissues (described in this study) and play an important role in stabilization of the soft corals hydroskeleton. I therefore included the manuscript within this thesis to present a different taxon that may be harmed by multiple environmental stressors. The mineralogy of sclerites from soft corals is hardly investigated (Rahman et al. 2011) but future Confocal Raman

Microscopy studies will serve as a helpful tool to analyse sclerites and their vulnerability towards ocean acidification.

3. Overview over the manuscripts and supplementary material

3. Overview of Manuscripts

Manuscript I:

Elevated CO_2 levels do not affect shell structure of the bivalve *Arctica islandica* from the Western Baltic

Kristina Stemmer, Gernot Nehrke, Thomas Brey

Conceived and designed the experiments: KS TB GN. Performed the sampling, culturing and staining of bivalves, perturbation experiments, seawater analyses, Scanning Electron Microscopy analysis: KS. Preparation of bivalve shells: KS with help of GN. Analyzed the data: KS with the help of TB GN. Contributed reagents/materials/analysis tools: TB GN. Wrote the manuscript: KS with help of GN TB.

The manuscript is accepted by *PLOS ONE*

Manuscript II:

Polyenes in the shell of *Arctica islandica* and their relation to the provenance of the shell: a confocal Raman microscopy study

Kristina Stemmer and Gernot Nehrke

Conceived and designed the experiment: KS GN. Prepared the shells: KS with help of GN. Performed the Confocal Raman Microscopy analysis: KS with the help of GN. Analyzed the data: KS GN. Contributed reagents/materials/analysis tools: GN. Wrote the manuscript: KS with help of GN.

The manuscript is submitted to *Journal of Molluscan Studies.*

Manuscript III:

In situ measurements of pH, Ca^{2+} and DIC dynamics within the extrapallial fluid of the ocean quahog *Arctica islandica*

Kristina Stemmer, Thomas Brey, Martin Glas, Martin Beutler, Burgel Schalkhausser, Dirk de Beer

Conceived and designed the experiment: KS MG DdB TB. Build the microsensors: KS. Prepared the bivalves and performed the microsensor measurements: KS MG. Analyzed data of microsensor measurements: KS MG with help of DdB and BS. Performed and analyzed microscopic pH measurements: KS MB. Performed DIC analysis: KS MG. Contributed reagents/materials/analysis tools: DdB TB. Wrote the manuscript: KS with contribution of MB DdB BS TB MG.

The manuscript is submitted to *Journal of Experimental Marine Biology and Ecology* (March 2013)

Supplementary Material:

S1:

Impact of ocean acidification on escape performance of the king scallop, Pecten maximus, from Norway

Burgel Schalkhausser, Christian Bock, Kristina Stemmer, Thomas Brey, Hans-O Pörtner, Gisela Lannig

K. Stemmer contributed to the development of the concept, helped with parts of the analyses, with the discussions of the results and gave editorial help to the manuscript.

This manuscript is published in *Marine Biology,* DOI 10.1007/s00227-012-2057-8, published online: 30 September 2012

S2:

Morphological and genetic analyses of xeniid soft coral diversity (Octocorallia; Alcyonacea)

Kristina Stemmer, Ingo Burghardt, Christoph Mayer, Götz B. Reinicke, Heike Wägele, Ralph Tollrian, Florian Leese

Conceived and designed the experiment: KS FL RT HW. Sampling of soft corals: KS. Sample preparation and genetic analyses: KS with help of FL. Analysis of genetic data: KS CM FL. Morphological analysis: KS IB with help of GBR. Scanning electron microscopy analysis: KS with the help of IB. Wrote the manuscript: KS FL HW. Contributed valuable comments to the manuscript: GBR CM. Contributed reagents/materials/analysis tools: RT HW.

4. Manuscripts

Manuscript I

Scanning electron microscope image of *Arctica islandica* shell. Cross-section of outer shell margin with intact periostracum.

Elevated CO_2 levels do not affect shell structure of the bivalve *Arctica islandica* from the Western Baltic

Kristina Stemmer[*1], Gernot Nehrke[2], Thomas Brey[1]

[1]*Functional Ecology,* [2]*BioGeoScience, Alfred Wegener Institute Helmholtz Centre for Polar and Marine Research, Bremerhaven, Germany*

Abstract

The shell of the bivalve *Arctica islandica* is used to reconstruct paleo-environmental conditions (e.g. temperature) via biogeochemical proxies, i.e. biogenic components that are related closely to environmental parameters at time of shell formation. Several studies have shown that proxies like element- and isotope-ratios can be affected by shell growth and structure. Thus it is essential to evaluate the impact of changing environmental parameters such as ocean acidification on shell properties to validate these biogeochemical proxies for a wider range of environmental conditions. Growth experiments with *Arctica islandica* from the Western Baltic Sea under different pCO$_2$ levels (from 380 to 1120 μatm) indicate no affect of elevated pCO$_2$ on shell growth or crystal microstructure, indicating that *A. islandica* shows an adaptation to a wider range of pCO$_2$ levels than reported for other species. Accordingly, proxy information derived from *A. islandica* shells of this region contains no pCO$_2$ related bias.

Introduction

Marine biogenic carbonates like the bivalve shell represent complex composites of organic and inorganic phases (Addadi et al. 2006; Cuif JP et al. 2011; Nudelman et al. 2006). Fossilized as well as recent shells are attractive bioarchives for paleo-climate reconstruction (Marchitto et al. 2000; Schoene et al. 2003; Wanamaker et al. 2009) and environmental monitoring (Krause-Nehring et al. 2012), as information on environmental conditions at times of shell formation is preserved in structural and biogeochemical shell properties (Epstein et al. 1953; Hickson et al. 1999; Schone et al. 2004). However, in bivalve shells, some of the "classic" proxy systems (e.g. element and isotope signatures) developed for paleo-temperature ($\delta^{18}O$ e.g. Schone et al. 2004), salinity and food availability have been shown to be affected by growth patterns, crystal structures, the organic- and the mineral- phase of the biogenic carbonate (calcite, the more soluble aragonite or both) (Addadi et al. 2003; Schoene et al. 2011; Strasser et al. 2008).

From the chemical point of view, increased seawater pCO$_2$ and therefore decreased pH leads to a reduced saturation level for calcium carbonates (Feely et al. 2004) and therefore hampers shell or skeleton formation (Gazeau et al. 2007; Ries et al. 2009). Apparently, several species of marine calcifiers can cope with such conditions (Langer et al. 2009; Ries et al. 2009; Thomsen et al. 2010; Tunnicliffe et al. 2009) albeit this adaptation may coincide with changes in shell structure and chemistry (Hahn et al. 2012; Melzner et al. 2011; Thomsen et al. 2010; Tunnicliffe et al. 2009). Raising atmospheric CO$_2$ and the corresponding decrease in ocean pH represents a challenge for marine calcifiers on a global scale (e.g. Doney 2009).

A number of studies evaluates the impact of high pCO$_2$ and low pH on marine bivalve shells (e.g.Gazeau et al. 2007; Michaelidis et al. 2005; Ries et al. 2009; Rodolfo-Metalpa et al. 2011) but just a few of these take a closer look on shell growth in height or thickness and on internal shell crystal structure (Hahn et al. 2012; Melzner et al. 2011; Thomsen et al. 2010). In the north-Atlantic bivalve *A. islandica*, Hiebenthal et al. (2012a) found shell stability, shell growth and tissue lipofuscin accumulation (indicating stress levels) to be unaffected by high pCO$_2$ (up to 1700 µatm), indicating that this species may be less vulnerable to ocean acidification. Our study analyzes whether *A. islandica* has to pay a price for this adaptation to more acidic conditions in terms of changes in shell microstructure.

Due to its longevity (up to several centuries, Abele et al. 2009; Strahl et al. 2007; Wanamaker et al. 2008a), its distinct internal growth band pattern (Epple et al. 2006; Ropes 1984), its wide distribution in the northern Atlantic (Dahlgren et al. 2000; Nicol 1951), and its long fossil record *A. islandica* represents a valuable bioarchive (Schoene et al. 2005; Schone et al. 2005; Weidman et al. 1994). Wanamaker et al. (2008b) e.g. used shell-derived temperature proxies ($\delta^{18}O_c$) of *A. islandica* to reconstruct ocean temperature variability over the last millennium.

The mineral phase present within the shell of *A. islandica* is aragonite with an outer shell layer (OSL) comprising the outer shell margin and forming the distinct shell increments and growth checks, and an inner shell layer (ISL) extending from the oldest part of the shell, the umbo, to the pallial line (Dunca et al. 2009; Morton 2011; Ropes et al. 1984). Both layers are separated by a thin myostracum, and a protective organic layer, the periostracum, covers the outer shell. The shell is formed at the inner shell surface (growth in thickness) and the shell margin (growth in height), i.e. at two separate locations of precipitation divided by the attachment of the mantle tissue at the pallial line: The inner EPF is in contact with the ISL that is not yet formed outward the pallial line where the outer EPF is in contact with the OSL. It is suggested that shell precipitates directly from extrapallial fluids (EPF) situated in space between secretory mantle tissue and shell surface (Crenshaw 1980; Wheeler 1992; Wilbur 1983). However, to what extent the EPF is involved in shell formation is not clear and subject of current research. Outer and inner shell layer are composed of distinct crystal morphotypes that can be differentiated in a shell cross-section, with different affinities of elemental uptake (Dunca et al. 2009; Ropes et al. 1984; Schoene et al. 2011). Irregular simple prisms, irregular complex crossed lamellar and crossed acicular-crossed lamellar microstructures are described by Ropes et al. (1984) and are also observed in *A. islandica* shells from the North Sea (Schoene et al. 2011), whereas the shells from the Kiel Bight (Western Baltic Sea) mostly display homogeneous crystals in the outer shell layer and simple crossed lamellar structures in the inner shell layer (Dunca et al. 2009).

There is substantial evidence that element- and isotope-signatures of biogenic carbonates used as proxy data are affected by the structure of the biogenic carbonate to some extent (Dauphin et al. 2003; Meibom et al. 2004). Crystal growth rate, size and structure within bivalve shells can strongly influence trace element concentrations, as shown by, e.g., Carré et al. (2006); Freitas et al. (2009). Regarding *A. islandica*, Schöne et al. (Schoene et al. 2011) recommends

to restrict sampling for geochemical analysis to one type of shell structure to avoid structure related bias.

In Kiel Bight, *Arctica islandica* inhabit the zone below the thermohaline pycnocline (> 15m), and thus are exposed to strong environmental fluctuations, i.e. low and variable salinity (18 - 23), periods of low oxygen availability during summer stratification and corresponding fluctuating $p\text{CO}_2$ levels with peaks over 1000 µatm (Boknis Eck Time Series Station, (Hansen et al. 1999). Shell growth and shell structure represent an integrated response of the physiological and biochemical activities in the organism to the surrounding environmental conditions (Riisgard & Randlov 1981). Compared to *A. islandica* from fully marine environments life span of Kiel Bight animals is distinctly shorter, the shells are generally thinner (Nicol 1951) and smaller and show a less organized microstructure (Dunca et al. 2009). Nevertheless, *A. islandica* is a prominent and abundant key species in Western Baltic benthic communities (Brey et al. 1990).

The aim of this study is to investigate the impact of $p\text{CO}_2$ on the shell microstructure of *A. islandica* from the Kiel Bight, in order to evaluate the possible impact such changes would have on shell based proxies.

Material and Methods

Aquaculture

Arctica islandica were collected in February 2010 from the "Süderfahrt" location (N 54°31'-32' E 10°41'-48') in Kiel Bight, Western Baltic. Clams were dredged from the seafloor in 20 m water depth and small animals of 15 to 25 mm height were chosen for this study. Clams were transported to the AWI Wadden Sea Station Sylt and kept in an aerated flow-through tank with natural sediment for an acclimation time of 3 months. *A. islandica* is a high saline species and shows optimum growth at between 6 and 10 °C (Hiebenthal et al. 2012a; Hiebenthal et al. 2012b; Mann 1982). Therefore, salinity and temperature of experimental seawater were slowly increased to experimental starting conditions with salinity of 29 and a temperature of 10 °C. During the experiments, artificial calcium carbonate free sediment (Vitakraft® quarz gravel 1-2 mm grain size) was used to avoid pH buffering. Food supply

(DT's Premium Blend, T's Plankton Farm, Sycamore, IL, containing *Nannochloropsis oculata*, *Phaeodactylum tricorutum* and *Chrorella* sp.) was added every two days.

Calcein staining

To mark the start of the experiment in the clamshell, the animals were immersed for 4 ½ hours in a calcein solution (100 mg/l seawater) followed by two washing steps as described in Riascos et al. (2007). Calcein is a fluorescent dye with an excitation and emission wavelength of 495/515 nm respectively. It is incorporated in biogenic calcium carbonate at the actual location of carbonate growth (Moran 2000), i.e. the outer shell margin in bivalves (Riascos et al. 2007) and was shown not to alter the element signature of the carbonate (Dissard et al. 2009). All clams were pumping water (shell open and siphons visible) during the staining period and were therefore exposed to the fluorochrome. No animal died during the staining was zero. The perturbation experiment started right after the staining procedure.

CO_2 perturbation experiment

A. islandica were kept at three different pCO_2 - gas-levels for 90 days: The control group at 380 µatm (ambient atmospheric CO_2 level) and experimental groups at 760 µatm (2x actual pCO_2) and 1120 µatm (4x preindustrial pCO_2), respectively. CO_2 concentrations of the experimental water were maintained by a gas mixing system (HTK, Hamburg, Germany). Experimental temperature was set to 10 °C but showed slight fluctuations over the 90 days owing to North Sea warming as well as slight differences between incubations related to technical conditions (Table 1). The experimental setup is shown in Figure 1.
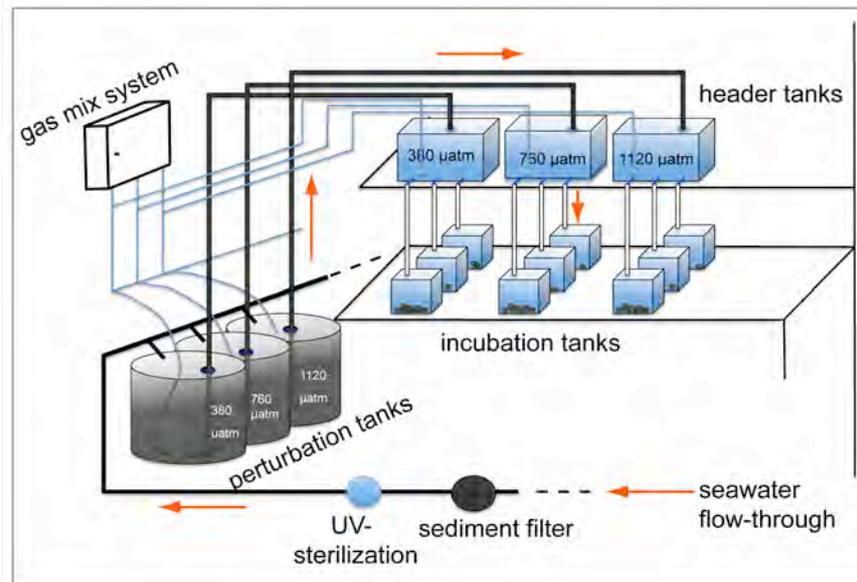
Figure 1: Experimental-setup for pCO_2 perturbation. The temperature controlled room was supplied with one filter-tank (sediment filter and UV-sterilization), one 250 l perturbation tank and one 30 l perturbed header tank per pCO_2-level. From the header tanks the CO_2-enriched water and the control water flowed down to triplicates of 4 l incubation tanks. In each tank 10 animals were incubated, i.e. a total of 30 clams per pCO_2-level. A plastic lid sealed all tanks to prevent gas exchange with the atmosphere. Seawater-flow rate from header to incubation tank was 150 ml/min.

Water chemistry and calculations

pH, salinity and temperature of the treatment tanks were measured once a day. Water samples (25 ml) for total alkalinity (A_T, determined by means of potentiometric titration using the Gran method) were collected once a week. The pH electrode (WTW 3310 pH meter with SenTix Mic electrode, Weilheim, Germany) was calibrated with NBS buffers before every measurement. Carbonate chemistry was calculated using the program CO2SYS (Lewis & Wallace 1998) with the input of pH (NBS scale), A_T and the constants of Mehrbach et al. (Mehrbach et al. 1973). Measured and calculated water parameters from our controlled perturbation experiment under different pCO_2 conditions are listed in Table 1.

Shell material

After 90 days experimental exposition, the clams were chucked and the soft tissue removed. Shells were carefully cleaned by hand and air-dried. From each treatment, 15 clamshells (5 per replicate) were randomly chosen for growth analysis. The staining with the fluorochrome calcein marked the start of the pCO_2 incubation and allowed to identify shell material grown under experimental conditions.

Table 1: Carbonate system parameters of the experimental seawater over time (90 days). Measured and calculated mean values. pCO_2-gas [µatm] = concentration of pCO_2 in perturbation gas; A_T [mmol kg^{-1}] = Total Alkalinity; Sal = Salinity; T (°C) = Temperature in Celsius; pH$_{NBS}$ = pH calibrated with Nist Buffer Standard; C_T [mmol kg^{-1}] = Total dissolved inorganic carbon; pCO_2-sw [µatm] = concentration of pCO_2 in seawater; Ω arag = saturation state of aragonite; SD = standard deviation

Measured parameters

pCO_2-gas [µatm]	A_T [mmol kg^{-1}]	SD	Sal	SD	T (°C)	SD	pH$_{NBS}$	SD
380	2328	(± 28)	30.9	(± 0.8)	10.6	(± 2.1)	8.07	(± 0.05)
760	2335	(± 26)	30.9	(± 0.8)	9.5	(± 2.1)	7.90	(± 0.07)
1120	2335	(± 26)	30.9	(± 0.8)	9.3	(± 1.3)	7.75	(± 0.07)

Calculated parameters

C_T [mmol kg^{-1}]	SD	pCO_2-sw [µatm]	SD	Ω arag	SD
2193	(± 48)	524	(± 83)	1.68	(± 0.30)
2263	(± 45)	800	(± 184)	1.14	(± 0.26)
2309	(± 45)	1140	(± 221)	0.83	(± 0.18)

Growth analysis

Shells were submerged in NaOCl (13%) solution for 1 h to remove the organic layer (periostracum) and subsequently washed with de-ionisized water two times. Shells were checked for calcein marks using a fluorescence stereoscope (Olympus SZX12, Figure 2). In most shells, the calcein mark was not found along the whole shell edge, but only intermittently. If the mark included the endpoint of the line of strongest growth (LSG, Fig.1), the shell was cross-sectioned along the LSG, if not, along a line through the calcein mark closest to the LSG. To prevent shell damage during cutting, metal epoxy (Toolcraft) was applied to the marked shell area one day before sectioning. Cross-sections were grinded using grinding paper (Buehler) with grits of P1200/P2400/P4000 grades followed by a polishing step with Buehler diamond polycrystalline suspensions (3 µm) and a final polish with aluminum oxide suspension (1 µm). The samples were then carefully rinsed using de-ionised water and air-dried.

Shell growth in height was measured from the end of the calcein mark (start of pCO_2 incubation) to the outer shell margin (end of pCO_2 incubation). If growth could not be measured directly on the LSG trajectory, the measurement was transformed to growth at LSG assuming isometric shell growth in all directions. Shell growth in thickness was measured at the end of the calcein mark perpendicular to the direction of growth (Figure 3). All

measurements were performed under a fluorescence stereoscope (Olympus SZX12) using the program ANALYSIS.

Differences in shell growth in height and thickness between treatments were analyzed by one-way ANOVA and subsequent TUKEY HSD post-hoc tests (significance level alpha = 0.05).
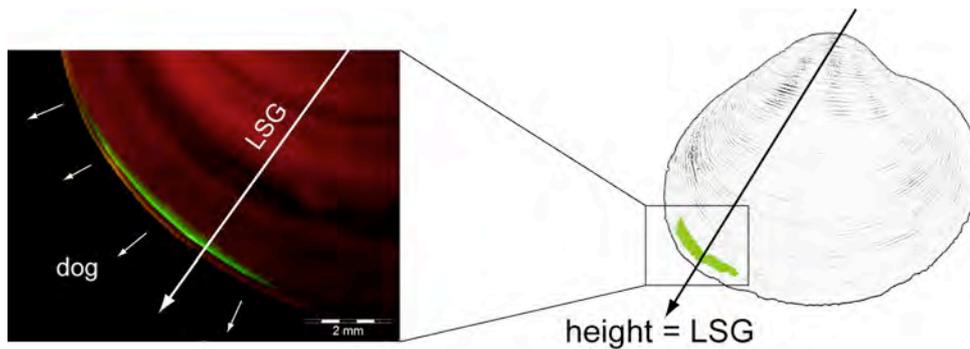
Figure 2: *Arctica islandica* shell showing a green calcein mark that indicates the start of the pCO_2 incubation. New grown shell was measured at the line of strongest growth (LSG). Arrows indicate the direction of growth (dog).
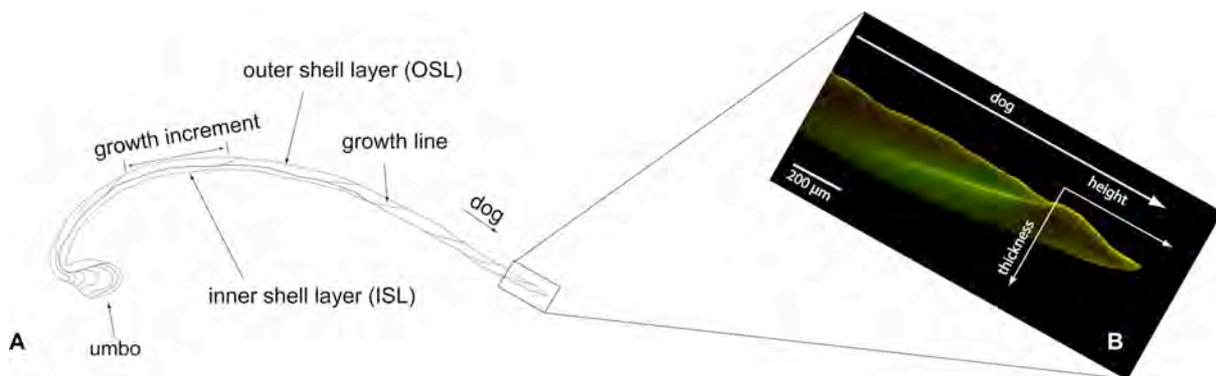
Figure 3: (A) Sketch of shell-cross-section with major shell structures. (B) Magnification of outer shell margin from the cross-section showing measurements of experimental shell growth in height and thickness.

Structural analysis

Microstructure of crystallites from different layers of shell material was compared via scanning electron microscopy (XL30 ESEM, Philips) on shell cross-sections from all treatments. Polished samples were coated with gold and scanned with an accelerating Voltage of 10 kV and a beam current of 1.7 nA. Shell-layers chosen for analysis are defined in Figure 4 A, B, C.
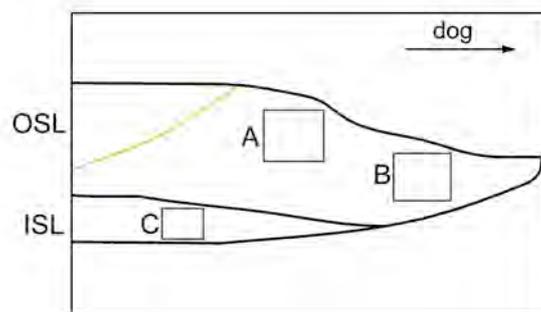
Figure 4: Sketch of outer shell margin from the cross section with areas where SEM images were taken. (A) Transition zone of shell material grown under normal and pCO_2 perturbated conditions in the outer shell layer (OSL) (green line = calcein mark). (B) Inner shell layer (ISL). (C) Last precipitated shell material at the very tip of the shell.

Results

Shell staining

The calcein mark used to mark the start of the experiment could be detected in 80 % of the shells (Table 2) etched with NaOCl. Within most shells the calcein mark did not appear along the whole shell margin but rather in just one, two or several segments (Figure 2). This indicates asynchronous shell growth of *Arctica islandica* during short time periods (4 ½ h calcein immersion). However, since this finding is outside the scope of this study we will not pursue it further here.

Growth rate

pCO$_2$ level had no significant effect on shell growth in height and thickness (one-way ANOVA, height: F = 0.503, p = 0.609; thickness: F = 1.227, p = 0.306). Growth varied between 0.96 µm/day and 9.14 µm/day in height and between 0.70 µm/day and 2.88 µm/day in thickness (Figure 5A, B respectively; Table 2).
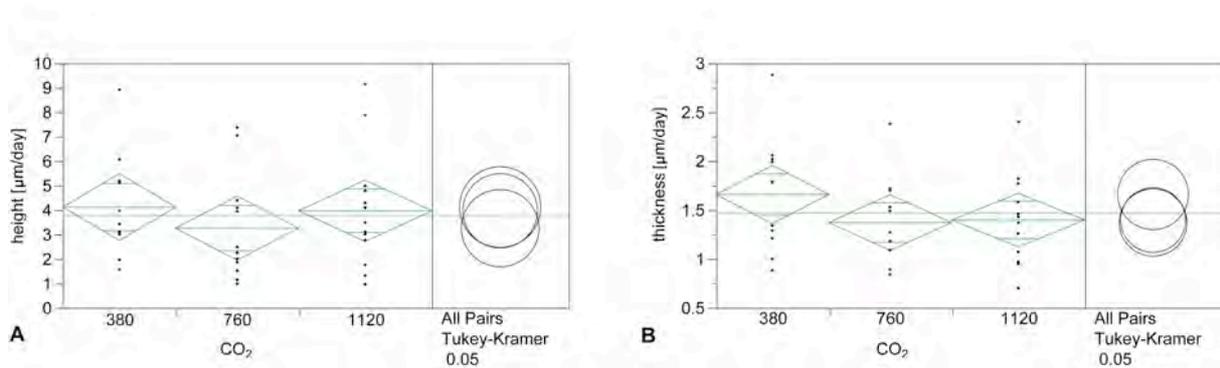
**Figure 5:** Shell growth in height (A) and thickness (B) did not differ significantly under three different pCO$_2$ levels (n = 11-13, one-way ANOVA, height: = 0.503, p = 0.609; thickness: F = 1.227, p = 0.306; JMP9)

Table 2: Daily growth rates of *Arctica islandica*. Column five and six give the shell growth rate per day at the line of strongest growth (LSG) in length and in thickness. To present shell growth rate per day, the measured total shell growth during the experiment was divided by the 90 days of the experiment. No. = continuous sample number; sample = sample code; pCO_2 [µatm] = concentration of gas-mix applied.

No.	sample	pCO_2 [µatm]	calcein mark	shell growth at LSG in length [µm/day]	in thickness [µm/day]
1	380A1	380	x	3.10	1.78
2	380A2	380	x	1.18	0.88
3	380A3	380	x	3.01	2.02
4	380A4	380	x	3.64	2.06
5	380A5	380	-	-	-
6	380B1	380	x	2.35	2.88
7	380B2	380	x	2.05	1.34
8	380B3	380	x	2.33	1.79
9	380B4	380	-	-	-
10	380B5	380	-	-	-
11	380C1	380	x	1.32	1.29
12	380C2	380	x	2.38	1.21
13	380C3	380	x	1.56	1.00
14	380C4	380	x	4.55	1.99
15	380C5	380	-	-	-
16	760A1	760	x	1.51	1.27
17	760A2	760	x	2.01	1.53
18	760A3	760	x	1.35	1.27
19	760A4	760	x	7.04	2.38
20	760A5	760	-	-	-
21	760B1	760	x	0.98	0.89
22	760B2	760	x	1.14	0.84
23	760B3	760	x	1.09	1.18
24	760B4	760	-	-	-
25	760B5	760	-	-	-
26	760C1	760	x	1.84	1.49
27	760C2	760	x	3.76	1.72
28	760C3	760	x	1.86	1.09
29	760C4	760	x	2.24	1.70
30	760C5	760	x	1.77	1.09
31	1120A1	1120	x	2.57	1.58
32	1120A2	1120	x	1.78	0.95
33	1120A3	1120	x	1.31	0.97
34	1120A4	1120	x	2.15	1.43
35	1120A5	1120	x	1.75	1.07
36	1120B1	1120	x	3.54	2.40
37	1120B2	1120	x	0.49	0.70
38	1120B3	1120	x	1.66	1.37
39	1120B4	1120	-	-	-
40	1120B5	1120	-	-	-
41	1120C1	1120	x	1.86	1.37
42	1120C2	1120	x	4.11	1.82
43	1120C3	1120	x	1.32	1.77
44	1120C4	1120	x	2.09	1.46
45	1120C5	1120	x	2.99	1.26

Shell microstructure

Crystal structures of shell material of *A. islandica* formed during the pCO_2 incubations did not differ between treatments (Figure 6). In the cross sections, outer and inner shell layer (OSL/ISL) were clearly distinguishable by their crystallites: The shell region of the OSL is characterized by a homogeneous distribution of irregular shaped crystallites with an average diameter of 1.5 µm (Figure 6A). The inner shell layer was build from distinct crossed lamellar crystallites (Dunca et al. 2009; Schoene et al. 2011) (Figure 4B; Figure 6B). The very tip of the new grown shell, i.e. the latest formed crystal structure looks the same in all experimental animals, too: It consists of homogeneous distributed but irregular shaped crystallites with an average diameter of 5 µm (Figure 4C; Figure 6C).
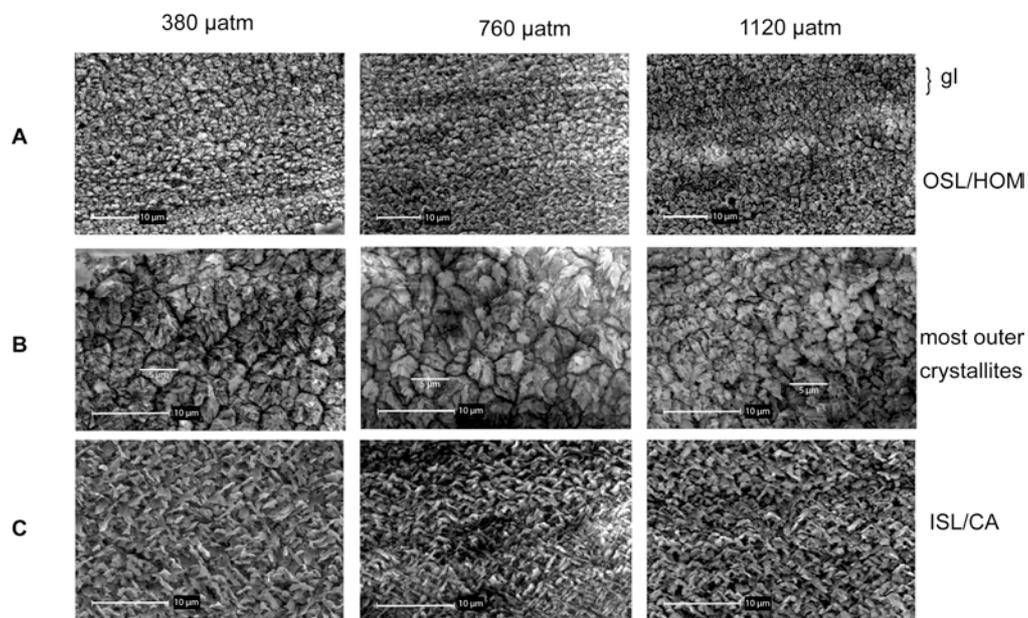
**Figure 6:** SEM images. Crystallites of new shell material grown under different pCO_2 levels. (A) The growth line (gl) stained with calcein at starter point of the pCO_2 incubation is visible due to smaller crystallites. HOM = homogeneous crystallites. (B) Inner shell layer (ISL) with distinct crossed-acicular crystallites. (C) Latest formed crystallites.

Discussion

Our study indicates that shell growth and crystal microstructure of *A. islandica* from Kiel Bight are not altered by pCO$_2$ in the range of 380 - 1120 µatm.

Individual shell growth rates varied over a wide range (0.96 – 9.14 µm/day in height and 0.70 -2.88 µm/day in thickness) but were not affected by pCO$_2$ treatment. Each shell formed new shell material with distinct and specific crystal structures in outer and inner shell layer. The widely accepted concept of extracellular matrix mediated mineralization in bivalves (Addadi et al. 2006; Weiner & Dove 2003) suggests that mineral formation requires a microenvironment that provides and maintains a sufficient supersaturation for nucleation and growth of the mineral phase. Our results indicate that *A. islandica* possess a high physiological control over the chemical composition at the site of calcification, even when exposed to elevated proton concentrations, i.e. low pH.

Current evidence indicates that elevated pCO$_2$ and lowered pH can have various effects on bivalve species, apparently depending on species and experimental conditions (Berge et al. 2006; Gazeau et al. 2007; Hahn et al. 2012; Melzner et al. 2011; Michaelidis et al. 2005). Accordingly, we are still far from a consistent picture of the cause-and-effect mechanisms involved.

To our knowledge there are few studies of pCO$_2$ effects on newly grown bivalve shell material. Hahn et al. (2012) report changes in shell ultrastructure in Mediterranean *Mytilus galloprovincialis* that were transplanted in the field from normal to a high pCO$_2$ level site. However, it remains unclear to which extent other (uncontrolled) environmental factors may have affected shell properties, too. Melzner et al. (2011) observed dissolution of the internal aragonite (nacre) layer in the blue mussel *Mytilus edulis* from Kiel Fjord under exposition to pCO$_2$ > 2000 µatm. These mussels experience seasonal pCO$_2$ peaks of > 4000 µatm and corresponding low pH down to 7.1 and thus are presumed to be adapted to such conditions (Hiebenthal et al. 2012a; Thomsen et al. 2010). However, a direct comparison with our findings is difficult because (i) the shell of *M. edulis* consists of two calcium carbonate polymorphs, calcite on the outside and aragonite on the inside and (ii) pCO$_2$ impact on newly grown shell material in shell regions comparable to those investigated in our study was not analyzed.

What makes Arctica islandica so special?

The fact that elevated $p\mathrm{CO_2}$ levels neither affect shell growth rate (Hiebenthal et al. 2012a, this study) nor shell microstructure (this study) indicates that *A. islandica* is in full physiological and chemical control of the shell formation process, including carbonate precipitation. This tolerance can have two possible explanations: (a) pre-adaptation through species-specific lifestyle; (b) pre-adaptation to regularly enhanced $p\mathrm{CO_2}$ levels in Kiel Bight.

(a) *A. islandica* is unique among bivalves as the deliberate exposition to high $p\mathrm{CO_2}$ and low pH conditions is part of its life strategy: *A. islandica* can perform extreme "metabolic rate depression" (MDR), i.e. animals may stop water pumping and bury deeper into the sediment for several days, while reducing metabolic activity to very low levels (Abele et al. 2009; Strahl et al. 2011). These sediments are often hypercapnic (physiological effects of elevated $p\mathrm{CO_2}$) and can be undersaturated with respect to aragonite (Green et al. 2004), whereas body fluids, i.e. haemolymph, mantle water, and extrapallial fluid are naturally acidified and may become even more acidic under anaerobic conditions (Crenshaw 1972; Melzner et al. 2012). Our findings support the hypothesis of Hiebenthal et al. (2012a) that the specific lifestyle of *A. islandica* may serve as a pre-adaptation to forthcoming elevated ocean $p\mathrm{CO_2}$. This feature may have added to the long-term success of *A. islandica*, too. *A. islandica* is the only remnant of an ancient genus of the once diverse Arcticidae (Nicol 1951) and apparently was able to survive major past climatic oscillations, showing a high abundance through geological times and a wide distribution in the Northern Atlantic.

(b) An alternative explanation would be that *A. islandica* from Kiel Bight, are well adapted to the strongly fluctuating conditions (salinity, temperature, oxygen availability, $p\mathrm{CO_2}$) of Kiel Bight, and therefore particularly this population can cope very well with elevated $p\mathrm{CO_2}$ levels. Adaption to fluctuating and increased $p\mathrm{CO_2}$ may add to the general expression of pronounced stress response at the expense of lifespan (Philipp et al. 2012) with that of Kiel Bight animals of ~ 40 yrs (Begum et al. 2009) compared to *A. islandica* from Island populations living up to 400 yrs in fully marine environment (Schone et al. 2005; Wanamaker et al. 2008b). The robustness towards changing conditions of Kiel Bight animals is also reflected in our experiment where *A. islandica* had no visual problem to cope with fully saline North Sea water used during the experiment.

Future research on *A. islandica* from different localities (Island, Kattegat, White Sea, ect.), possibly in combination with genetic approaches (e.g. transciptomics) (Philipp et al. 2012) will show whether or not the observed $p\mathrm{CO_2}$ tolerance of this bivalve is unique in the Kiel Bight population or a species-specific feature.

However, synergistic effects of $p\mathrm{CO_2}$ and other parameters such as temperature, food availability and salinity have not been considered yet. Furthermore, we still lack a detailed understanding of the mechanisms and controls of shell formation, which are a matter of ongoing and future research. We need to uncover the processes involved in biomineralization and before resolving this interdisciplinary enigma we can only report species-specific responses and hypothesize the processes behind it.

Conclusions

Our study shows that shell growth and shell microstructure of young *A. islandica* from Kiel Bight are not affected by the $p\mathrm{CO_2}$ up to 1120 μatm. Correspondingly, isotope- and element-based proxies derived from *A. islandica* shells are unbiased regarding changes in shell structure caused by varying environmental $p\mathrm{CO_2}$ levels. Whether or not this robustness applies to all *A. islandica* populations or just to the one from the Western Baltic remains to be seen.

Acknowledgements

References

Abele, D., Brey, T. & Philipp, E. 2009 Bivalve models of aging and the determination of molluscan lifespans. *Experimental Gerontology* **44**, 307-315.

Addadi, L., Joester, D., Nudelman, F. & Weiner, S. 2006 Mollusk shell formation: A source of new concepts for understanding biomineralization processes. *Chemistry-a European Journal* **12**, 981-987.

Addadi, L., Raz, S. & Weiner, S. 2003 Taking advantage of disorder: Amorphous calcium carbonate and its roles in biomineralization. *Advanced Materials* **15**, 959-970.

Begum, S., Basova, L., Strahl, J., Sukhotin, A., Heilmayer, O., Philipp, E., Brey, T. & Abele, D. 2009 A metabolic model for the ocean quahog *Arctica islandica* - effects of animal mass and age, temperature, salinity, and geography on respiration rate. *Journal of Shellfish Research* **28**, 533-539.

Berge, J. A., Bjerkeng, B., Pettersen, O., Schaanning, M. T. & Oxnevad, S. 2006 Effects of increased sea water concentrations of CO2 on growth of the bivalve *Mytilus edulis* L. *Chemosphere* **62**, 681-687.

Brey, T., Arntz, W. E., Pauly, D. & Rumohr, H. 1990 *Arctica (Cyprina) islandica* in Kiel Bay (western Balzic) - growth, production and ecological significance *Journal of Experimental Marine Biology and Ecology* **136**, 217-235.

Carre, M., Bentaleb, I., Bruguier, O., Ordinola, E., Barrett, N. T. & Fontugne, M. 2006 Calcification rate influence on trace element concentrations in aragonitic bivalve shells: Evidences and mechanisms. *Geochimica Et Cosmochimica Acta* **70**, 4906-4920.

Crenshaw, M. A. 1972 Inorganic composition of molluskan extrapallial fluid. *Biological Bulletin* **143**, 506-512.

Crenshaw, M. A. 1980 Mechanisms of shell formation and dissolution. *Topics in Geobiology* **1**, 115-132.

Cuif JP, Dauphin Y & Sorauf JE. 2011 *Biominerals and fossils through time*: Cambridge University Press.

Dahlgren, T. G., Weinberg, J. R. & Halanych, K. M. 2000 Phylogeography of the ocean quahog (*Arctica islandica*): influences of paleoclimate on genetic diversity and species range. *Marine Biology* **137**, 487-495.

Dauphin, Y., Guzman, N., Denis, A., Cuif, J. P. & Ortlieb, L. 2003 Microstructure, nanostructure and composition of the shell of Concholepas concholepas (Gastropoda, Muricidae). *Aquatic Living Resources* **16**, 95-103.

Dissard, D., Nehrke, G., Reichart, G. J., Nouet, J. & Bijma, J. 2009 Effect of the fluorescent indicator calcein on Mg and Sr incorporation into foraminiferal calcite. *Geochemistry Geophysics Geosystems* **10**.

Doney, S. C. F. V. F. R. K. J. 2009 Ocean Acidification: the other CO_2 Problem. *Annual Review of Marine Science* **1**, 169 - 92.

Dunca, E., Mutvei, H., Goransson, P., Morth, C.-M., Schoene, B. R., Whitehouse, M. J., Elfman, M. & Baden, S. P. 2009 Using ocean quahog (*Arctica islandica*) shells to reconstruct palaeoenvironment in A-resund, Kattegat and Skagerrak, Sweden. *International Journal of Earth Sciences* **98**, 3-17.

Epple, V. M., Brey, T., Witbaard, R., Kuhnert, H. & Paetzold, J. 2006 Sclerochronological records of *Arctica islandica* from the inner German Bight. *Holocene* **16**, 763-769.

Epstein, S., Buchsbaum, R., Lowenstam, H. A. & Urey, H. C. 1953 Revised carbonate-water isotopic temperature scale *Geological Society of America Bulletin* **64**, 1315-1325.

Feely, R. A., Sabine, C. L., Lee, K., Berelson, W., Kleypas, J., Fabry, V. J. & Millero, F. J. 2004 Impact of anthropogenic CO2 on the CaCO3 system in the oceans. *Science* **305**, 362-366.

Freitas, P. S., Clarke, L. J., Kennedy, H. & Richardson, C. A. 2009 Ion microprobe assessment of the heterogeneity of Mg/Ca, Sr/Ca and Mn/Ca ratios in *Pecten maximus* and *Mytilus edulis* (bivalvia) shell calcite precipitated at constant temperature. *Biogeosciences* **6**, 1209-1227.

Gazeau, F., Quiblier, C., Jansen, J. M., Gattuso, J.-P., Middelburg, J. J. & Heip, C. H. R. 2007 Impact of elevated CO2 on shellfish calcification. *Geophysical Research Letters* **34**.

Green, M. A., Jones, M. E., Boudreau, C. L., Moore, R. L. & Westman, B. A. 2004 Dissolution mortality of juvenile bivalves in coastal marine deposits. *Limnology and Oceanography* **49**, 727-734.

Hahn, S., Rodolfo-Metalpa, R., Griesshaber, E., Schmahl, W. W., Buhl, D., Hall-Spencer, J. M., Baggini, C., Fehr, K. T. & Immenhauser, A. 2012 Marine bivalve shell geochemistry and ultrastructure from modern low pH environments: environmental effect versus experimental bias. *Biogeosciences* **9**, 1897-1914.

Hansen, H. P., Giesenhagen, H. C. & Behrends, G. 1999 Seasonal and long-term control of bottom-water oxygen deficiency in a stratified shallow-water coastal system. *Ices Journal of Marine Science* **56**, 65-71.

Hickson, J. A., Johnson, A. L. A., Heaton, T. H. E. & Balson, P. S. 1999 The shell of the Queen Scallop *Aequipecten opercularisis* (L.) as a promising tool for palaeoenvironmental reconstruction: evidence and reasons for equilibrium stable-isotope incorporation. *Palaeogeography Palaeoclimatology Palaeoecology* **154**, 325-337.

Hiebenthal, C., Philipp, E., Eisenhauer, A. & Wahl, M. 2012a Effects of seawater pCO_2 and temperature on shell growth, shell stability, condition and cellular stress of Western Baltic Sea *Mytilus edulis* (L.) and *Arctica islandica* (L.). *Marine Biology*.

Hiebenthal, C., Philipp, E. E. R., Eisenhauer, A. & Wahl, M. 2012b Interactive effects of temperature and salinity on shell formation and general condition in Baltic Sea Mytilus edulis and Arctica islandica. *Aquatic Biology* **14**, 289-298.

Krause-Nehring, J., Brey, T. & Thorrold, S. R. 2012 Centennial records of lead contamination in northern Atlantic bivalves (*Arctica islandica*). *Marine Pollution Bulletin* **64**, 233-240.

Langer, G., Nehrke, G., Probert, I., Ly, J. & Ziveri, P. 2009 Strain-specific responses of Emiliania huxleyi to changing seawater carbonate chemistry. *Biogeosciences* **6**, 2637-2646.

Lewis & Wallace. 1998 Basic program for CO_2 system in seawater. Oak Ridge National Laboratory.

Mann, R. 1982 The seasonal cycle of gonadal development in Arctica islandica from the southern New England shelf. *U S Fish and Wildlife Service Fishery Bulletin* **80**, 315-326.

Marchitto, T. M., Jones, G. A., Goodfriend, G. A. & Weidman, C. R. 2000 Precise temporal correlation of holocene mollusk shells using sclerochronology. *Quaternary Research* **53**, 236-246.

Mehrbach, C., Culberso.Ch, Hawley, J. E. & Pytkowic.Rm. 1973 Measurement of apparent dissociation-constants of carbonic-acid in seawater at atmospheric pressure *Limnology and Oceanography* **18**, 897-907.

Meibom, A., Cuif, J. P., Hillion, F. O., Constantz, B. R., Juillet-Leclerc, A., Dauphin, Y., Watanabe, T. & Dunbar, R. B. 2004 Distribution of magnesium in coral skeleton. *Geophysical Research Letters* **31**.

Melzner, F., Stange, P., Truebenbach, K., Thomsen, J., Casties, I., Panknin, U., Gorb, S. N. & Gutowska, M. A. 2011 Food Supply and Seawater pCO(2) Impact Calcification and Internal Shell Dissolution in the Blue Mussel *Mytilus edulis*. *Plos One* **6**.

Melzner, F., Thomsen, J., Koeve, W., Oschlies, A., Gutowska, M. A., Bange, H., Hansen, H. P. & Körtzinger, A. 2012 Future ocean acidification will be amplified by hypoxia in coastal habitats. *Marine Biology*, DOI 10.1007/s00227-012-1954-1.

Michaelidis, B., Ouzounis, C., Paleras, A. & Portner, H. O. 2005 Effects of long-term moderate hypercapnia on acid-base balance and growth rate in marine mussels *Mytilus galloprovincialis*. *Marine Ecology-Progress Series* **293**, 109-118.

Moran, A. L. 2000 Calcein as a marker in experimental studies newly-hatched gastropods. *Marine Biology* **137**, 893-898.

Morton, B. 2011 The biology and functional morphology of *Arctica islandica* (Bivalvia: Arcticidae): A gerontophilic living fossil. *Marine Biology Research* **7**, 540-553.

Nicol, D. 1951 Recent species of the veneroid pelecypod Arctica. *Jour Washington Acad Sci* **41**, 102-106.

Nudelman, F., Gotliv, B. A., Addadi, L. & Weiner, S. 2006 Mollusk shell formation: Mapping the distribution of organic matrix components underlying a single aragonitic tablet in nacre. *Journal of Structural Biology* **153**, 176-187.

Philipp, E. E. R., Wessels, W., Gruber, H., Strahl, J., Wagner, A. E., Ernst, I. M. A., Rimbach, G., Kraemer, L., Schreiber, S., Abele, D. & Rosenstiel, P. 2012 Gene Expression and Physiological Changes of Different Populations of the Long-Lived Bivalve *Arctica islandica* under Low Oxygen Conditions. *Plos One* **7**, e44621. doi:10.1371/journal.pone.0044621.

Riascos, J., Guzman, N., Laudien, J., Heilmayer, O. & Oliva, M. 2007 Suitability of three stains to mark shells of *Concholepas concholepas* (Gastropoda) and *Mesodesma donacium* (Bivalvia). *Journal of Shellfish Research* **26**, 43-49.

Ries, J. B., Cohen, A. L. & McCorkle, D. C. 2009 Marine calcifiers exhibit mixed responses to CO_2-induced ocean acidification. *Geology* **37**, 1131-1134.

Riisgard, H. U. & Randlov, A. 1981 Energy budgets, growth and filtration-rates in *Mytilus edulis* at different algal concentrations *Marine Biology* **61**, 227-234.

Rodolfo-Metalpa, R., Houlbreque, F., Tambutte, E., Boisson, F., Baggini, C., Patti, F. P., Jeffree, R., Fine, M., Foggo, A., Gattuso, J. P. & Hall-Spencer, J. M. 2011 Coral and mollusc resistance to ocean acidification adversely affected by warming. *Nature Climate Change* **1**, 308-312.

Ropes, J. W. 1984 Procedures for preparing acetate peels and evidence validating the annual periodicity of growth lines formed in the shells of the ocean quahogs, *Arctica islandica Marine Fisheries Review* **46**, 27-35.

Ropes, J. W., Jones, D. S., Murawski, S. A., Serchuk, F. M. & Jearld, A. 1984 Documentation of annual growth lines in ocean quahogs, *Arctica islandica* L. . *Fishery Bulletin* **82**, 1-19.

Schoene, B. R., Hickson, J. & Oschmann, W. 2005 Reconstruction of subseasonal environmental conditions using bivalve mollusk shells-A graphical model. In *Isotopic and Elemental Tracers of Cenozoic Climate Change*, vol. 395, pp. 21-31.

Schoene, B. R., Kroencke, I., Houk, S. D., Castro, A. D. F. & Oschmann, W. 2003 The cornucopia of chilly winters: Ocean quahog (*Arctica islandica*, L., Mollusca) master chronology reveals bottom water nutrient enrichment during colder winters (North Sea). *Senckenbergiana Maritima* **32**, 165-175.

Schoene, B. R., Radermacher, P., Zhang, Z. & Jacob, D. E. 2011 Crystal fabrics and element impurities (Sr/Ca, Mg/Ca, and Ba/Ca) inshells of Arctica islandica - implications for paleoclimate reconstructions. *Palaeogeography Palaeoclimatology Palaeoecology* **DOI:10.1016/j.palaeo.2011.05.013**.

Schone, B. R., Castro, A. D. F., Fiebig, J., Houk, S. D., Oschmann, W. & Kroncke, I. 2004 Sea surface water temperatures over the period 1884-1983 reconstructed from oxygen isotope ratios of a bivalve mollusk shell (*Arctica islandica,* southern North Sea). *Palaeogeography Palaeoclimatology Palaeoecology* **212**, 215-232.

Schone, B. R., Fiebig, J., Pfeiffer, M., Gless, R., Hickson, J., Johnson, A. L. A., Dreyer, W. & Oschmann, W. 2005 Climate records from a bivalved Methuselah (Arctica islandica, Mollusca; Iceland). *Palaeogeography Palaeoclimatology Palaeoecology* **228**, 130-148.

Strahl, J., Brey, T., Philipp, E. E. R., Thorarinsdottir, G., Fischer, N., Wessels, W. & Abele, D. 2011 Physiological responses to self-induced burrowing and metabolic rate depression in the ocean quahog *Arctica islandica*. *Journal of Experimental Biology* **214**, 4223-4233.

Strahl, J., Philipp, E., Brey, T., Broeg, K. & Abele, D. 2007 Physiological aging in the Icelandic population of the ocean quahog *Arctica islandica*. *Aquatic Biology* **1**, 77-83.

Strasser, C. A., Mullineaux, L. S. & Walther, B. D. 2008 Growth rate and age effects on Mya arenaria shell chemistry: Implications for biogeochemical studies. *Journal of Experimental Marine Biology and Ecology* **355**, 153-163.

Thomsen, J., Gutowska, M. A., Saphoerster, J., Heinemann, A., Truebenbach, K., Fietzke, J., Hiebenthal, C., Eisenhauer, A., Koertzinger, A., Wahl, M. & Melzner, F. 2010 Calcifying invertebrates succeed in a naturally CO2-rich coastal habitat but are threatened by high levels of future acidification. *Biogeosciences* **7**, 3879-3891.

Tunnicliffe, V., Davies, K. T. A., Butterfield, D. A., Embley, R. W., Rose, J. M. & Chadwick, W. W., Jr. 2009 Survival of mussels in extremely acidic waters on a submarine volcano. *Nature Geoscience* **2**, 344-348.

Wanamaker, A. D., Jr., Heinemeier, J., Scourse, J. D., Richardson, C. A., Butler, P. G., Eiriksson, J. & Knudsen, K. L. 2008a Very long-lived mollusks confirm 17th century ad tephra-based radiocarbon reservoir ages for north Islandic shelf-waters *Radiocarbon* **50**, 399-412.

Wanamaker, A. D., Jr., Kreutz, K. J., Schoene, B. R., Maasch, K. A., Pershing, A. J., Borns, H. W., Introne, D. S. & Feindel, S. 2009 A late Holocene paleo-productivity record in the western Gulf of Maine, USA, inferred from growth histories of the long-lived ocean quahog (*Arctica islandica*). *International Journal of Earth Sciences* **98**, 19-29.

Wanamaker, A. D., Jr., Kreutz, K. J., Schoene, B. R., Pettigrew, N., Borns, H. W., Introne, D. S., Belknap, D., Maasch, K. A. & Feindel, S. 2008b Coupled North Atlantic slope water forcing on Gulf of Maine temperatures over the past millennium. *Climate Dynamics* **31**, 183-194.

Weidman, C. R., Jones, G. A. & Kyger. 1994 The long-lived mollusk *Arctica islandica* - a new paleoceanographic tool for the reconstruction of bottom temperatures for the continental shelves of the northern North-Atlantic ocean. *Journal of Geophysical Research-Oceans* **99**, 18305-18314.

Weiner, S. & Dove, P. 2003 An Overview on Biomineralization Processes and the Problem of the Vital Effect.

Wheeler, A. P. 1992 Mechanisms of molluscan shell formation. In *Calcification in biological systems.*, pp. 179-216.

Wilbur, K. M. 1983 Shell formation. In *The Mollusca. Volume 4. Physiology. Part 1.*, pp. 253-287.

Manuscript II
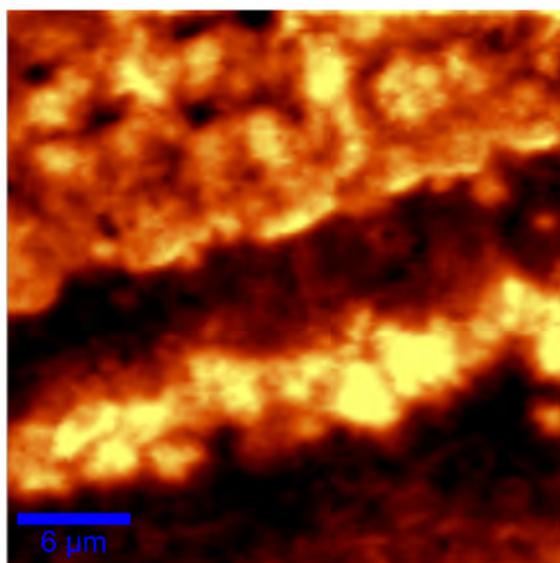
Raman high resolution-scan of polyenes from *Acrtica islandica* shell.

Polyenes in the shell of *Arctica islandica* and their relation to the provenance of the shell: a confocal Raman microscopy study

Kristina Stemmer[1] and Gernot Nehrke[2]

[1]Functional Ecology, [2]BioGeoScience, Alfred Wegener Institute Helmholtz Centre for Polar and Marine Research, Bremerhaven, Germany

Abstract

Many pigments, which are widely found in coloured parts of mollusc shells, are constituted by polyenes, i.e., molecules with a central polyenic chain. Due to a resonant coupling of these molecules at wavelengths typically used in Raman spectroscopy, this method is very well suited to investigate their occurrence in biogenic materials. Here we use confocal Raman microscopy to map the spatial distribution of polyenes within the shell of the bivalve *Arctica islandica*, and to determine their chemical characteristics (chain length). Polyene chain length does not differ between shells from different locations (off Iceland, Baltic Sea and North Sea). I.e., we cannot confirm the hypothesis that polyene chain length is related to external factors such as food source. We also show that the pigment polyenes are not only located at the outside of the shell, but also within the shell, adjacent to the typical shell growth banding pattern. This finding raises the question whether polyenes may play a role in the biomineralization process itself.

Introduction

Pigment polyenes are polyunsaturated organic compounds that are recently described to occur in several mollusc shells (Hedegaard et al. 2006). In general, pigments are substances that modify the colour of reflected or transmitted light by absorbing specific wavelengths and exist in many structures like the human retina, bird feathers, hair and calcium carbonate shells (Britton 2008). Pigment polyenes are identified from coloured parts of mollusc shells and were previously related to food source but mostly their origin and function are still unknown (Hedegaard et al. 2006; Karampelas et al. 2007; Merlin & Delé-Dubois 1986). In recent years mollusc shells gained much attention in biomineralization research, primarily due to their valuable fossil record and their vulnerability with respect to ocean acidification.

Polyenes contain conjugated linear carbon-carbon single and double bonds building a polyenic chain. Confocal Raman Microscopy (CRM) allows to determine the spectral position related to the vibrational modes of the C-C single and C=C double bonds (Hedegaard et al. 2006; Karampelas et al. 2007; Nehrke & Nouet 2011) and subsequently to estimate the number of C=C double bonds (Schaffer et al. 1991). The shell of the bivalve pectinid *Chlamys senatoria* appears in varying colours with each colour correlating to a different estimated amount of C=C double bonds of the polyenic chain (Hedegaard *et al.* 2006). In their study the authors discussed the relation of colour variations to different food sources available within varied habitats.

So far only a few studies exist on polyenes in calcareous mollusc shells. These studies mostly focused on the correlation between polyenes and the colour of the pigments (Barnard & de Waal 2006; Hedegaard et al. 2006) or analytical methods (Karampelas et al. 2007; Withnall et al. 2003).

We investigated shells of the burrowing bivalve *A. islandica*, one of the longest living animals on earth (Wanamaker et al. 2008), from four different locations, to measure i) whether polyenes are present and if yes ii) to evaluate their origin. We can then estimate the number of conjugated C=C double bonds of the polyenes within their shells by determining the spectral position of the vibrational modes related to the C-C single and C=C double bonds using Raman spectroscopy. In addition we characterize for the first time the spatial distribution of polyenes within cross-sections of a bivalve shell.

Material and Methods

Target specimen

To investigate pigment polyenes within the shell of *Arctica islandica* (Linnaeus, 1767) we used longitudinal cross-sections (polished) of shells from four different geographic locations (three per location) (Figure 1). Shell cross-sections from the Western Baltic Sea (Mecklenburg Bight), North Sea, and North Atlantic (NE Iceland) are obtained from the shell collection at the Alfred-Wegener-Institute in Bremerhaven (Germany), whereas shells from the Kiel Bight (Western Baltic Sea) are from a previously performed culture experiment (see below).

The shell of *A. islandica* is composed of aragonite as the only mineral phase and is divided in inner and outer shell layer (ISL and OSL) covered by a pale to a dark organic cuticle layer throughout ontogeny, the periostracum (Brey et al. 1990; Ridgway et al. 2010; Schoene et al. 2005a). The ISL is responsible for the thickening of the shell whereas the OSL provides additional growth in height forming calcium carbonate increments and organic rich growth lines (i.e. slowing of shell growth) that can be used for age determination (Figure 1) (Ropes 1984; Thompson et al. 1980; Witbaard et al. 1994). It has been proposed that both shell layers are proposed to form in separate compartments between the mantle tissue and the inner shell (Wheeler 1992). Shells vary in size and shape depending on the environment in which they were secreted as can be seen from the specimens shown in Figure 1. *A. islandica* from the Western Baltic Sea build thinner shells and are generally smaller compared to the shells from the North Sea and around Iceland. Maximum age varies between populations and range from ~40 yrs in the Western Baltic Sea over ~125 yrs in the North Sea up to over 350 yrs within the populations around Iceland (Basova et al. 2012; Begum et al. 2010; Schoene et al. 2005b) making *A. islandica* the longest lived animal on earth and a valuable study organism for several research disciplines (e.g. physiologists, geneticists, sclerochronologists)
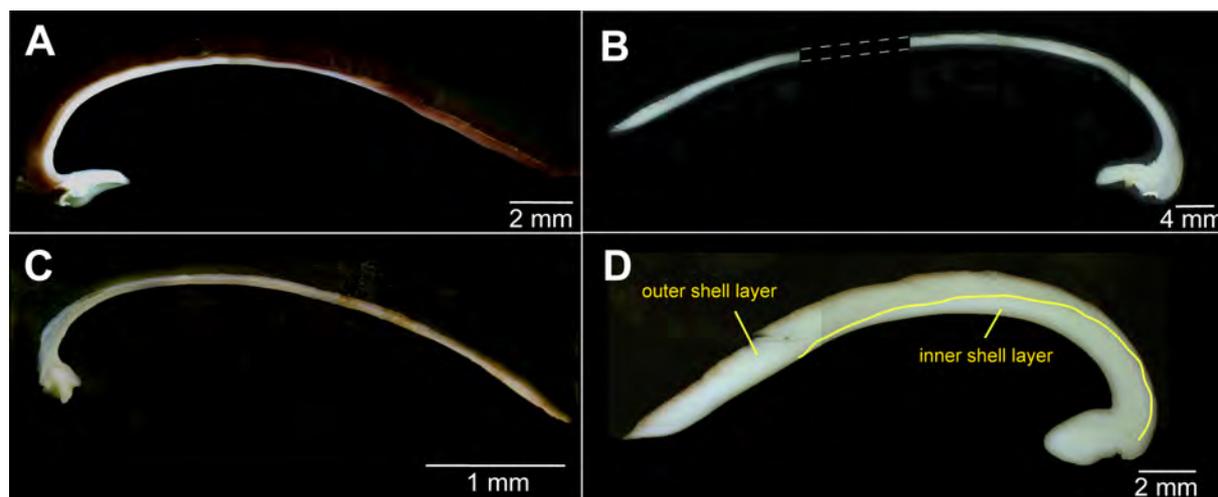
Figure 1. Shell-cross-sections of *Arctica islandica* from four different locations showing coloured areas in the outer shell layer and the distal part of the shell. A) Kiel Bight; B) North Sea; C) Mecklenburg Bight; D) North Atlantic (NE Iceland).

Confocal Raman microscopy

For the investigation of the pigments we used a WITec alpha 300 R (WITec GmbH, Germany) Confocal Raman Microscope (CRM). The spatial distribution of the polyenes was mapped via intensity distribution of the Raman peaks related to vibrational modes induced by the C-C single and C=C double bonds. The experimental settings are reported in Table 1 and a detailed description of the method is found in Nehrke and Nouet (2011). For all Raman measurements a 488 nm diode laser was used. Single Raman spectra for the exact determination of the peak position of polyene peaks was done by integrating 10 spectra each measured for 0.5 s.

Spectral analysis and image processing was conducted using the WITecProject software (version 2.04, WITec GmbH, Germany). Peak positions were determined using the "Multipeak Fitting 2" routine of IGOR Pro assuming a Gauss shape for the Raman peaks (version 6.11, WaveMetrics, Inc. USA) (Figure 2). Spectra were normalized to the peak position of the Rayleigh peak.

Table 1. Experimental parameters of Raman mapping in shell-cross-section from *A. islandica* from Kiel Bight shown in Figure 4B. Wavelength of the laser was 488 nm with 600 gratings per mm.

label	scan type	size (µm)	points per line	objective	integration time (s)
scan 1	large area scan	900 x 450	450 x 225	20x N.A. 0.4	0.05
scan 2	large area scan	700 x 400	350 x 200	20x N.A. 0.4	0.05
scan 3	high resolution scan	90 x 90	360 x 360	50x N.A. 0.8	0.01

Results and Discussion

Coloured shell areas

Shell cross-sections of *A. islandica* from all four locations show irregular colouring of brownish-pigmented areas (Figure 1). The outer shell layer (OSL) and shell material towards the outer shell margin (distal part) are most intensely coloured. The inner shell layer (ISL) is predominantly white. Qualitative differences in colour intensities between shell cross-sections from the four different locations can be observed. Within shells from the Kiel Bight (A) the outer shell layer shows a strong red-brown colour with a distinct colour-gradient from the latest formed shell at the outer shell margin and the outer outer shell layer (oOSL) decreasing in intensity towards the ISL and the older shell. Shells from Mecklenburg Bight (C) show a similar proportion of coloured to non-coloured areas. However, the colour is yellow-brown, less intense and patchier distributed than in shells from the Kiel Bight (A). Shells from the North Sea (B) and the North Atlantic (NE Iceland) (D) are mostly white with coloured areas only along the very outer shell.

During the ontogeny of *A. islandica* the colour of the organic periostracum changes from pale brown to dark brown (Murawski et al. 1982), probably caused by iron depositions or by the degradation of certain proteins and consequent changes of their molecular structure (Brey et al. 1990). The sample shells for this study were not yet outgrown and the colour of their periostracum was similar to the colour shown along the corresponding shell-cross-sections.

Polyene peak position

Using CRM we measured strong peaks belonging to the vibrational modes of polyenic chains. Peaks marked with R_1 and R_4 in Figure 2 resemble conjugated C-C single and C=C double bond vibrational modes of the major polyene peaks at ~1130 cm^{-1} and 1520 cm^{-1}, respectively. We calculated the expected number of C-C single (N_1) and C=C double bonds (N_4) after Schaffer *et al.* (1991) by:

$$N_1 = \frac{476}{R1 - 1082} \quad \text{and} \quad N_4 = \frac{830}{R4 - 1438}$$
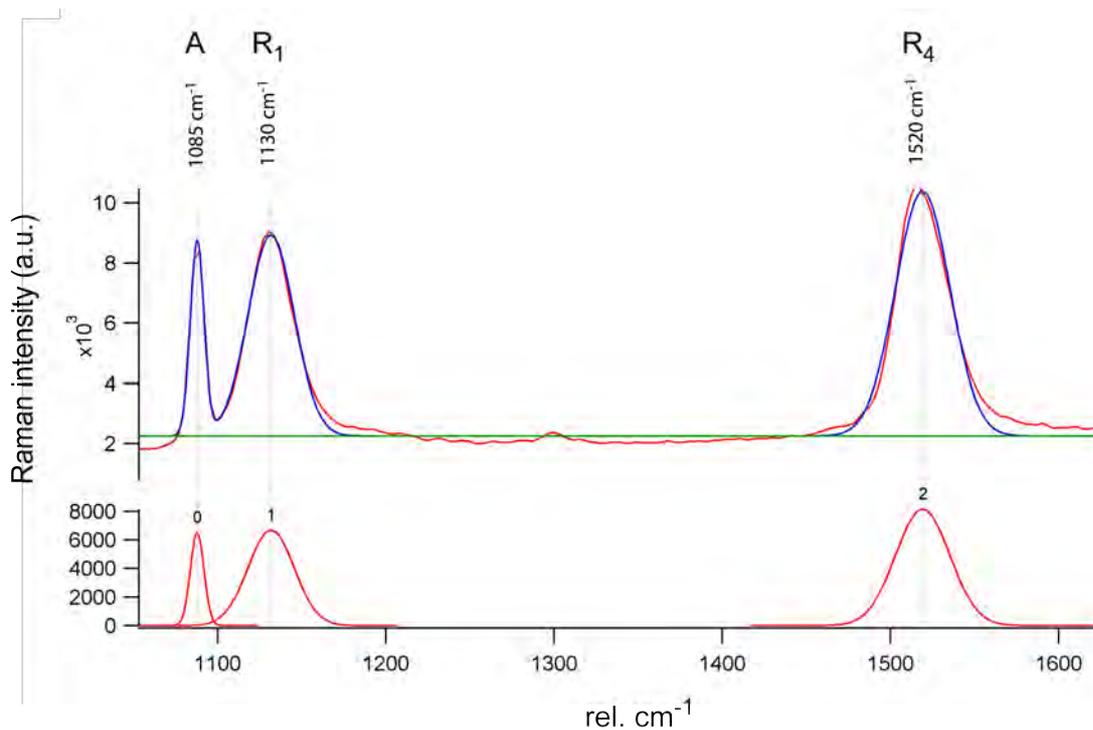
Figure 2. Exemplified Raman-spectra from *A. islandica* shell-cross-sections together with the peak fit assuming Gaussian peak shape as used to determine the exact peak position. The signal at 1085 cm^{-1} marked with A belongs to the aragonite spectra. R_1 and R_4 correspond to the major vibrational modes of polyenic chains (C-C carbon-carbon single bonds and C=C carbon-carbon double bond stretching vibrations, respectively).

The position of the Raman peak belonging to the C-C single and the C=C double bond of all investigated *A. islandica* shells is reproducible within ± 2cm^{-1} and results in the same estimated number of N=10 C=C double bonds. We see no qualitative differences in the measured Raman spectra and conclude that *A. islandica* always contains pigment polyenes with the same chain length indicating that these polyenes are species-specific. Supporting the hypothesis that pigments are habitat dependent is not supported for *A. islandica*. However, the questions of weather the pigment polyenes represent altered molecules partly related to the food source cannot be answered with this study and is matter for further investigations.

A comparison of our data to selected data from Hedegard et al. (2006) is given in Table 2 and Figure 3. Hedegaard and co-authors (2006) investigated five different coloured shells of the species *Chlamys senatoria* and found that the peak position of the polyenes showed a range of up to 10 cm^{-1}. *A. islandica* shells do not show such a variation in shell colours, i.e. the phenotype, which could be the reason for the much smaller range we measured for *A. islandica* in this study (2 cm^{-1}). However, the colours are distinctly different (Figure 1),

especially between the shells from Kiel Bight and Mecklenburg Bight (Figure A, C), and yet contain the same polyenic chain length.

Table 2. Investigated bivalve shells for pigment polyenes (n=3). Location, wavenumbers of the two major polyene peaks, the calculated number of conjugated C=C double bonds (N_1/N_4) (after Schaffer et al. 1991).

species	colour	location	R (cm^{-1})	R$_4$ (cm$_{-1}$)	N$_1$	N$_4$
Arctica islandia	red browm	Kiel Bight	1131 ± 0.7	1519 ± 0.3	9.8 ± 0.1	10.3 ± 0
A. islandia	pale brown	Mecklenburg Bight	1133 ± 0.6	1521 ± 1.4	9.3 ± 0.1	10.0 ± 0.2
A. islandia	pale brown	North Sea	1131 ± 0.7	1518 ± 1.2	9.8 ± 0.1	10.4 ± 0.2
A. islandia	pale brown	NE Iceland	1130 ± 0.7	1519 ± 2.0	9.8 ± 0.2	10.3 ± 0.3
Chlamys senatoria	orange	Hedegaard *et al.* (2006)	1135	1526	9.0	9.4
C. senatoria	yellow	Hedegaard *et al.* (2006)	1125	1509	11.1	11.7
C. senatoria	red	Hedegaard *et al.* (2006)	1130	1517	9.9	10.5
C. senatoria	purple	Hedegaard *et al.* (2006)	1128	1511	10.3	11.4
C. senatoria	brownish	Hedegaard *et al.* (2006)	1130	1516	9.9	10.6
Mytilus edulis	blue	Hedegaard *et al.* (2006)	1098	1484	29.8	18.0

Due to the nature of the resonance Raman signal even small amounts of polyenes within the sample (down to 10^{-8} M, (Merlin & Delé-Dubois 1986)) can induce detectable peaks. In a confocal system like the Raman microscope the intensity of the signal strongly depends on the roughness and tilt of the scanned sample surface. This sensitivity to surface features and the fact that a) every polished cross section of a given sample represents "one of a kind" and b) the exact distance between objective and sample is never 100 % reproducible between scans renders a quantification of the amount of pigments based on the measured intensity impossible. Nonetheless quantitatively the intensity of the measured Raman signal can be attributed to the presence of polyenes and corresponds with the observed colour distribution. In the following section we describe the relative spatial distribution of pigment polyenes within the polished shell-cross-section of *A. islandica* from the Kiel Bight.
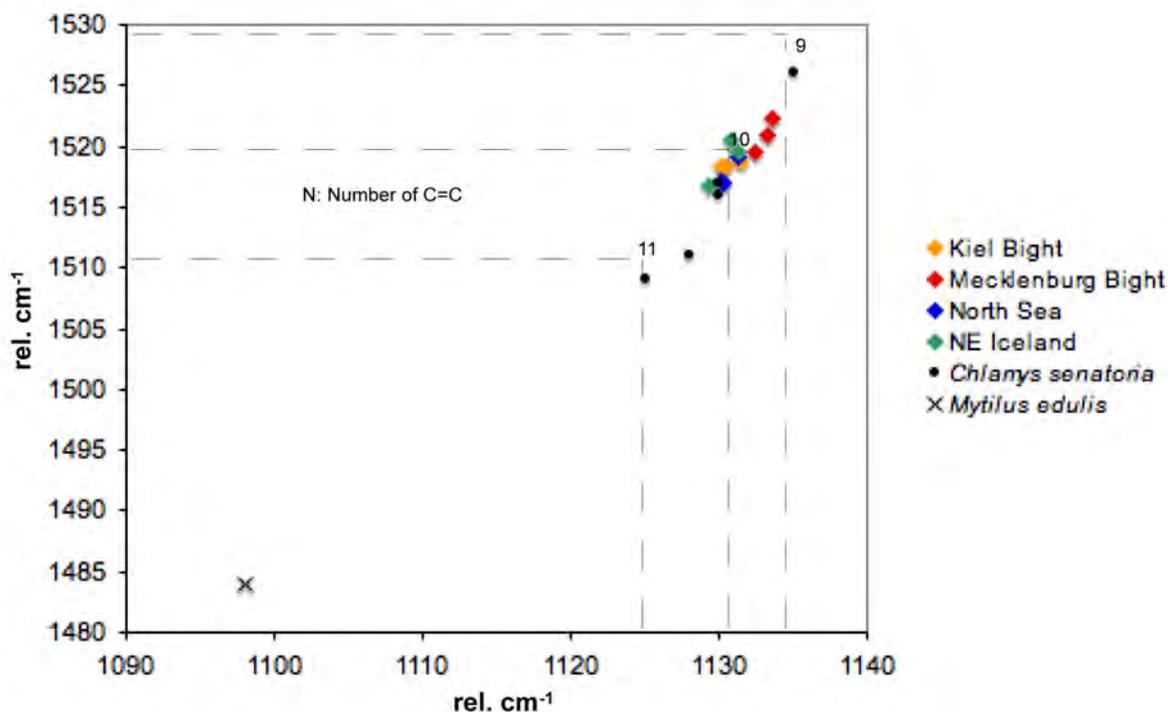
Figure 3. Plot of the relative wavenumbers after Hedegaard et al. (2006) for pigment polyenes measured in the shell of *A. islandica* from different locations together with data published in Hedegaard et al. (2006). The numbers within the plots represent the calculated number of C=C double bonds as given in Table 2 (the number of the double bonds of *Mytilus edulis* falls outside the plotted range).

Spatial distribution of pigment polyenes

The shells of *A. islandica* used to analyse the spatial distribution of polyenes had been collected and cultured within a project related to ocean acidification. The latter study showed that the micro-structural features did not differ between natural and cultured shells (Stemmer *et al.* in review). The animals were originally collected from Kiel Bight and cultured over three months under ambient conditions (Stemmer et al. 2013). Polyenes present in the shell cross-sections produced well detectable Raman signals well within detectable ranges. To visualize the polyene distribution we plotted the intensity distribution of the major peak at 1530 cm^{-1} (Figure 4). Details on that method can be found in Nehrke and Nouet (2011). Raman scans performed across shell cross-sections showed that polyenes are inhomogeneously distributed. The signal was strong along the oOSL and the outer shell margin. However, polyene pigments could not be detected in the inner shell layer, which

leads to the assumption, that only the outer extrapallial fluid (Wheeler 1992), distal to the pallial line, secretes polyenes together with the outer shell layer.

Polyenes are incorporated along growth lines (Figure 4C) that form during slowing of growth in the OSL and contain a high amount of organic material (Lutz & Rhoads 1977; Schoene et al. 2004), especially in coloured shell areas as shown in Figure 4A.
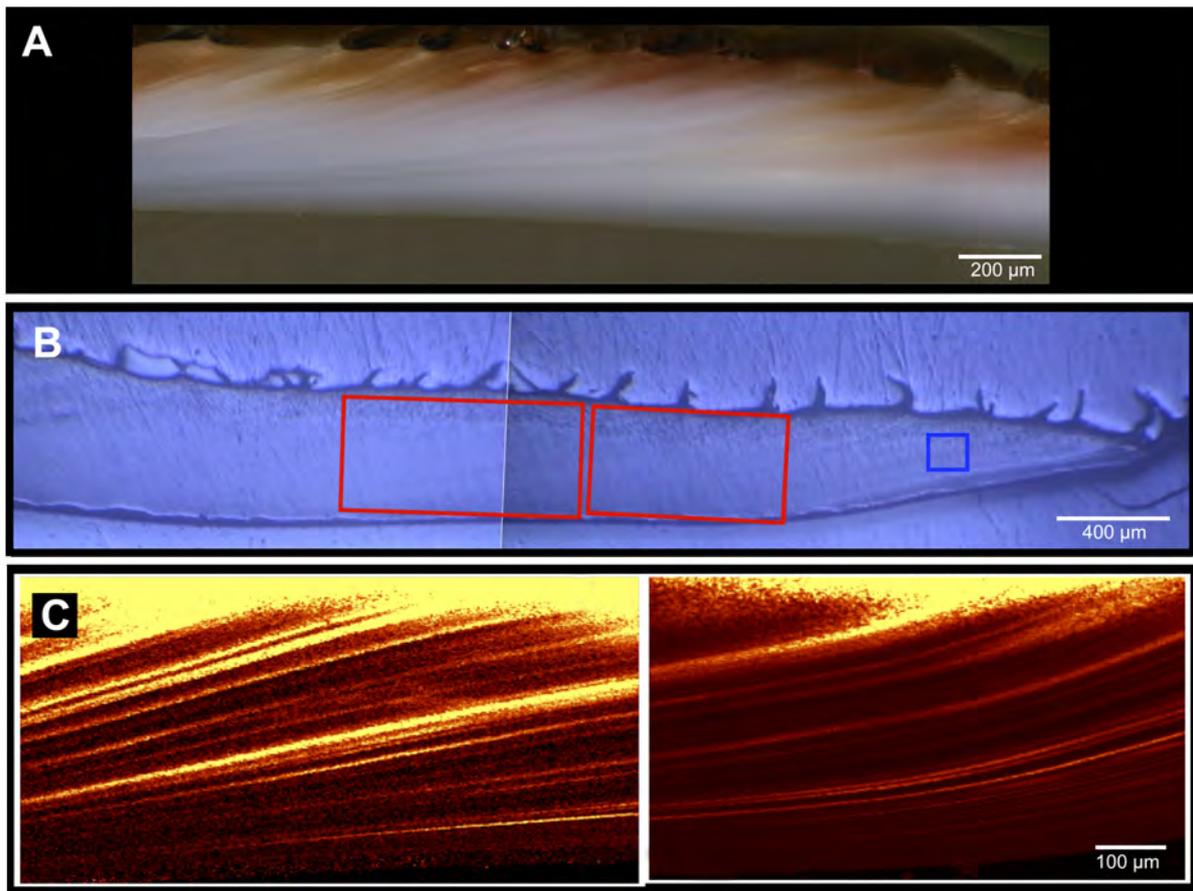
Figure 4. Distribution of pigment polyenes in a shell-cross-section of *Arctica islandica* from the Kiel Bight. A) Colour gradient from the outer to the inner shell layer; B) Distal part of shell-cross-section indicating areas scanned by CRM (red square: scan 1 and 2 shown in Figure C. Blue square: scan 3 shown in Figure 5); C) polyene distribution showing the same banding pattern well known as the growth banding in many bivalve shells.

The intensity distribution of the polyenes is shown in Figure 4C. Within these maps the polyenes show a banding pattern congruent with the characteristic growth lines described for *A. islandica* (Thompson et al. 1980). In addition an enhanced abundance of polyenes along the very outer shell layer adjacent to the organic periostracum becomes visible. The presence of polyenes in this extreme outer shell has been previously documented (Barnard & de Waal 2006; Hedegaard et al. 2006), however, the banding pattern within shell cross-sections is described for the first time in this study.

Annual growth lines of bivalve shells are often used to determine the age of the bivalve when the date of death is known (Jones 1980; Schoene et al. 2005a). The shell increments (shell material between growth lines) can be further investigated for biochemical signatures and are a valuable tool for environmental reconstruction (Schoene et al. 2005a). Since the investigated shell material is obtained from culture experiments in which the growth increments can be determined by means of labelling the beginning of the experiment (Stemmer *et al.* under review) it is revealed that this bandings pattern exhibit intra annual resolution (~10 bands are formed during the three month lasting culturing period) (Figure 4C). The potential of this information to sclerochronological and paleoclimatic research has to be further investigated.

High resolution (~300 nm) Raman scans of growth lines (Figure 5) were used to investigate how the polyenes are incorporated into the shell material. Figure 5A shows a Raman map based on the intensity distribution of the aragonite peak at ~1085 cm^{-1}. This map nicely illustrates the occurrence of aragonitic granules, which is typical for many biogenic carbonates (Cuif et al. 2011; Cuif et al. 2012). From the same area the intensity distribution of the polyene related peak at ~1530 cm^{-1} is plotted in (Figure 5B). This map shows two growth bands related to polyene bands (Figure 4C). An overlay of both maps (Figure 5C) indicates that the polyenes are incorporated within the aragonite granules, and do not surround them. For many biogenic carbonates it is described that organic molecules surround the aragonitic (or calcitic) granules like an envelope (Cuif et al. 2012). We cannot determine from the Raman scan if an organic envelope around the aragonitic granules is apparent, since most of the organic molecules expected within the organic matrix do not exhibit a resonance Raman signal, the prerequisite to detect the very low concentrations in which they are expected to be present. However, two major questions arise from the spatial distribution of polyenes determined in this study.

a) What is the reason for the inhomogeneous distribution of polyenes being present in the outer part of the shell, and disappearing in the older parts of the shell? b) Does association of polyene occurrence with growth bands in shells of *A. islandica* indicate an important role of the polyenes in the biomineralization process itself?
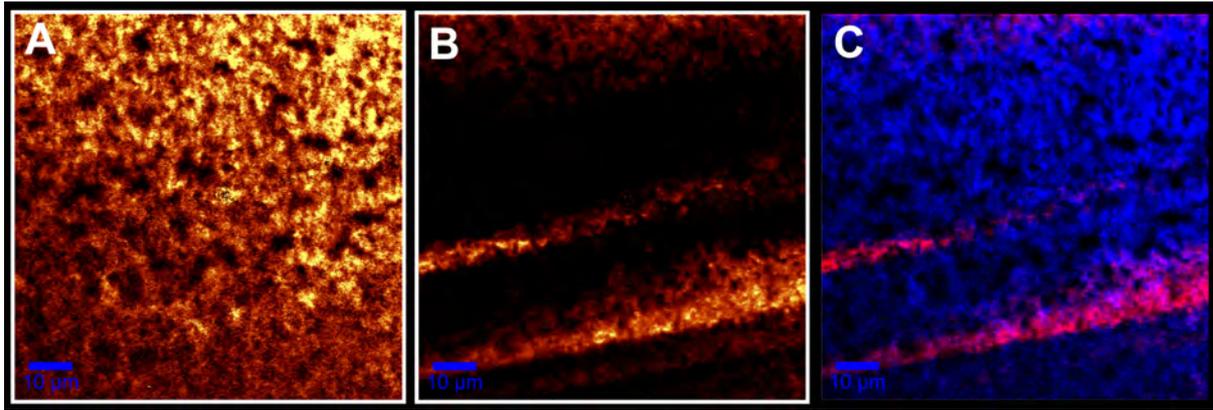
Figure 5. High resolution (~ 300 nm) Raman scan of shell area indicated as blue square in Figure 4B. A) Aragonite distribution; B) Polyene distribution showing two lines of the growth pattern shown in Figure 4C; C) Overlay of A) and B) showing polyenes integrated into the aragonitic granules.

Conclusions

This study demonstrated for the first time the presence of pigment polyenes in the shell of *A. islandica*:

1) These pigment polyenes have 10 C=C conjugated double bonds. This is in the range published for other species. Comparison of shell material from different regions does not show habitat specific differences in the calculated number of conjugated double bonds. This renders the origin of pigment polyenes from food sources unlikely, albeit a detailed examination of the food source was outside of the scope of this study.

2) We detected polyenes in the outer shell layer only. This can be explained by the general assumption that the inner and the outer shell layers are formed from two different compartments.

3) Congruent to the colour gradient within the shell cross-section we see a gradient of the polyene pigments. Polyene concentrations decrease from young to old and from outer to inner parts of the shell. This pattern remains an enigma so far. It can only be hypothesized that the molecules have been altered with time in such a way that they no longer contain polyenic chains that can induce a resonance Raman signal.

4) Polyenes are closely related to the growth-banding pattern and may play an important role in the biomineralization process, which leads to the formation of the shell.

5) Polyenes are most likely incorporated within the aragonitic granules.

Acknowledgements

References

Barnard, W. & de Waal, D. 2006 Raman investigation of pigmentary molecules in the molluscan biogenic matrix. *Journal of Raman Spectroscopy* **37**, 342-352.

Basova, L., Begum, S., Strahl, J., Sukhotin, A., Brey, T., Philipp, E. & Abele, D. 2012 Age-dependent patterns of antioxidants in *Arctica islandica* from six regionally separate populations with different lifespans. *Aquatic Biology* **14**, 141-152.

Begum, S., Basova, L., Heilmayer, O., Philipp, E. E. R., Abele, D. & Brey, T. 2010 Growth and energy budget models of the bivalve *Arctica islandica* at six different sites in the Northeast Atlantic realm *Journal of Shellfish Research* **29**, 107-115.

Brey, T., Arntz, W. E., Pauly, D. & Rumohr, H. 1990 *Arctica - (Cyprina) - islandica* in Kiel Bay (Western Baltic) - growth, production and ecological significance *Journal of Experimental Marine Biology and Ecology* **136**, 217-235.

Britton, G. 2008 Functions of Intact Carotenoids. In *Carotenoids*, vol. 4, pp. 189-212.

Cuif, J. P., Dauphin Y & Sorauf JE. 2011 *Biominerals and fossils through time*: Cambridge University Press.

Cuif, J. P., Dauphin, Y., Nehrke, G., Nouet, J. & Perez-Huerta, A. 2012 Layered growth and crystallization in calcareous biominerals: Impact of structural and chemical evidence on two major concepts in invertebrate biomineralization studies. *Minerals* **2**, 11-39.

Hedegaard, C., Bardeau, J. F. & Chateigner, D. 2006 Molluscan shell pigments: An in situ resonance Raman study. *Journal of Molluscan Studies* **72**, 157-162.

Jones, D. S. 1980 Annual cycle of shell growth increment formation in 2 continental-shelf bivalves and its paleoecologic significance *Paleobiology* **6**, 331-340.

Karampelas, S., Fritsch, E., Mevellec, J. Y., Gauthier, J. P., Sklavounos, S. & Soldatos, T. 2007 Determination by Raman scattering of the nature of pigments in cultured freshwater pearls from the mollusk *Hyriopsis cumingi*. *Journal of Raman Spectroscopy* **38**, 217-230.

Lutz, R. A. & Rhoads, D. C. 1977 Anaerobiosis and a theory of growth line formation *Science* **198**, 1222-1227.

Merlin, J. C. & Delé-Dubois, M. L. 1986 Resonance Raman Characterization of Polyacetylenic pigments in the calcareous skeleton. *Comparative Biochemistry and Physiology B-Biochemistry & Molecular Biology* **84**, 97-103.

Murawski, S. A., Ropes, J. W. & Serchuk, F. M. 1982 Growth of the ocean quahog, *Arctica islandica*, in the middle Atlantic Bight *Fishery Bulletin* **80**, 21-34.

Nehrke, G. & Nouet, J. 2011 Confocal Raman microscope mapping as a tool to describe different mineral and organic phases at high spatial resolution within marine biogenic carbonates: case study on *Nerita undata* (Gastropoda, Neritopsina). *Biogeosciences* **8**, 3761-3769.

Ridgway, I. D., Richardson, C. A. & Austad, S. N. 2010 Maximum Shell Size, Growth Rate, and Maturation Age Correlate With Longevity in Bivalve Molluscs. *Journals of Gerontology Series a-Biological Sciences and Medical Sciences* **66**, 183-190.

Ropes, J. W. 1984 Methods for aging oceanic bivalves. *Underwater Naturalist* **15**, 12-15.

Schaffer, H. E., Chance, R. R., Silbey, R. J., Knoll, K. & Schrock, R. R. 1991 Conjugation length dependence of Raman-Scattering in a series of linear polyenes - implications for polyacetylene *Journal of Chemical Physics* **94**, 4161-4170.

Schoene, B. R., Castro, A. D. F., Fiebig, J., Houk, S. D., Oschmann, W. & Kroncke, I. 2004 Sea surface water temperatures over the period 1884-1983 reconstructed from oxygen isotope ratios of a bivalve mollusk shell (*Arctica islandica*, southern North Sea). *Palaeogeography Palaeoclimatology Palaeoecology* **212**, 215-232.

Schoene, B. R., Fiebig, J., Pfeiffer, M., Gless, R., Hickson, J., Johnson, A. L. A., Dreyer, W. & Oschmann, W. 2005a Climate records from a bivalved Methuselah (*Arctica islandica*, Mollusca; Iceland). *Palaeogeography Palaeoclimatology Palaeoecology* **228**, 130-148.

Schoene, B. R., Hickson, J. & Oschmann, W. 2005b Reconstruction of subseasonal environmental conditions using bivalve mollusk shells-A graphical model. In *Isotopic and Elemental Tracers of Cenozoic Climate Change*, vol. 395, pp. 21-31.

Stemmer, K., Nehrke, G. & Brey, T. 2013 Elevated CO2 levels do not affect shell structure of the bivalve *Arctica islandica* from the Western Baltic. *Plos One*

Thompson, I., Jones, D. S. & Dreibelbis, D. 1980 Annual internal growth banding and and life-history of the ocean quahog *Arctica islandica* (Mollusca, Bivalvia) *Marine Biology* **57**, 25-34.

Wanamaker, A. D., Jr., Heinemeier, J., Scourse, J. D., Richardson, C. A., Butler, P. G., Eiriksson, J. & Knudsen, K. L. 2008 Very long-lived mollusks confirm 17th century ad tephra-based radiocarbon reservoir ages for North Icelandic shelf waters *Radiocarbon* **50**, 399-412.

Wheeler, A. P. 1992 Mechanisms of molluscan shell formation. In *Calcification in biological systems.*, pp. 179-216.

Witbaard, R., Jenness, M. I., Vanderborg, K. & Ganssen, G. 1994 Verification of annual growth increments in *Arctica islandica* from the North Sea by means of oxygen and carbon isotopes *Netherlands Journal of Sea Research* **33**, 91-101.

Withnall, R., Chowdhry, B. Z., Silver, J., Edwards, H. G. M. & de Oliveira, L. F. C. 2003 Raman spectra of carotenoids in natural products. *Spectrochimica Acta Part a-Molecular and Biomolecular Spectroscopy* **59**, 2207-2212.

Manuscript III
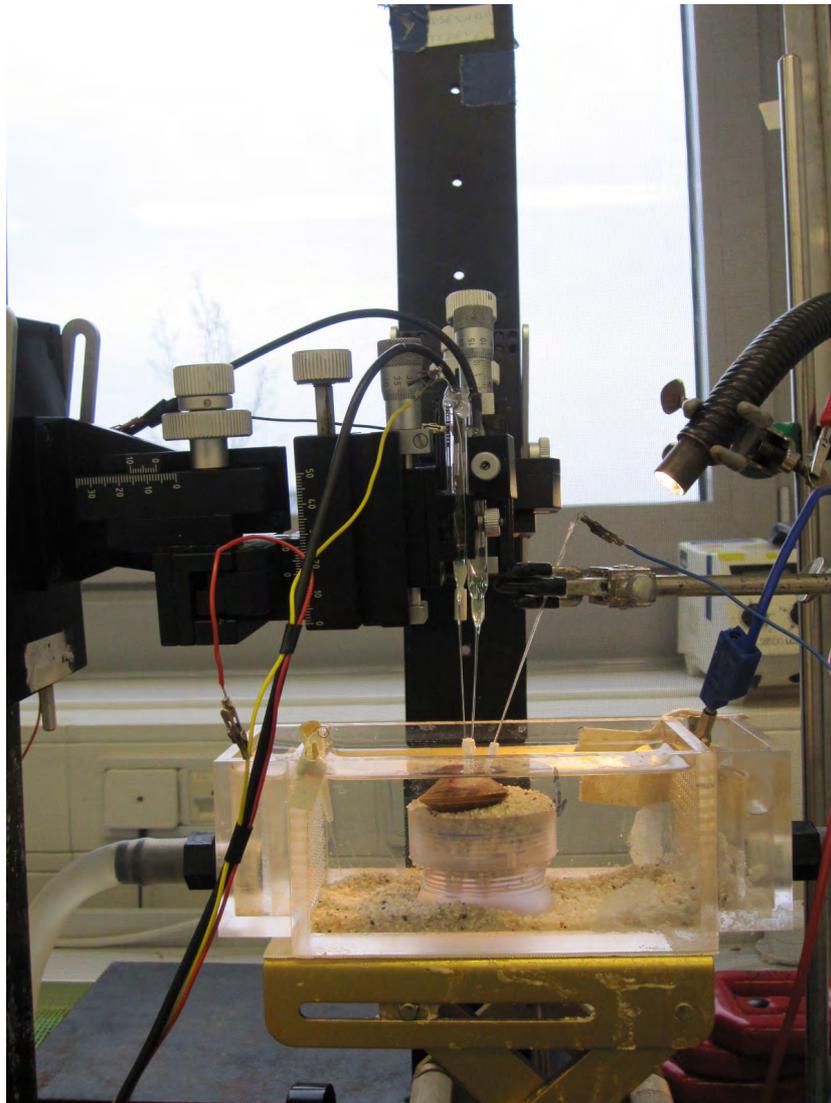
Microsensor set up showing the flow-through chamber with *Arctica islandica* and the applied microsensors fixed on a micromanipulator.

In situ measurements of pH, Ca^{2+} and DIC dynamics within the extrapallial fluid of the ocean quahog *Arctica islandica*

Kristina Stemmer[*1,2], Thomas Brey[1], Martin Glas[2], Martin Beutler[2], Burgel Schalkhausser[1], Dirk de Beer[2]

[1]*Alfred Wegener Institute Helmholtz Centre for Polar and Marine Research, Bremerhaven, Germany*
[2] *Max Planck Institute for Marine Microbiology, Bremen, Germany*

Abstract

We studied in the bivalve *Arctica islandica* to what extent the extrapallial fluid (EPF) is involved in shell formation. *In situ* pH microscopy identified pH gradients between inner shell surface and outer mantle epithelium (OME). pH at the OME varied rapidly between neutral and values above 9, suggesting active proton pumping. With microsensors we also measured remarkable short-term dynamics in pH and Ca^{2+} concentrations, again suggesting active pumping. We further focussed on pH, calcium and dissolved inorganic carbon (DIC) dynamics within the EPF to determine whether calcium carbonate precipitation is possible within the EPF. Our data show that the bulk of the inner EPF rarely reaches calcium carbonate saturation, thus cannot be the site of shell formation. However, at OME surface we observed pH levels up to 9.5, corresponding to a 15-20 fold carbonate supersaturation. Thus ion pumping by the OME can drive calcification when the OME is just a few μm distant from the inner shell surface, as it is the case in the outer EPF.

Introduction

Biomineralization is a regulated process within living organisms where calcium carbonate precipitates on an organic matrix (Crenshaw 1972b; Falini et al. 1996; Lowenstam 1981; Nudelman et al. 2006). Shell-formation in bivalves (referred to as calcification throughout the following text) happens extracellular with a strong biological control (Crenshaw 1980; Weiner & Dove 2003; Weiner & Traub 1980). The shell is thought to form from an extracellular fluid, the extrapallial fluid (EPF) that is located between the inner shell surface and outer mantle epithelium (OME) (Wada & Fujinuki 1976; Wilbur 1983). The OME is a thin barrier between the hemolymph and the EPF and is the secreting organ for the shell constitutions and hence is suggested to control the concentrations of inorganic ions (i.e. calcium, protons, bicarbonate) and organic components (i.e. proteins, glycoproteins and polysaccharides) entering the EPF or the actual site of calcification (Crenshaw 1972a; Falini et al. 1996; Hattan et al. 2001). Where this site is located and how $CaCO_3$ is exactly precipitated is matter of ongoing research (Addadi et al. 2006; Levi-Kalisman et al. 2001; Nudelman et al. 2007; Weiss 2010).

The EPF is in direct contact with the shell and mostly divided in an inner and outer section, forming the inner shell surface, and the increments of the outer shell layer, respectively (Wilbur 1983). The two compartments are divided by the pallial line where the OME is attached via numerous retractor muscles to the inner shell surface (Wheeler 1992; Wilbur 1983). Sampling of the fluid is difficult due to the small volumes and analyses are mostly reduced to the inner EPF (Crenshaw 1972a; Ip et al. 2006; Wada & Fujinuki 1976).

Previous investigations of the EPF form a controversial picture of its organic and inorganic composition and ion-transportation mechanisms. Regarding calcium-ion concentration that has to be necessarily increased for $CaCO_3$ precipitation, only a little fraction of Ca^{2+} was found freely dissolved within the EPF of the blue mussel *Mytilus edulis* (Misogianes & Chasteen 1979). Some organic molecules have been identified to reversely bind to calcium, probably presenting a building block of the soluble organic shell matrix (Hattan et al. 2001). Coimbra et al. (1988) reported calcium concentrations within the EPF quite similar to seawater but with higher carbonate-ion concentrations. The OME is highly permeable to calcium and different pathways for Ca^{2+}-transport through the mantle tissue have been previously discussed (Carre et al. 2006; Gillikin et al. 2005; Klein et al. 1996; Wheeler 1992).

Melzner et al. (2009) measured high pCO$_2$ values in extracellular fluids (hemolymph, EPF) that form a diffusion barrier for metabolic CO$_2$ excretion. Consequently the pH values of the EPF are below that of ambient seawater for most of the time and the fluid is undersaturated with respect to CaCO$_3$ (Crenshaw & Neff 1969; Heinemann et al. ; Melzner et al. 2009; Thomsen et al. 2010). Some bivalves can even calcify at high rates under acidified conditions of the surrounding seawater with a saturation state of CaCO$_3$ < 0.5 (Stemmer et al. 2013; Thomsen et al. 2010; Thomsen & Melzner 2010). The microenvironment in which calcification occurs has to be highly supersaturated with respect to shell minerals and therefore might not occur in the EPF.

The EPF is an enclosed compartment, thus its chemistry can be well controlled, e.g. by ion-transport. It functions as a reservoir for all compounds necessary for calcification (e.g. Crenshaw 1972a; Hattan et al. 2001; Misogianes & Chasteen 1979). Several studies were dedicated to the EPF but the concept of ion-transportation mechanisms driving calcification is still controversial and the precise function of the EPF has yet stayed unresolved (Carre et al. 2006; Crenshaw 1972a; McConnaughey & Gillikin 2008; Thomsen et al. 2010).

In the current study we wanted to clarify the role of the EPF in the calcification process within young specimen of the ocean quahog *A. islandica* by directly measuring ion-dynamics with high temporal resolution. We performed optical pH measurements within the inner EPF and used pH and Ca^{2+} microsensors to measure short- and long-term dynamics. We also measured the DIC over time to evaluate the internal carbonate system of the EPF. We contribute data for a further understanding of the function of the EPF and present new approaches for *in situ* measurements.

Material and Methods

Clam maintenance and preparation

All measurements were conducted on the North Atlantic bivalve *Arctica islandica*. Young bivalves were recovered from the Kiel Bight area in the Western Baltic Sea and maintained in aquaria at 14 °C with a salinity of 25. Seawater was exchanged every 2 days. As a food source, live marine plankton (DT's Premium Blend, DT's Plankton Farm, Sycamore, USA) was added ever two days.

For microsensor measurements we drilled three holes in the bivalve shell using a hand held drill (Dremel, "MultiPro" 395, Germany), similar to a dentist drill. The first layers of the outer shell were removed carefully with a polishing tool in the area before or behind the pallial line and between the adductor muscles depending on the compartment of interest. Preventing heating of the shell and accumulation of $CaCO_3$-powder the shell was flushed constantly with a water stream. When the shell at the aimed area was thin enough, a small drilling head was used. Carefully three holes of 2 mm in diameter were drilled into the bivalve shell: Two entrances for the microsensors (Ca^{2+} and pH) and one entrance for the reference.

As an extension of the holes, pipette tips were cut to at least 5 mm of length and glued onto the holes using two-component glue. Preventing gas exchange, parafilm was applied to seal the pipette tips (further referred to as catheter). Clams were put back into the aquaria overnight for acclimation. The catheters were above the seawater level all the time. For microscopic pH measurements a PVC measuring window (with an area of ~ 1 cm^2) was attached onto a similarly drilled opening of the shell (Figure 1). The pH indicator was injected into the EPF through a small hole in the window that was then sealed with parafilm.

After these operations the bivalves were checked for tissue damages after measurement. Data retrieved on specimens with damaged mantle tissue where excluded for further analyses on the EPF. All bivalves were actively filtrating shortly after preparation.
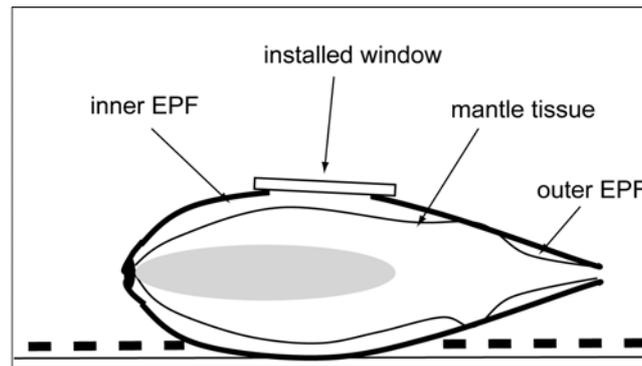
Figure 1: Sketch of prepared clam for microscopic pH measurements. The installed window allows to view into the inner EPF and onto the outer mantle epithelium (OME) of the mantle tissue. The connection of the mantle tissue with the shell (on the pallial line) separates the inner and the outer EPF. The animal was embedded in a thin sand layer (dashed line) for stability.

Microscopic pH analysis

The microscopic pH indicator, a pH sensitive non-membrane permeable dye, BCECF-dextran (Invitrogen), was dissolved just before the measurement (2 g/l) and 50 µl was injected in the EPF. The excitation intensity ratio of BCECF at 458 nm and 488 nm (emission: 505 nm – 550 nm) changes with changing pH enabling measurements independent from the dye concentration. Fluorescence measurements were done with an upright confocal microscope (LSM 510, Zeiss, Germany) using an argon laser (458 nm and 488 nm, blue light) for excitation of the indicator dye. Fluorescence emission was measured between 505 nm and 550 nm.

By integrating the measured intensities of each image of a stack a pH depth profile between the installed window (referred to as "shell" in the following) and the OME of the animal has been calculated. Calibration was performed using BCECF in seawater with pH 8.85 and pH 5.75 after the Invitrogen Manual. Optical sections of extracellular pH of the clam were taken in 50 µm steps every 5.6 seconds. Parameters of the measurement-series are listed in Table 1. The window was clearly visible when in focus, due to autofluorescence, and defined as the zero depth. The end point (meaning the OME was reached) was defined when fluorescence signals decreased down to the dimension of the signal offset, as the dye molecules cannot penetrate membranes and tissues.

During measurements the bivalves were placed in a petri dish submerged in seawater. Only the installed window was positioned above the surface. By adding cooled water several times during the measurements, the seawater temperature was kept around 14°C with a salinity of 25. During all measurements the bivalves were open and filtrating.

Table 1: Parameters used for microscopic pH measurements within the inner EPF of two specimens of *A. islandica*. The stack size comprises the amount of measurement points. Several stacks have been measured consecutively = # stacks.

specimen	stack size	# stacks	steps [μm]	total distance [μm]	time per measurement [s]	time between each stack [s]	total time [min]
#1	32	13	50	1600	5.6	600	358.83
#2	24	28	50	1200	5.6	300	197.72

Microsensor set up and measurements

Liquid membrane type pH and Ca^{2+} microsensors (LIX) were build and calibrated as described in de Beer et al. (1997, 2000). Microsensors had a tip diameter of approximately 10 μm and were installed on a micromanipulator fixed on a heavy stand to enable careful positioning within the installed tubes on the clam to reach the EPF. The clam was submerged and the installed catheters were reaching out of the water covered by parafilm. A polycarbonate flow-chamber ensured the circulation with aerated seawater at constant temperature of 14°C and a salinity of 25. The experimental set-up can be seen in Figure 2.

All electrodes were guided carefully through the punctured parafilm of each catheter. The reference electrode was first fixed within one catheter with the tip of the reference reaching shortly behind the shell into the EPF. The fluid reached about 1-2 mm into the catheters so that contact of the sensors with the fluid was ensured. Positioning of the microsensors was performed manually with help of a stereoscope. Signals were recorded every 3-10 seconds and plotted on a connected computer (strip-chart recorder).

pH and calcium values were taken before and after the measurements from the experimental seawater and used as baselines for calculations of the ΔpH and ΔCa^{2+} in the EPF of *A. islandica*. Measurements shown in this study were conducted under ambient light conditions.
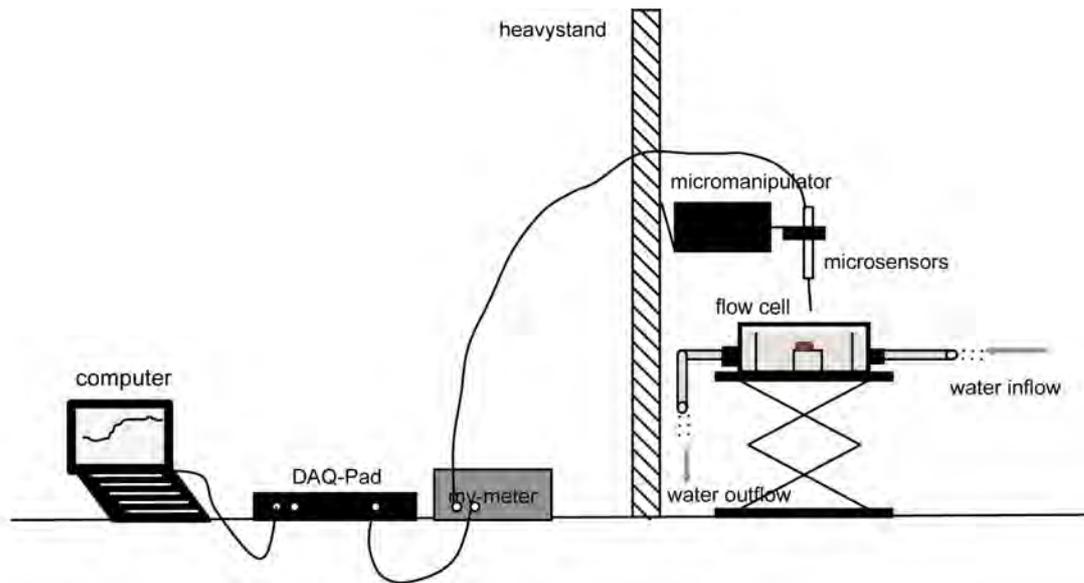
Figure 2: Microsensor set up.

DIC measurements

EPF samples were taken during microsensor measurements using a glass syringe. From the fluid that filled the installed catheters a volume of at least 80 µl was drawn carefully to avoid gas entry and immediately transferred to a DIC analyser. Standard preparation and DIC analysis via small volume flow-injection were performed after Hall & Aller (1992). This procedure was repeated as long as fluid from the EPF was accessible.

Results

Optical pH measurements

Using BCECF-dextran as a pH indicator it was possible to measure a pH gradient over depth within the inner EPF of *A. islandica* between the shell and the OME of the animal. All pH depth profiles of specimen #1 and the first 17 depth profiles of specimen #2 show a decrease in pH towards the OME. These measurements show that the pH at the OME surface is very low over a long period of time, probably due to respiration. These profiles were averaged and are displayed in Figure 3.

On several occasions we observed the pH at the OME to increase strongly (Figure 4). This can only be due to proton pumping processes. The last 11 pH depth profiles of specimen #2

show an inversion of a decreasing to an increasing pH gradient towards the OME (Figure 4). The gradual inversion of the pH in depth (Figure 4) indicates uptake of protons that leads to an increase in pH from 7.3 up to 9.5 at the OME surface in less than 20 minutes. The pH at the shell did not follow the OME pH dynamics, but was rather constant.
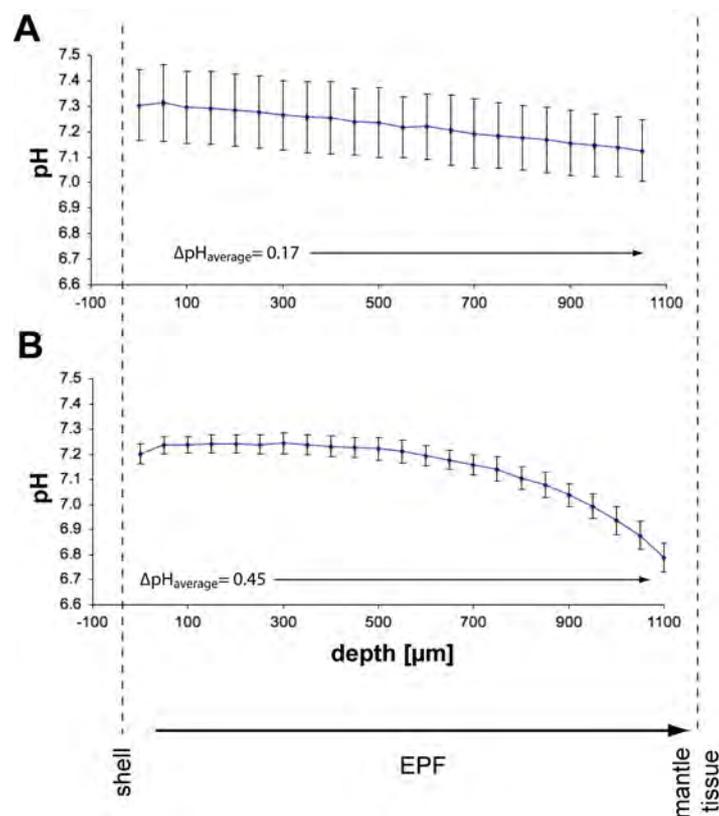

Figure 3: Averages of microscopically imaged pH profiles showing a decrease from the shell to the outer mantle epithelium (OME) of the extrapallial fluid (EPF) in two individuals of *A. islandica*. A) n = 13. B) n = 17 profiles. Arrow indicates the measuring direction.
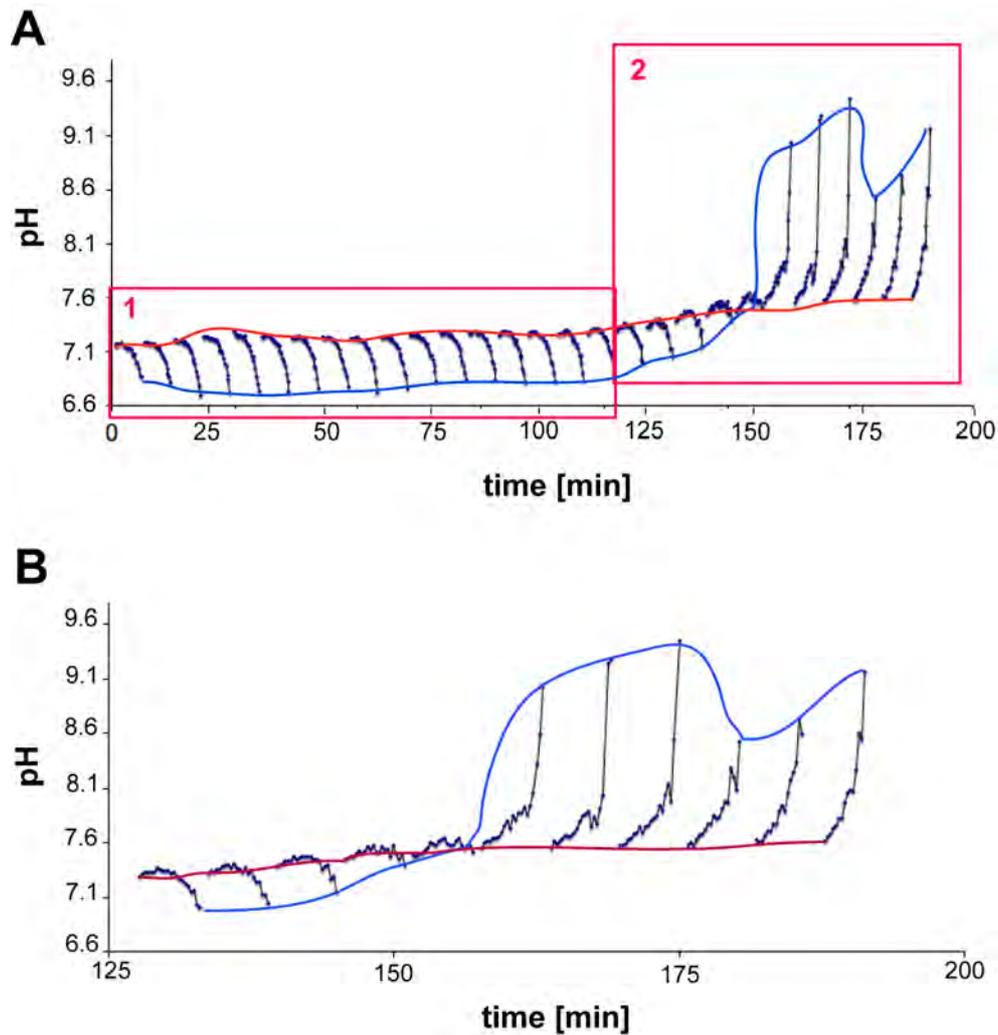
Figure 4: Time series of microscopic pH depth profiles through the extrapallial fluid (EPF) of *A. islandica* specimen #2. A) 28 pH depth profiles over time. Box 1 shows the 17 profiles averaged in Figure 3C. Profiles within box 2 are magnified in B). B) Inversion of decreasing to increasing pH gradient. The red line follows the pH close to the shell; the blue line shows the pH increase around the outer mantle epithelium (OME) of up to 9.5.

Simultaneous pH, Ca^{2+} and DIC dynamics

Using LIX-microsensors, pH and calcium concentrations were measured *in situ* and simultaneously within the inner EPF of *A. islandica* while the valves of the calm were open. The short-term dynamics show that when pH moves up calcium concentration also goes up and vice versa for most of the time (Figure 5). Occasionally, the synchronous dynamics change and move in opposite directions. Measurements were performed every 3 seconds and demonstrate the fast change of the two parameters.
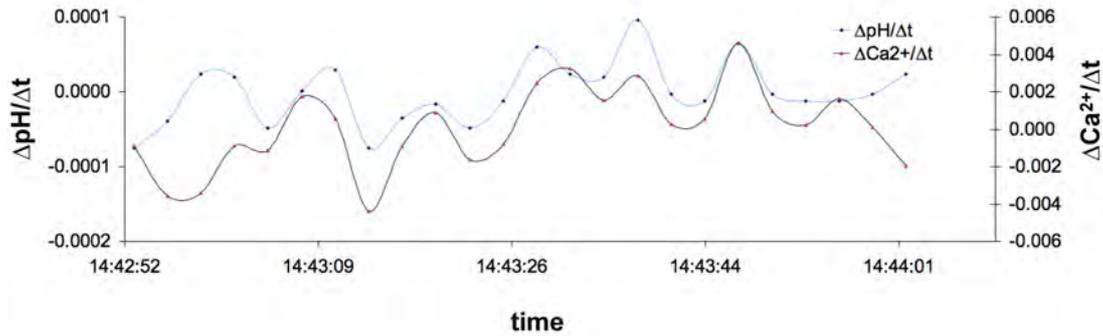
Figure 5: Simultaneous measurements of pH and Ca^{2+} short-term dynamics within the inner EPF of *A. islandica*. The change in pH and Ca^{2+} are plotted against the change over time. Concentrations were measured every 3 seconds.

Simultanous microsensor long-term measurements of pH and calcium within the inner EPF of *A. islandica* were performed over 7 hours. The valves of the clam were open over the whole period of time. pH of the EPF was between ~ 0.2 and ~ 0.6 units lower compared to the surrounding pH of experimental seawater that was used as a baseline for ΔpH. Calcium concentrations were higher and we measured an increase of up to 2.5 mM over seawater calcium concentrations used as a baseline for the ΔCa^{2+} (Figure 6A). Both parameters increased and decreased synchronously. During this microsensor measurement, EPF samples were taken and analysed for DIC (Figure 6B). Interestingly, DIC values also oscillate but are not as synchronous.

DIC was measured six times during the microsensor measurements and the difference to the surrounding experimental seawater was calculated. The dynamics of ΔDIC can be seen in Figure 6B. During the first two hours of the measurements when pH and calcium concentrations increase the DIC concentration is more or less the same as in seawater with a slight decrease of ~ 174 μmol/kg. The following three measurements show a steep increase in DIC of up to 3191 μmol/kg that is over 50% higher than the seawater concentration. During this high DIC values the two other parameters, pH and Ca^{2+}, show a simultaneous oscillation. From the measurements it seems that DIC and pH are on a maximum value at the same time and calcium concentration shows also a strong sudden increase with all three parameters decrease rapidly together. Although the DIC values appear with a small delay compared to the other two parameters the last measurement point reaches almost seawater values again. The delay can be due to the lesser measurement points of DIC compared to the microsensor measurements of pH and Ca^{2+} with every 3 seconds.
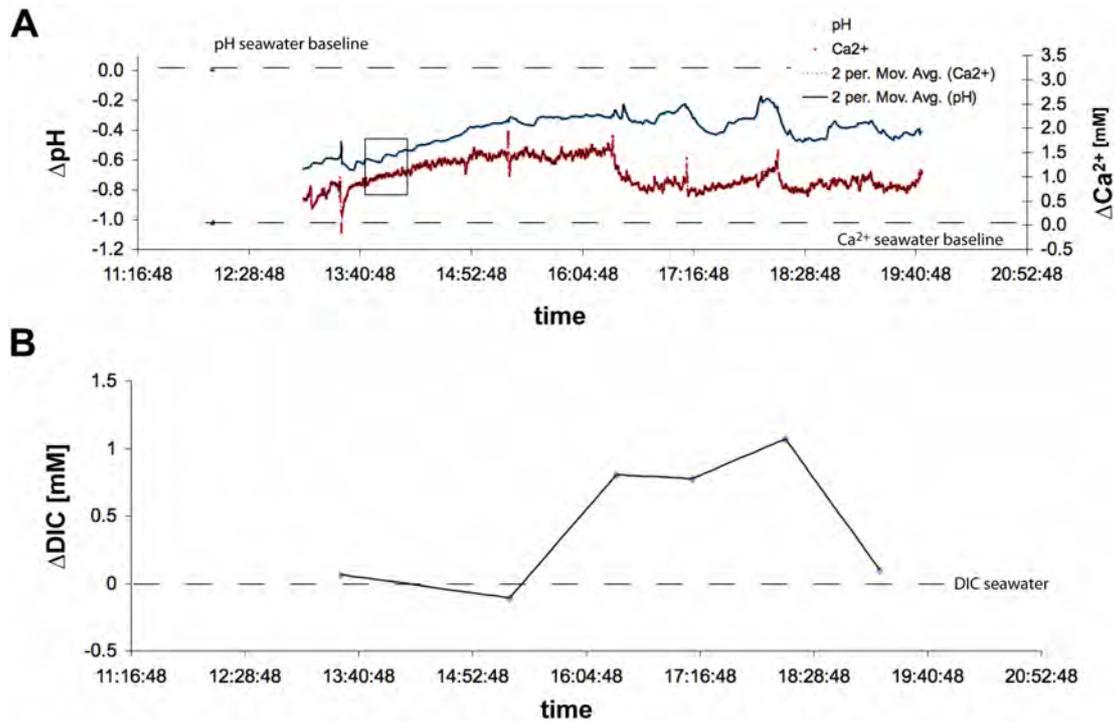
Figure 6: Simultaneous measurements of pH, Ca^{2+} and DIC long-term dynamics over time within the inner EPF of *A. islandica*. A) ΔpH and ΔCa^{2+} relative to seawater pH and Ca^{2+} concentrations respectively (see legend). Box indicates the short-term dynamics shown in Figure 5. B) DIC concentrations simultaneously measured during microsensor measurements shown in A). Displayed as ΔDIC relative to seawater.

Discussion

For the detailed understanding of the shell-formation process, mechanisms of ion-transportation close to the site of calcification need to be identified (e.g. (Carre et al. 2006; McConnaughey & Gillikin 2008). In bivalve shell-formation the two major compartments, the inner and the outer extrapallial fluid (EPF) are closest to the site of biomineralization (Wheeler 1992). However, analysis of the outer EPF is not accessible for analysis due to the small area and volume. Therefore, in this study we focussed on the inner EPF of young specimen of *Arctica islandica*.

The transparent (PVC) window in the shell enabled optical measurements of pH up of the outer mantle epithelium (OME) and potentially encourages other similar studies using different ionic fluorescent dyes. Insertion of Ca^{2+} and pH microsensors into the EPF through small operational holes was successful but the exact distance of the microsensor tips to the

OME could not be determined. However, their advantage is that synchronous recordings of Ca^{2+} and pH were possible with high temporal resolution.

The low pH that was mostly recorded in the EPF and especially at the tissue surface can only be driven by respiratory CO_2 production. The sudden elevation of the pH to levels of above 9.5 can only be caused by active proton uptake by the epithelium, which costs metabolic energy. The pH and Ca^{2+} dynamics supply extra information on the possible transporter. We propose that the dynamics are driven by a Ca^{2+}/H^+-exchanger (Ca^{2+}-ATPase). Such a counterporter is most frequently associated with calcium carbonate precipitation (McConnaughey & Gillikin 2008).

In the bivalves *Anodonta cygnea* the presence of a V-type proton pump in the OME has been demonstrated (da Costa et al. 1999). This H^+ transporter can be active in parallel to the Ca^{2+}/H^+-exchanger.

The synchronous pH and Ca^{2+} dynamics measured with microsensors can be explained by active counter pumping of H+ and Ca2+ ions. Ca-H-ATPase can transport calcium-ions across the mantle epithelia to the EPF in exchange for $2H^+$ (e.g. Schwiening et al. 1993). Their activity was shown to induce synchronous Ca^{2+} and pH dynamics at the surface of macroalgae (McConnaughey & Falk 1991). These transporters have been described in detail and are suggested to play a role in the calcification process (Ip & Lim 1991; Kingsley & Watabe 1985). Moreover, Fan et al. (2007) found evidence for Ca^{2+}-ATPase on the OME of pearl oysters. Interestingly, similar pH and Ca^{2+} dynamics were measured in the calcification site of coral polyps, the calicoblastic fluid (Al-Horani et al. 2003). The authors validated the activity of Ca^{2+}-ATPase enzyme via Ca^{2+}-ATPase inhibitors.

Our data do not allow conclusions on whether the observed elevated DIC in the EPF is caused by active pumping or passive influx from respiration. Several mechanisms have been proposed for active transport of DIC (Melzner et al. 2009; Miyamoto et al. 1996). To uncover processes of DIC accumulation goes beyond our study but our data suggests a correlation between DIC and H^+/Ca^{2+} pumping (Figure 4).

We propose that these pumps are in involved in shell formation, although these pumps cannot induce calcification within the EPF. The proton pumps can induce a pH at the tissue surface that is high enough to induce calcification, but the pH at the shell surface of the inner EPF

stays too low due to the distance between OMU and shell. At the observed pH of ~ 9.5 the supersaturation of $CaCO_3$ can be calculated. Assuming a DIC of 2300 µmol/kg (seawater DIC) we calculated with CO2sys (Lewis & Wallace 1998) that the oversaturation can be 15-20 fold. $CaCO_3$ precipitation does not occur on the tissue surface, probably by inhibition mechanisms (Marin & Luquet 2004; Miyamoto et al. 2005). It is documented that $CaCO_3$ precipiation only occur under strong local supersaturation, e.g. in calcifying algae it was > 30 fold (McConnaughey & Falk 1991), in freshwater stromatolites it was > 20 fold (Bissett et al. 2008), in corals ~25 fold (Al-Horani et al. 2003) and in hypersaline microbial mats oversaturation of ~ 25 fold were recorded (Ludwig et al. 2005). Thus the pH values we found on the tissue surface can induce calcification. We propose that this can only happen when the tissue is in close contact with the shell, as for example in the outer EPF. Here the distance is in the order of microns, and in this enclosed volume even more extreme pH values can develop. This pumping may offer the organism several options to control the shell building. Firstly, the pumps may be actively regulated, like in other complex organisms. Secondly, the animal may control the distance between shell and tissue in which the active pumps are located (OME). We have no information on the distribution of the pumps over the OME. It might be most optimal to have these concentrated in the area where most growth is occurring, however our data indicate that these pumps are also present in the OME adjacent to the inner EPF, where calcification is less needed.

Conclusions

In the present study the inner EPF of *A. islandica* was investigated as a highly dynamic compartment with regards to pH, Ca^{2+} and DIC. A sudden increase in pH from below 7 up to 9.5 at the OME shows active proton pumping and is consistent with the hypothesis of H^+-pumps being integrated in the OME. Simultaneous pH and Ca^{2+} microsensor measurements revealed remarkable short-term dynamics and demonstrate the power of this method for *in situ* measurements of ion-dynamics. The function of this active pumping process might play a role in the calcification process. Calculations of the saturation state within the inner EPF indicate an environment that can reach very strong $CaCO_3$ oversaturation when a microsite is created. Lifting of the OME up to the inner shell surface can create such a microenvironment where ion pumping by the tissue drives calcification.

Future *in situ* investigations on the OME in the inner and in the outer EPF, using Ca^{2+} markers will help to uncover possible calcium pumps or channels and get us closer to resolve the enigma of the biomineralization process within *A. islandica*.

Acknowledgements

References

Addadi, L., Joester, D., Nudelman, F. & Weiner, S. 2006 Mollusk shell formation: A source of new concepts for understanding biomineralization processes. *Chemistry-a European Journal* **12**, 981-987.

Al-Horani, F. A., Al-Moghrabi, S. M. & de Beer, D. 2003 The mechanism of calcification and its relation to photosynthesis and respiration in the scleractinian coral *Galaxea fascicularis*. *Marine Biology* **142**, 419-426.

Bissett, A., de Beer, D., Schoon, R., Shiraishi, F., Reimer, A. & Arp, G. 2008 Microbial mediation of stromatolite formation in karst-water creeks. *Limnology and Oceanography* **53**, 1159-1168.

Carre, M., Bentaleb, I., Bruguier, O., Ordinola, E., Barrett, N. T. & Fontugne, M. 2006 Calcification rate influence on trace element concentrations in aragonitic bivalve shells: Evidences and mechanisms. *Geochimica Et Cosmochimica Acta* **70**, 4906-4920.

Coimbra, J., Machado, J., Fernandes, P. L., Ferreira, H. G. & Ferreira, K. G. 1988 Electrophysiology of the mantle of *Anodonta cygnea Journal of Experimental Biology* **140**, 65-88.

Crenshaw, M. A. 1972a Inorganic composition of molluscan extrapallial fluid *Biological Bulletin* **143**, 506-512.

Crenshaw, M. A. 1972b The soluble matrix from *Mercenaria mercenaria* shell. *Biomineralization Res Rep* **6**, 6.

Crenshaw, M. A. 1980 Mechanisms of shell formation and dissolution. *Topics in Geobiology* **1**, 115-132.

Crenshaw, M. A. & Neff, J. M. 1969 Decalcification at mantle-shell interface in mollusks *American Zoologist* **9**, 881-&.

da Costa, A. R., Oliveira, P. F., Barrias, C. & Ferreira, H. G. 1999 Identification of a V-type proton pump in the outer mantle epithelium of *Anodonta cygnea*. *Comparative Biochemistry and Physiology a-Molecular and Integrative Physiology* **123**, 337-342.

de Beer, D., Glud, A., Epping, E. & Kuhl, M. 1997 A fast-responding CO_2 microelectrode for profiling sediments, microbial mats, and biofilms. *Limnology and Oceanography* **42**, 1590-1600.

de Beer, D., Kuhl, M., Stambler, N. & Vaki, L. 2000 A microsensor study of light enhanced Ca2+ uptake and photosynthesis in the reef-building hermatypic coral *Favia* sp. *Marine Ecology Progress Series* **194**, 75-85.

Falini, G., Albeck, S., Weiner, S. & Addadi, L. 1996 Control of aragonite or calcite polymorphism by mollusk shell macromolecules. *Science* **271**, 67-69.

Fan, W., Li, C., Li, S., Feng, Q., Xie, L. & Zhang, R. 2007 Cloning, characterization, and expression patterns of three sarco/endoplasmic reticulum Ca2+-ATPase isoforms from pearl oyster (*Pinctada fucata*). *Acta Biochimica Et Biophysica Sinica* **39**, 722-730.

Gillikin, D. P., Lorrain, A., Navez, J., Taylor, J. W., Keppens, E., Baeyens, W. & Dehairs, F. 2005 Strong biological controls on Sr/Ca ratios in aragonitic marine bivalve shells. *Geochemistry Geophysics Geosystems* **6**.

Hall, P. O. & Aller, R. C. 1992 Rapid, small-volume, flow-injection analysis for $\sum$-CO_2 and NH^{4+} in marine and fresh-waters. *Limnology and Oceanography* **37**, 1113-1119.

Hattan, S. J., Laue, T. M. & Chasteen, N. D. 2001 Purification and characterization of a novel calcium-binding protein from the extrapallial fluid of the mollusc, *Mytilus edulis*. *Journal of Biological Chemistry* **276**, 4461-4468.

Heinemann, A., Fietzke, J., Melzner, F., Boehm, F., Thomsen, J., Garbe-Schoenberg, D. & Eisenhauer, A. Conditions of *Mytilus edulis* extracellular body fluids and shell composition in a pH-treatment experiment: Acid-base status, trace elements and delta B-11. *Geochemistry Geophysics Geosystems* **13**.

Ip, Y. K. & Lim, A. L. L. 1991 Are calcium and strontium transported by the same mechanism in the hermatypic coral *Galaxea fascicularis Journal of Experimental Biology* **159**, 507-513.

Ip, Y. K., Loong, A. M., Hiong, K. C., Wong, W. P., Chew, S. F., Reddy, K., Sivaloganathan, B. & Ballantyne, J. S. 2006 Light induces an increase in the pH of and a decrease in the ammonia

concentration in the extrapallial fluid of the giant clam *Tridacna squamosa. Physiological and Biochemical Zoology* **79**, 656-664.

Kingsley, R. J. & Watabe, N. 1985 Ca-ATPase localization and inhibition in the gorgonian *Leptogorgia virgulata* (lamarck) (Coelenterata, Gorgonacea) *Journal of Experimental Marine Biology and Ecology* **93**, 157-167.

Klein, R. T., Lohmann, K. C. & Thayer, C. W. 1996 Sr/Ca and C-13/C-12 ratios in skeletal calcite of *Mytilus trossulus*: Covariation with metabolic rate, salinity, and carbon isotopic composition of seawater. *Geochimica Et Cosmochimica Acta* **60**, 4207-4221.

Levi-Kalisman, Y., Falini, G., Addadi, L. & Weiner, S. 2001 Structure of the nacreous organic matrix of a bivalve mollusk shell examined in the hydrated state using Cryo-TEM. *Journal of Structural Biology* **135**, 8-17.

Lewis & Wallace. 1998 Basic program for CO_2 system in seawater. Oak Ridge National Laboratory.

Lowenstam, H. A. 1981 Minerals formed by organisms *Science* **211**, 1126-1131.

Ludwig, R., Al-Horani, F. A., de Beer, D. & Jonkers, H. M. 2005 Photosynthesis-controlled calcification in a hypersaline microbial mat. *Limnology and Oceanography* **50**, 1836-1843.

Marin, F. & Luquet, G. 2004 Molluscan shell proteins. *Comptes Rendus Palevol* **3**, 469-492.

McConnaughey, T. A. & Falk, R. H. 1991 Calcium-Proton exchange during algal calcification *Biological Bulletin* **180**, 185-195.

McConnaughey, T. A. & Gillikin, D. P. 2008 Carbon isotopes in mollusk shell carbonates. *Geo-Marine Letters* **28**, 287-299.

Melzner, F., Gutowska, M. A., Hu, M. & Stumpp, M. 2009 Acid-base regulatory capacity and associated proton extrusion mechanisms in marine invertebrates: An overview. *Comparative Biochemistry and Physiology a-Molecular & Integrative Physiology* **153A**, S80-S80.

Misogianes, M. J. & Chasteen, N. D. 1979 Chemical and spectral characterization of the extrapallial fluid of *Mytilus edulis Analytical Biochemistry* **100**, 324-334.

Miyamoto, H., Miyashita, T., Okushima, M., Nakano, S., Morita, T. & Matsushiro, A. 1996 A carbonic anhydrase from the nacreous layer in oyster pearls. *Proceedings of the National Academy of Sciences of the United States of America* **93**, 9657-9660.

Miyamoto, H., Miyoshi, F. & Kohno, J. 2005 The carbonic anhydrase domain protein nacrein is expressed in the epithelial cells of the mantle and acts as a negative regulator in calcification in the mollusc *Pinctada fucata. Zoological Science* **22**, 311-315.

Nudelman, F., Chen, H. H., Goldberg, H. A., Weiner, S. & Addadi, L. 2007 Spiers memorial lecture: Lessons from biomineralization: comparing the growth strategies of mollusc shell prismatic and nacreous layers in *Atrina rigida. Faraday Discussions* **136**, 9-25.

Nudelman, F., Gotliv, B. A., Addadi, L. & Weiner, S. 2006 Mollusk shell formation: Mapping the distribution of organic matrix components underlying a single aragonitic tablet in nacre. *Journal of Structural Biology* **153**, 176-187.

Schwiening, C. J., Kennedy, H. J. & Thomas, R. C. 1993 Calcium Hydrogen exchange by plasma-membrane Ca-ATPase of voltage-clamped snail neurons. *Proceedings of the Royal Society B-Biological Sciences* **253**, 285-289.

Stemmer, K., Nehrke, G. & Brey, T. 2013 Elevated CO2 levels do not affect shell structure of the bivalve *Arctica islandica* from the Western Baltic. *Plos One*

Thomsen, J., Gutowska, M. A., Saphoerster, J., Heinemann, A., Truebenbach, K., Fietzke, J., Hiebenthal, C., Eisenhauer, A., Koertzinger, A., Wahl, M. & Melzner, F. 2010 Calcifying invertebrates succeed in a naturally CO_2-rich coastal habitat but are threatened by high levels of future acidification. *Biogeosciences* **7**, 3879-3891.

Thomsen, J. & Melzner, F. 2010 Moderate seawater acidification does not elicit long-term metabolic depression in the blue mussel *Mytilus edulis*. *Marine Biology* **157**, 2667-2676.

Wada, K. & Fujinuki, T. 1976 Biomineralization in bivalve molluscs with emphasis on the chemical composition of the extrapallial fluid. *Belle W. Baruch Library in Marine Science* **5**, 175-190.

Weiner, S. & Dove, P. 2003 An Overview on Biomineralization Processes and the Problem of the Vital Effect.

Weiner, S. & Traub, W. 1980 X-ray-diffraction study of the insoluble organic matrix of mollusk shells *Febs Letters* **111**, 311-316.

Weiss, I. M. 2010 Jewels in the Pearl. *Chembiochem* **11**, 297-300.

Wheeler, A. P. 1992 Mechanisms of molluscan shell formation. In *Calcification in biological systems.*, pp. 179-216.

Wilbur, K. M. 1983 Shell formation. In *The Mollusca. Volume 4. Physiology. Part 1.*, pp. 253-287.

5. Synthesis

5. Synthesis

Primarily the work within this thesis is dedicated to ocean acidification research and contributes valuable information about the possible adaptation mechanisms of *Arctica islandica* and its bivalve shell. Subsequently this thesis highlights important knowledge gaps and the necessity of a fundamental understanding of single processes involved in the shell formation process. In the following section I will shortly discuss the main results of this thesis and put them into perspective of the role of *A. islandica* shell and other marine organisms in a high pCO$_2$ world.

In the first part of this thesis (manuscript I) *A. islandica* from the Kiel Bight was evaluated as well adapted to changing pCO$_2$ and shell growth as well as crystal microstructure stayed unaffected when grown under different pCO$_2$ levels. The results validate proxy information that can be affected by shell growth and structure, derived from *A. islandica* shells from this population containing no pCO$_2$ related bias. However, recent studies showed various effects of low pH and high pCO$_2$ on different bivalve species indicating species-specific responses partly depending on the experimental conditions (Gazeau et al. 2007; Hahn et al. 2012; Melzner et al. 2011; Michaelidis et al. 2005). Comparison of previous studies with the findings presented in manuscript I is difficult because of i) experimental disparities (Gazeau et al. 2007; Hahn et al. 2012) and ii) studies on bivalve shells with different crystal motifs than *A. islandica* (e.g. *Mytilus edulis* shell consists of two calcium carbonate polymorphs) (Melzner et al. 2011; Thomsen & Melzner 2010) and analysis of different shell regions (Hahn et al. 2012). In future investigations a consistency of experimental set-ups and analytical methods will help producing comparable data.

Arctica islandica is a living fossil which developed specific survival strategies e.g. a thick organic periostracum shielding the shell from corrosive water or self-induced metabolic depression for saving energy (Abele et al. 2008; Strahl et al. 2011). In the Kiel Bight smaller shells and the decrease of life-span may be the trait for the strongly fluctuating environment (i.e. salinity, temperature, O$_2$ and pCO$_2$) (Hiebenthal et al. 2012a; Hiebenthal et al. 2012b; Philipp et al. 2012) whereas populations under favourable conditions in very stable environments build thicker and bigger shells and can live up to several hundred years (e.g. off Iceland) (Schoene et al. 2005; Wanamaker et al. 2008). Thus the results of this study lead to the assumption that tolerance to high pCO$_2$ levels of *A. islandica* is induced by i) the species-specific lifestyle serving as pre-adaptation or ii) seasonal enhanced pCO$_2$ levels within Kiel

Bight area that trigger pre-adaptation and thus add to a general expression of a pronounced stress response at the expense of life-span.

Why shells do not completely dissolve when exposed to $CaCO_3$ undersaturated conditions and how $CaCO_3$ can still precipitate when even internal body fluids (i.e. haemolymph, mantle water, extrapallial fluid) are naturally acidified (Crenshaw 1972; Melzner et al. 2012) manuscript III) are unresolved questions. Hence it was a fundamental task of this thesis to investigate organic shell properties and the biomineralization process itself. As a biogenic carbonate, *A. islandica* shell is a composite of inorganic and organic phases and especially the latter raises attention on the formation of an organic-matrix, dictating the biomineralization process (Levi-Kalisman et al. 2001; Nudelman et al. 2006; Weiss 2010).

Pigment polyenes are suggested to be associated with the organic matrix but besides their appearance in coloured parts of mollusk shells, not much is known about their origin or their function (Hedegaard et al. 2006). In part two of this thesis (manuscript II), polyenes were identified as a common compound for *A. islandica* from four different regions. If this molecule promotes the robustness of the shell is still questionable but shells from the Kiel Bight contained pigment polyenes in a banding pattern similar to growth lines with an intra-annual resolution indicating a powerful tool for sclerochronology. Being not habitat related as suggested by Hedegaard et al. (2006) raises the hypothesis that pigment polyenes are synthesised or chemically altered by the animal (Barnard & de Waal 2006), probably independently from the food source. Growth experiments including different food sources and different ontogenetic stages of *A. islandica* can give more valuable insights of the polyene nature and its origin. Their distinct appearance in the outer shell layer leads to the hypothesis that polyenes get only incorporated from the outer extrapallial fluid (EPF) from which the outer shell layer is getting generated and is thus suggested as a matter of future investigations. In this study, polyenes were also found incorporated within the aragonitic granules. Cuif et al. (2012) describe organic molecules surrounding aragonite or calcite granules like an envelope. The organic periostracum covering the shell and organic molecules being intertwined with $CaCO_3$ granules would shelter the shell from corrosion. However, altered shells via erosion (e.g. by digging), bioerosion (e.g. by worms) or hampered assemblage of organic phases are most probably threatened by dissolution (e.g. Thomsen & Melzner 2010). To what extend polyenes are associated with the organic-matrix and if polyenes play an important role in the shell formation process remains to be seen. Confocal Raman spectroscopy proofed to be a

suitable method to study pigment polyenes and is suggested for further studies on single shell molecules.

No effect of high pCO$_2$ on shell growth rate (also shown by Hiebenthal et al. 2012a) or shell microstructure indicates full physiological and chemical control by *A. islandica* over the biomineralization process. In part three of this thesis the actual site of calcification as part of the biomineralization process was investigated (manuscript III). The EPF is in direct contact with the inner shell surface and was long assumed to be the place of shell formation (Wada & Fujinuki 1976; Wilbur 1983). Whether precipitation of CaCO$_3$ takes place in the microenvironment of the EPF or somewhere else is a matter of debate (Addadi et al. 2006; Crenshaw 1972; Heinemann et al. 2011). The site of calcification needs to be highly supersaturated with respect to CaCO$_3$ and few studies present the EPF as a naturally acidified compartment (Crenshaw 1972; Melzner et al. 2012). In manuscript III, I present the bulk EPF of *A. islandica* as an undersaturated environment where calcification just cannot happen. However, the secreting outer mantle epithelium (OME) of the animal can extremely elevate extracellular pH by ion pumping shown also in manuscript III. Thus the OME may function as a dynamic membrane, creating a microsite when in close contact with the inner shell surface. Ion pumping would then drive calcification.

Weiss (2010) presented a new model for biomineralization combined with previous proposals (Levi-Kalisman et al. 2001; Nudelman et al. 2006; Suzuki et al. 2009) and suggested the dynamic movement of a chitinous membrane close to a few μm to the inner shell layer. Controlled secretion of a special organic mix and the active pumping of Ca^{2+}/H$^+$ via ion pumps would create a microsite highly supersaturated and ready for processing not only calcification but providing all constituents for biomineralization. The chitinous membrane would need to be a preformed layer between OME and inner shell surface probably secreted right at that microsite. The third study of this thesis (manuscript III) agrees partly with this model and contributes valuable *in situ* information of ion pumping by the OME. Application of microsensors and optical measurements of the pH within the EPF enabled *in situ* measurements and are valuable approaches for future ion-dynamic studies on the site of bivalve calcification. Investigation of the OME in the inner and the outer EPF e.g. using calcium imaging similar to optical pH measurements performed in the inner EPF (manuscript III) will further help to determine Ca^{2+}-transport ways.

Within the supplementary material, S1 and S2 illustrate and expand the range of organisms, methods and disciplines that need to be addressed to enable reliable future predictions of life in a changing ocean. For S1) the thermal tolerance window from the actively swimming king scallop, *Pecten maximus*, was observed to be narrowed by high pCO$_2$ which results in elevated vulnerability to temperature changes of the species influencing its escape performance and thus its fitness capacities in an acidic ocean and S2) describes that minute calcareous spicules are abundant in many invertebrate taxa, like soft corals, that have not yet been thoroughly considered to be harmed by ocean acidification.

Many open questions remain concerning the future impact of ocean acidification on marine organisms and synergistic effects of pCO$_2$, and other parameters (salinity, temperature, food availability) need to be combined in future studies. The fact that marine calcifiers like *A. islandica* stay unaffected by high pCO$_2$ levels may seem optimistic towards future projections of a warm acidic ocean. But we are far from understanding effects of long-term exposure to rapidly increasing pCO$_2$ levels and the possible consequence for the marine ecosystem e.g. loss of biodiversity, which in return could impact the food web structure. Nevertheless, without knowing *where* or *what* or *when* to look for from a nanoscale to an ecosystem level we might miss out on some very important details for evaluating future impacts on calcifying organisms. I propose to specifically subordinate the question whether *A. islandica* is solely robust to elevated pCO$_2$ and to rather focus on the complex biogenic composite of the shell and the mechanistic understanding of biomineralization. Due to its shell that serves as an environmental recorder and above all its immense longevity, *A. islandica* remains a valuable candidate for future research on shell properties and biomineralization processes. A multidisciplinary approach is needed in order to better understand the role of single components (i.e. ions, cells, organic matrices) and processes involved in shell-formation.

References

Abele, D., Strahl, J., Brey, T. & Philipp, E. E. R. 2008 Imperceptible senescence: Ageing in the ocean quahog *Arctica islandica*. *Free Radical Research* **42**, 474-480.

Addadi, L., Joester, D., Nudelman, F. & Weiner, S. 2006 Mollusk shell formation: A source of new concepts for understanding biomineralization processes. *Chemistry-a European Journal* **12**, 981-987.

Barnard, W. & de Waal, D. 2006 Raman investigation of pigmentary molecules in the molluscan biogenic matrix. *Journal of Raman Spectroscopy* **37**, 342-352.

Crenshaw, M. A. 1972 Inorganic composition of molluscan extrapallial fluid *Biological Bulletin* **143**, 506-512.

Cuif, J. P., Dauphin, Y., Nehrke, G., Nouet, J. & Perez-Huerta, A. 2012 Layered growth and crystallization in calcareous biominerals: Impact of structural and chemical evidence on two major concepts in invertebrate biomineralization studies. *Minerals* **2**, 11-39.

Gazeau, F., Quiblier, C., Jansen, J. M., Gattuso, J.-P., Middelburg, J. J. & Heip, C. H. R. 2007 Impact of elevated CO_2 on shellfish calcification. *Geophysical Research Letters* **34**.

Hahn, S., Rodolfo-Metalpa, R., Griesshaber, E., Schmahl, W. W., Buhl, D., Hall-Spencer, J. M., Baggini, C., Fehr, K. T. & Immenhauser, A. 2012 Marine bivalve shell geochemistry and ultrastructure from modern low pH environments: environmental effect versus experimental bias. *Biogeosciences* **9**, 1897-1914.

Hedegaard, C., Bardeau, J. F. & Chateigner, D. 2006 Molluscan shell pigments: An in situ resonance Raman study. *Journal of Molluscan Studies* **72**, 157-162.

Heinemann, A., Hiebenthal, C., Fietzke, J., Eisenhauer, A. & Wahl, M. 2011 Disentangling the biological and environmental control of *M. edulis* shell chemistry (vol 12, May, 2011). *Geochemistry Geophysics Geosystems* **12**.

Hiebenthal, C., Philipp, E., Eisenhauer, A. & Wahl, M. 2012a Effects of seawater pCO_2 and temperature on shell growth, shell stability, condition and cellular stress of Western Baltic Sea *Mytilus edulis* (L.) and *Arctica islandica* (L.). *Marine Biology*.

Hiebenthal, C., Philipp, E. E. R., Eisenhauer, A. & Wahl, M. 2012b Interactive effects of temperature and salinity on shell formation and general condition in Baltic Sea *Mytilus edulis* and *Arctica islandica*. *Aquatic Biology* **14**, 289-298.

Levi-Kalisman, Y., Falini, G., Addadi, L. & Weiner, S. 2001 Structure of the nacreous organic matrix of a bivalve mollusk shell examined in the hydrated state using Cryo-TEM. *Journal of Structural Biology* **135**, 8-17.

Melzner, F., Stange, P., Truebenbach, K., Thomsen, J., Casties, I., Panknin, U., Gorb, S. N. & Gutowska, M. A. 2011 Food Supply and Seawater pCO(2) Impact Calcification and Internal Shell Dissolution in the Blue Mussel *Mytilus edulis*. *Plos One* **6**.

Melzner, F., Thomsen, J., Koeve, W., Oschlies, A., Gutowska, M. A., Bange, H., Hansen, H. P. & Körtzinger, A. 2012 Future ocean acidification will be amplified by hypoxia in coastal habitats. *Marine Biology*.

Michaelidis, B., Ouzounis, C., Paleras, A. & Portner, H. O. 2005 Effects of long-term moderate hypercapnia on acid-base balance and growth rate in marine mussels *Mytilus galloprovincialis*. *Marine Ecology-Progress Series* **293**, 109-118.

Nudelman, F., Gotliv, B. A., Addadi, L. & Weiner, S. 2006 Mollusk shell formation: Mapping the distribution of organic matrix components underlying a single aragonitic tablet in nacre. *Journal of Structural Biology* **153**, 176-187.

Philipp, E. E. R., Wessels, W., Gruber, H., Strahl, J., Wagner, A. E., Ernst, I. M. A., Rimbach, G., Kraemer, L., Schreiber, S., Abele, D. & Rosenstiel, P. 2012 Gene Expression and Physiological Changes of Different Populations of the Long-Lived Bivalve *Arctica islandica* under Low Oxygen Conditions. *Plos One* **7**.

Schoene, B. R., Fiebig, J., Pfeiffer, M., Gless, R., Hickson, J., Johnson, A. L. A., Dreyer, W. & Oschmann, W. 2005 Climate records from a bivalved Methuselah (*Arctica islandica*, Mollusca; Iceland). *Palaeogeography Palaeoclimatology Palaeoecology* **228**, 130-148.

Strahl, J., Brey, T., Philipp, E. E. R., Thorarinsdottir, G., Fischer, N., Wessels, W. & Abele, D. 2011 Physiological responses to self-induced burrowing and metabolic rate depression in the ocean quahog Arctica islandica. *Journal of Experimental Biology* **214**, 4223-4233.

Suzuki, M., Saruwatari, K., Kogure, T., Yamamoto, Y., Nishimura, T., Kato, T. & Nagasawa, H. 2009 An Acidic Matrix Protein, Pif, Is a Key Macromolecule for Nacre Formation. *Science* **325**, 1388-1390.

Thomsen, J. & Melzner, F. 2010 Moderate seawater acidification does not elicit long-term metabolic depression in the blue mussel *Mytilus edulis*. *Marine Biology* **157**, 2667-2676.

Wada, K. & Fujinuki, T. 1976 Biomineralization in bivalve molluscs with emphasis on the chemical composition of the extrapallial fluid. *Belle W. Baruch Library in Marine Science* **5**, 175-190.

Wanamaker, A. D., Jr., Heinemeier, J., Scourse, J. D., Richardson, C. A., Butler, P. G., Eiriksson, J. & Knudsen, K. L. 2008 Very long-lived mollusks confirm 17th century ad tephra-based radiocarbon reservoir ages for North Icelandic shelf waters *Radiocarbon* **50**, 399-412.

Weiss, I. M. 2010 Jewels in the Pearl. *Chembiochem* **11**, 297-300.

Wilbur, K. M. 1983 Shell formation. In *The Mollusca. Volume 4. Physiology. Part 1.*, pp. 253-287.

Supplementary material

S1

ORIGINAL PAPER

Impact of ocean acidification on escape performance of the king scallop, *Pecten maximus*, from Norway

Burgel Schalkhausser · Christian Bock ·
Kristina Stemmer · Thomas Brey ·
Hans-O Pörtner · Gisela Lannig

Abstract The ongoing process of ocean acidification already affects marine life, and according to the concept of oxygen and capacity limitation of thermal tolerance, these effects may be intensified at the borders of the thermal tolerance window. We studied the effects of elevated CO_2 concentrations on clapping performance and energy metabolism of the commercially important scallop *Pecten maximus*. Individuals were exposed for at least 30 days to 4 °C (winter) or to 10 °C (spring/summer) at either ambient (0.04 kPa, normocapnia) or predicted future PCO_2 levels (0.11 kPa, hypercapnia). Cold-exposed (4 °C) groups revealed thermal stress exacerbated by PCO_2 indicated by a high mortality overall and its increase from 55 % under normocapnia to 90 % under hypercapnia. We therefore excluded the 4 °C groups from further experimentation. Scallops at 10 °C showed impaired clapping performance following hypercapnic exposure. Force production was significantly reduced although the number of claps was unchanged between normocapnia- and hypercapnia-exposed scallops. The difference between maximal and resting metabolic rate (aerobic scope) of the hypercapnic scallops was significantly reduced compared with normocapnic animals, indicating a reduction in net aerobic scope. Our data confirm that ocean acidification narrows the thermal tolerance range of scallops resulting in elevated vulnerability to temperature extremes and impairs the animal's performance capacity with potentially detrimental consequences for its fitness and survival in the ocean of tomorrow.

B. Schalkhausser (✉) · C. Bock · H.-O. Pörtner · G. Lannig
Integrative Ökophysiologie, Alfred Wegener Institut für
Polar- und Meeresforschung in der Helmholtz-Gemeinschaft,
Am Handelshafen 12, 27570 Bremerhaven, Germany
e-mail: Burgel.Schalkhausser@awi.de

K. Stemmer · T. Brey
Funktionelle Ökologie, Alfred Wegener Institut für
Polar- und Meeresforschung in der Helmholtz-Gemeinschaft,
Columbusstrasse, 27570 Bremerhaven, Germany

Introduction

Atmospheric temperature and CO_2 concentrations have been rising dramatically over the last decades due to anthropogenic influences (IPCC 2007). In oceans, an increase in dissolved CO_2 results in reduced seawater pH and altered carbonate chemistry, known as ocean acidification (OA). The oceans' average pH has already declined by more than 0.1 units below the pH of pre-industrial times (Caldeira and Wickett 2003). If trends continue at current rates, pH values are predicted to decrease by 0.3–0.4 units by the end of this century (Orr 2011). These changes will affect a variety of biological processes that depend on pH and/or the components of the CO_2/bicarbonate/carbonate system. Such effects are predicted to be especially significant for calcifying organisms (Fabry et al. 2008; Doney et al. 2009; Kroeker et al. 2010). Besides the obvious effect on calcification, OA exposure influences the rate of energy metabolism in invertebrates (Langenbuch and Pörtner 2004; Michaelidis et al. 2005; Lannig et al. 2010; Melatunan et al. 2011) via changes in extracellular and, possibly, intracellular pH values that cause alterations in energy partitioning. At the cellular level (muscle, liver), an extracellular acidosis causes metabolic depression by reducing the rate and costs of acid–base and ion regulation (Pörtner 1987; Pörtner et al. 2000; Pörtner and Bock 2000) and/or of protein synthesis (Langenbuch and Pörtner 2003).

At whole animal level, this is paralleled either by a decrease (Pörtner et al. 1998; Michaelidis et al. 2005) or by a stimulation in whole organism metabolic rate (Beniash et al. 2010; Stumpp et al. 2011), likely depending on whether and to what extent transepithelial mechanisms of acid–base regulation are depressed or stimulated by OA scenarios (Pörtner et al. 2000). Each of these shifts may result in trade-offs in energy allocation between different biological processes such as ion regulation, calcification, growth or development (Pörtner et al. 2000, 2004; Guderley and Pörtner 2010), possibly leading to constraints in one or more of these processes (Wood et al. 2008; Beniash et al. 2010; Stumpp et al. 2011).

The interactions between ocean acidification and other environmental factors are not well understood, and recent studies suggest a high complexity, with mainly synergistic effects. With respect to temperature, ocean acidification clearly reduced acute heat tolerance of the edible crab, *Cancer pagurus* (PCO_2 of 1 kPa, Metzger et al. 2007), and narrowed the thermal tolerance range of the spider crab, *Hyas araneus,* indicated by a PCO_2-dependent lowering of the critical temperature of the animals (OA scenarios: 0.07 and 0.3 kPa, Walther et al. 2009). A temperature rise of 5 °C and a PCO_2 elevated by 0.1 kPa caused respiration rates and adenylate nucleotide concentrations to fall in the snail *Littorina littorea* (Melatunan et al. 2011). An OA exposure of 0.3 kPa in combination with acute heat stress (delta 8–11 °C) impaired the locomotion capacity of the spider crab, *H. araneus* (Zittier et al. 2012). In Sydney rock oyster, *Saccostrea glomerata,* fertilization and larval development was explicitly reduced under hypercapnia (OA scenarios: 0.6, 0.7 and 1 kPa PCO_2) above optimum temperature (delta 4 °C) (Parker et al. 2009). All of these findings indicate that thermal sensitivity is enhanced under projected OA conditions. Conversely, sensitivity to OA is presumably enhanced at thermal extremes. OA exposure also interferes synergistically with other stressors. A study on juvenile oysters *Crassostrea virginica* revealed that the combined exposure to low salinity (15 vs. 30 psu) and high PCO_2 (0.07–0.08 kPa) produced greater changes in shell properties than each of the factors alone (Dickinson et al. 2012). Internal shell dissolution in *Mytilus edulis* under hypercapnic conditions was intensified in animals stressed by limited food supply, emphasizing a key role for food and thus energy availability in maximizing resistance to ocean acidification (Melzner et al. 2011).

The concept of oxygen- and capacity-limited thermal tolerance (OCLTT, Pörtner 2002) may offer a suitable approach towards a mechanistic understanding of the synergistic interaction between thermal stress and OA/pH effects (Pörtner and Farrell 2008). According to the OCLTT concept, maximal aerobic capacity and thus available metabolic power (energy use per unit time) are limited to the organism's specific thermal tolerance window. As outlined by Guderley and Pörtner (2010), the maximal metabolic power must be partitioned between biological processes. Given that metabolic power depends on environmental parameters such as temperature or pH, environmental conditions outside the optimum range reaching the pejus (= getting worse) and critical range will impair an animal's aerobic scope, resulting in less metabolic power to sustain major fitness-related processes such as growth, reproduction, immune response or the avoidance of predators (see Pörtner 2010; Sokolova et al. 2012).

Our model organism, *Pecten maximus*, belongs to the family Pectinidae (common name scallops). Scallops are distributed worldwide and are unique among bivalves due to their swimming behaviour. To escape from predators, other bivalves close their valves tightly or use their foot for burrowing and/or somersaults. Due to a reduced foot and shells not tightly closing, scallops use a different escape strategy by fast shell closure or jet-like propulsion enabling them to swim (Wilkens 2006). Given that swimming is used to escape, for example, from predator attacks by starfish or crabs (Winter and Hamilton 1985; Ansell et al. 1991), the scallops' swimming capacity is an important performance parameter. Events of swimming activity have been shown to depend on various biotic (e.g. predator abundance or size/age (Wiborg 1963; Brand 2006) and abiotic factors such as displacement from preferred sites (Winter and Hamilton 1985), effects of currents (Gruffydd 1976) or temperature (Scheibling et al. 1995).

The aim of our study was to investigate the impact of long-term OA exposure on the physiology of the scallop, *Pecten maximus*, at two temperatures, 4 °C (winter) versus 10 °C (spring/summer) against the background of the OCLTT concept. To analyse for energetic trade-offs and associated restrictions in performance capacities under expected OA conditions, we determined clapping performance and oxygen consumption rates under resting and exercise conditions of the commercially important scallop *P. maximus* after long-term incubation at elevated CO_2 level.

Materials and methods

Animals and holding conditions

In February 2011, wild-cultured *Pecten maximus* (Linnaeus 1758) were obtained from a sea farm (Kvitsøy Edelskjell AS) in the northern North Sea near Stavanger (58° 58′ 12″ N, 5° 42′ 36″ E). They were collected by scuba divers at a depth of approximately 20 m and a temperature of 3–5 °C. Environmental mean temperatures at a depth of 20 m vary

from 4.5 to 15.2 °C (monthly means from station Indre Utsira since 2000; data reported by the Institute of Marine Research, http://www.imr.no/forskning/forskningsdata/stasjoner/dato.php?page=0&year=2011&stid=5869) and ambient CO_2 levels of around 390 µatm (Pfeil et al. 2012).

Animals wrapped in wood wool were transported on ice to the Alfred Wegener Institute by airplane and kept in a recirculated aquarium system at 5 °C. After 2 weeks of recovery, the shells were carefully scrubbed to remove epibionts. The incubations started and all measurements were carried out in March and April 2011 to avoid possible interference with reproduction as the presumable single spawning event takes place in June as shown for *P. maximus* from Fosen (a location close to Stavanger; Strand and Nylund 1991).

Randomized groups of labelled animals were incubated in recirculating systems in temperature-control rooms at either 4 °C or at 10 °C (one system per group, comprising header, receiver and reservoir tanks and 2 experimental tanks (each equipped with 10 animals maximum) similar to the systems described by Michaelidis et al. 2005 or Findlay et al. 2010). Temperature treatments were combined with different PCO_2 levels, controls with ~0.039 kPa (390 µatm, normocapnia) and elevated exposures with 4 times pre-industrial PCO_2 at ~0.112 kPa (1120 µatm, hypercapnia). All tanks were continuously bubbled with the specific CO_2 concentration that was made using a gas mixing system (HTK, Hamburg, Germany). Incubation lasted a minimum of 33 days up to 60 days (see supplementary materials). According to their suspension-feeding lifestyle, scallops were drip-fed live phytoplankton 3 times per week (DT′s Premium Reef Blend (*Nannochloropsis osculata, Phaeodactylum, Chlorella*, 25.3 µg/L phytoplankton dry weight; Philipp et al. 2008). Feeding lasted for ≥6 h at a concentration of at least 6.10×10^5 cells gram^{-1} bivalve biomass hour^{-1} (4 °C) and 9.15×10^5 cells gram^{-1} bivalve biomass hour^{-1} (10 °C) (water circulation was stopped during feeding times). To ensure good water quality, water of the recirculated systems was exchanged at least twice a week and animal tanks were cleaned from faeces and remaining food items at least 3 times per week. Water physicochemistry was determined at least twice a week to ensure stable conditions (see Table 1): pH was measured with a pH electrode (WTW portable pH meter ProfiLine pH 3310) that was calibrated at the respective temperature with NIST buffers and salinity with a conductivity meter (WTW conductivity meter ProfiLine Cond 1970i), and total dissolved inorganic carbon (DIC) was determined with Seal Analysis SFA QuAAtro; pump Technicon trAAcs 800 TM. The pH was converted to total scale via measurement of Dickson standards. PCO_2 values were calculated using CO2sys (constants of Mehrbach et al. 1973 refitted by Dickson and

Table 1 Physicochemical conditions of seawater after long-term incubations of *P. maximus* during normocapnia and hypercapnia at different temperatures (4 and 10 °C acclimation)

Parameter	Normocapnia	Hypercapnia
4 °C		
PCO_2 [kPa]	0.040 ± 0.009	0.110 ± 0.028
Temperature [°C]	3.9 ± 0.8	3.5 ± 0.7
pH (NBS scale)	8.19 ± 0.06	7.76 ± 0.10
pH (total scale)	8.08 ± 0.09	7.65 ± 0.11
Salinity [psu]	31.1 ± 0.6	31.2 ± 0.8
DIC [µmol/L]	2308.5 ± 47.4	2392.4 ± 39.3
10 °C		
PCO_2 [kPa]	0.040 ± 0.006	0.115 ± 0.028
Temperature [°C]	9.8 ± 0.4	9.6 ± 0.7
pH (NBS scale)	8.25 ± 0.10	7.81 ± 0.07
pH (total scale)	8.08 ± 0.06	7.65 ± 0.10
Salinity [psu]	31.1 ± 0.7	31.2 ± 0.7
DIC [µmol/L]	2315.0 ± 57.9	2387.3 ± 40.8

Data are mean $\pm$ SD with $N = 25$–30 (4 °C), $N = 23$ (10 °C)

NBS National Bureau of Standards, PCO_2 seawater partial pressure of CO_2, *DIC* dissolved inorganic carbon

Millero 1987; programme developed by Lewis and Wallace 1998). Water quality was monitored by measurements of ammonia and nitrite values using photometric test kits (Machery-Nagel, Nanocolor test 0–68 and test 0–03). Animals were starved for 12–24 h prior to measurements to avoid interference with postprandial metabolism and faeces excretion (Wieser and Medgyesy 1990).

Shell dimensions of the scallops in the different incubation experiments did not differ between groups prior to and after incubation resulting in overall mean $\pm$ SD of 108.52 ± 2.44 mm (height), 94.99 ± 2.63 mm (length) and 26.63 ± 1.88 mm (width) ($N = 44$–47).

Calculation of condition index

To obtain data about the wellbeing of the animals, we calculated the condition index CI and the muscle index MI after Shiver et al. (2002) and Pazos et al. (1997) as follows:

$$CI = \frac{tissue_{DW}}{shell_{DW}} \cdot 100 \tag{1}$$

and

$$MI = \frac{muscle_{DW}}{shell_{DW}} \cdot 100 \tag{2}$$

with DW = dry weight of the total soft tissue and of the adductor muscle, respectively, and of the shell in [g]. Dry weights were determined after drying at 75 °C for as long as no detectable changes in weight were observed.

Measurement of haemolymph acid–base parameters

Haemolymph parameters were analysed as described in Lannig et al. (2010) using a blood gas analyser (MT 33, Eschweiler, Germany) with glass electrodes for PCO_2, PO_2 and pH that were calibrated at the respective temperature with NIST buffers or calibration gases, respectively.

Scallops were kept on ice and manually immobilized to avoid any claps while carefully sampling about 2 mL haemolymph out of the tonic adductor muscle with gastight, sterile syringes (0.60-mm cannula). Haemolymph samples were immediately transferred to the blood gas analyser (about 300 μL). For the determination of total CO_2 in the haemolymph (C_eCO_2), 200 μL of haemolymph were put into glass vials with 3 mL 0.1 M HCl via a microlitre precision syringe (Hamilton, 1700 series) and analysed by a gas chromatograph (Agilent 6890 N GC System, Agilent Technologies, USA). The rest was deep frozen in liquid nitrogen (N_2) and stored at -20 °C for further analysis.

The concentration of apparent bicarbonate in the haemolymph $[HCO_3^-]_e$ was calculated as:

$$[HCO_3^-]_e = C_eCO_2 - (\alpha CO_2 \cdot P_eCO_2) \quad (3)$$

with C_eCO_2 = total CO_2 concentration [mM], αCO_2 = solubility of CO_2 in seawater (calculated from Weiss 1974: 4 °C, 31.15 psu: 0.5610 mmol L^{-1} kPa^{-1}; 10 °C, 31.15 psu: 0.4583 mmol L^{-1} kPa^{-1}), P_eCO_2 = partial pressure of CO_2 in haemolymph [kPa].

After haemolymph sampling, animals were dissected, the wet soft tissues were weighed (to the nearest 0.1 g) and tissues samples were freeze clamped and stored in liquid N_2 or at -80 °C for further analysis.

Measurement of clapping performance

Experimental temperature was adjusted with a thermostat (Julabo, F32-HD), and the respective PCO_2 levels of ~ 0.039 kPa (normocapnia) and ~ 0.112 kPa (hypercapnia) were reached by bubbling the water with either air or a mixture of CO_2 and air via a multi-gas controller (MKS, PR4000). Determination of clapping performance was carried out following procedures described in previous studies (see Bailey et al. 2003; Fleury et al. 2005 and Guderley et al. 2009).

The measurements were performed using a force gauge (Mecmesin Advanced Force Gauge, 50 N). In the experimental tank, scallops were fixed on a plate using a hook-and-loop fastener (see Fig. 1 a for experimental set up). The lower valve was additionally immobilized with two clamps and stabilized with dental wax. The force gauge was placed on the front side of the scallop with a hook between its valves at an opening width, which was

observed for the undisturbed scallop (between 0.8 and 1.5 cm depending on the animal). After at least 12 h of recovery, clapping was induced by introducing aqua$_{dest}$ via a thin, gas-tight tube into the mantle cavity (see Bailey et al. 2005; Denny and Miller 2006). When the scallop stopped clapping, the stimulation was repeated until animals were fatigue and showed no response to further stimulation (after ~ 50 min). The force of the adductor muscle during time of clapping was measured with a frequency of 10 Hz. The opening width during claps was determined using a ruler and by video analysis (Logitech, Quick Cam E2500).

Force recordings were normalized before each analysis. A "clap" was defined as a short interval of great force difference produced by the scallop with a rapid valve closing via phasic contraction as described in Fleury et al. (2005). Number of claps and force strength were determined from force per time recordings. We calculated the total force F_{total} [N] of each animal by dividing the "force impulse" (measurement force [N] multiplied by measured time [s]) by total time [s]:

$$F_{total} = \frac{\int f dt}{t_{total}} \quad (4)$$

F_{total} is subdivided in a phasic part (force produced by the phasic adductor muscle) and a tonic part (force produced by the tonic muscle). The phasic force F_{phasic} [N] was calculated as sum of the clap force F_{clap} [N] (see Fig. 1 b). F_{clap} is the difference of the maximal force and the starting force during one clap. To calculate the mean phasic force $F_{mean\ phasic}$ [N] per one clap, F_{phasic} was divided by the number of claps:

$$F_{meanphasic} = \frac{\sum_i^n F_{clap}}{n} = \frac{F_{phasic}}{n} \quad (5)$$

where the claps are numbered from i to n.

The tonic force F_{tonic} [N] was calculated from the difference of F_{total} and F_{phasic}:

$$F_{tonic} = F_{total} - F_{phasic} = F_{total} - \frac{\sum_i^n F_{clap} \cdot t_{clap}}{t_{tonic}} \quad (6)$$

where t_{clap} is the average time per clap (0.25 s) and t_{total} is the total measurement time until the animal was fatigued, while t_{tonic} is the total time of all tonic phases. We calculated with t_{total} instead of t_{tonic}, which makes a negligible difference of 0.53 %, because $t_{tonic} = t_{total} - t_{phasic}$ and $t_{total} \approx t_{tonic}$ (with $t_{total} \sim 3000$ s compared with $t_{phasic} \sim 16$ s).

Measurement of metabolic rate

We measured respiration rates of normocapnia- and hypercapnia-exposed scallops using intermitted flow respirometry (cf. Heilmayer and Brey 2003; Tremblay et al.
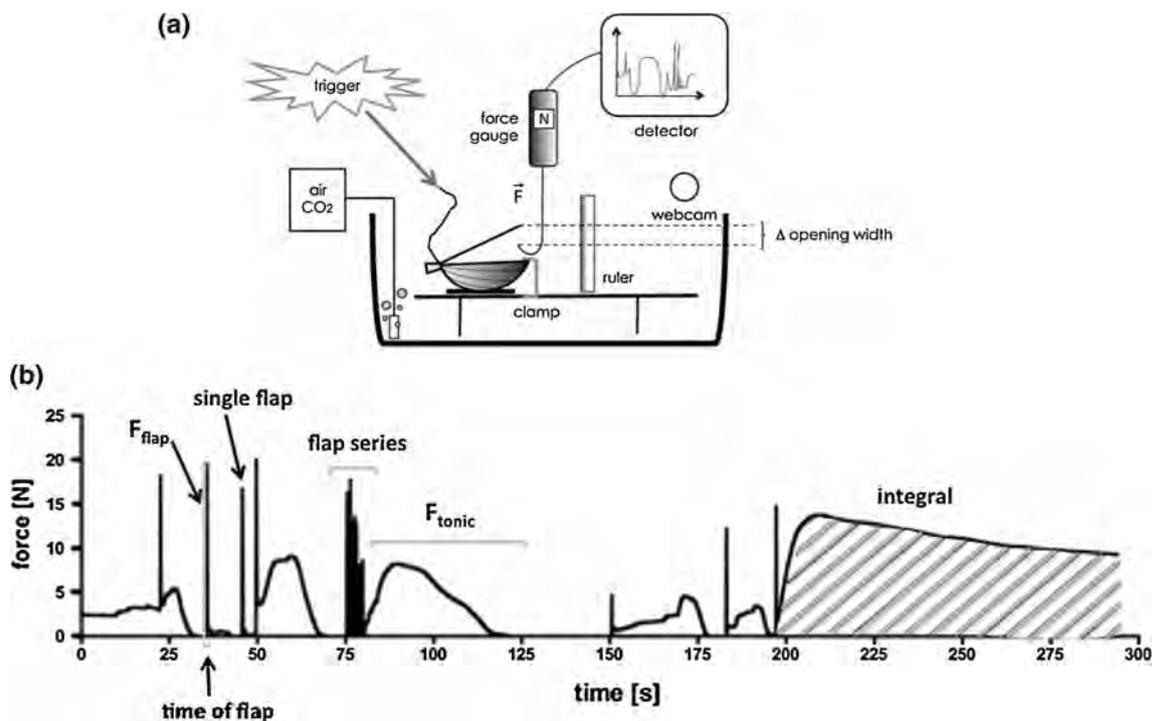
Fig. 1 Scheme of clapping performance data collection on *P. maximus*. **a** Experimental set up for force measurements. **b** Example for force recording and visualization of clap force (F_{clap}), single clap, clap series, tonic force (F_{tonic}), time of a clap (t_{phasic}), time of a tonic phase (t_{tonic}) and part of an integral (see text for details)

2006). The scallops were placed in respiration chambers (plexiglas chambers with a volume of ca. 1.5 L; one chamber per animal) and immobilized on the bottom of the chamber using hook-and-loop fastener. The respiration chambers were placed into the experimental tank with defined temperature and PCO_2 levels (see above). Oxygen saturation was measured with O_2 optodes from PreSens (Microx TX2 or TX3, PreSens, Neuweiler, Germany), and continuous water circulation inside the respiratory setup was performed by a peristaltic pump (Ismatec, type Ism404B; Ismatec MCP). In order to exclude animals with potential atypical behaviour without causing disturbances during measurements (similar to Heilmayer and Brey 2003), the scallops were monitored using a web cam under continuous, shaded light. For changes between flow-through and closed system, plastic quick couplings were used in a different compartment of the experimental tank separated by a water-permeable wall in order to avoid irritations and disturbances for the scallops. Prior to measurements, scallops were allowed to recover for at least 12 h. In each experiment, 3 respiration chambers were used simultaneously. Respiration in empty chambers was measured before and after each experiment to account for potential bacterial respiration (observed values were negligible).

Experimental runs were stopped when oxygen saturation was decreased to 75–70 % inside the chamber. Two to four runs were measured for each animal within 12 h. During nights, chambers were flooded and connected to the flow-through system. After measuring the oxygen consumption during resting metabolism, the respiration chambers were opened and the scallops were triggered to swim until fatigue as described above. After exhaustion, chambers were closed and the oxygen consumption measurements were started immediately and recorded until animals regained resting metabolic rates. The dry mass was calculated by applying the conversion factor 0.162, which was evaluated before using 20 separate *P. maximus*.

We calculated the oxygen consumption ($\dot{M}_{O2}$) [μmol O_2 h^{-1} gDW^{-1}] of the animal under resting and fatigue conditions as follows:

$$\dot{M}_{O2} = \alpha_{O2} \cdot V_{H2O} \cdot m\text{DM}^{-1} \cdot \frac{ds(O_2)}{dt} \qquad (7)$$

where α_{O2} is the oxygen solubility in seawater [μmol O_2 L^{-1} kPa^{-1}], V_{H2O} is the water volume [L] of the chamber $V_{chamber} - V_{animal}$, m_{DM} is the dry mass [g] of the animal and $s(O_2)$ is the oxygen consumption [kPa] over time t [h].

The net aerobic scope (NAS) [μmol O_2 h^{-1} gDW^{-1}] was calculated after Fry (1947) as

$$NAS = \dot{M}_{O2_{max}} - \dot{M}_{O2_{rest}} \qquad (8)$$

where $\dot{M}_{O2_{max}}$ is the maximal metabolic rate (MMR) after exercise and the $\dot{M}_{O2_{rest}}$ is the resting metabolic rate (RMR).

Statistical analysis

Data sets were analysed using SigmaPlot (Version 12.0, Systat Software, Inc.) and GraphPad Prism (Version 4.0a, GraphPad Software Inc.). Interactions between effects of CO_2 exposure and exercise on haemolymph parameters and respiration measurements as well as differences within these groups were considered significant if the probability of Type II error was less than 0.05 using Two Way Analysis of Variance and Two Way Repeated Measures ANOVA, respectively, in combination with a Holm–Sidak Test. Unpaired t test (Mann–Whitney rank sum test if normality test failed) was used to identify significant differences between normocapnia- and hypercapnia-exposed scallops in net aerobic scope (NAS) and for morphological parameters and force measurements. Results are presented in box plots, and values are given as mean $\pm$ SD if not stated otherwise.

Results

Scallop condition and mortality

From day 20 (normocapnia) and day 38 (hypercapnia) onward, 55 % of normocapnia- and 90 % of hypercapnia-exposed scallops died at 4 °C, whereas none of the scallops incubated at 10 °C died under normocapnic and just one under hypercapnic conditions (see Fig. 2). Condition indices of scallops before and after incubation did not differ between groups with a CI of 11.38 $\pm$ 1.38 (control group at the start of the experiment, $N = 20$) and with CIs at the end of the experiment of 11.70 $\pm$ 1.94 (4 °C normocapnia, $N = 8$), 11.24 $\pm$ 0.96 (10 °C normocapnia, $N = 19$) and 11.63 $\pm$ 1.35 (10 °C hypercapnia, $N = 19$)
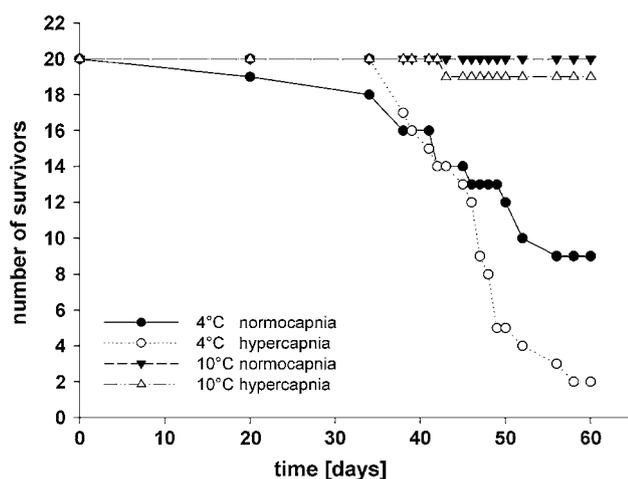

Fig. 2 Survival rate of *P. maximus* after long-term incubation under normocapnia (seawater PCO_2 $\sim$ 0.040 kPa) and hypercapnia (seawater PCO_2 $\sim$ 0.112 kPa) at two temperatures (4 and 10 °C), starting with $N = 20$

(mean $\pm$ SD, $F_{2,45} = 0.539$; $p = 0.587$). Muscle indices of scallops after incubation did not differ between groups with 3.66 $\pm$ 0.44 (4 °C normocapnia, $N = 8$), 3.34 $\pm$ 0.42 (10 °C normocapnia, $N = 19$) and 3.61 $\pm$ 0.42 (10 °C hypercapnia, $N = 19$) (mean $\pm$ SD, $F_{2,45} = 2.417$; $p = 0.1012$). Despite similar condition and muscle indices between the two temperature groups, we excluded both normocapnia- and hypercapnia-exposed scallops at 4 °C from further experimentation due to their stress level at rest as indicated by their high mortality.

Haemolymph acid–base parameters

Following OA exposure at 10 °C, scallops displayed significantly elevated P_eCO_2 ($F_{1,37} = 84.425$, $p < 0.001$), C_eCO_2 ($F_{1,36} = 42.403$, $p < 0.001$) and $[HCO_3^-]_e$ ($F_{1,35} = 27.039$, $p < 0.001$) and significantly lowered pH_e ($F_{1,36} = 61.861$, $p < 0.001$) values in both groups, resting and fatigued animals (Table 2). After exhaustive exercise, haemolymph values changed in a similar manner irrespective of ambient CO_2 level, resulting in significantly lowered P_eO_2 ($F_{1,36} = 28.385$, $p < 0.001$) and pH_e ($F_{1,36} = 15.652$, $p < 0.001$) and significantly elevated P_eCO_2 ($F_{1,37} = 35.293$, $p < 0.001$), C_eCO_2 ($F_{1,36} = 37.968$, $p < 0.001$) and $[HCO_3^-]_e$ ($F_{1,35} = 23.730$, $p < 0.001$) in

Table 2 Haemolymph parameters of *P. maximus* at rest and after exercise following long-term incubation under normocapnia (seawater PCO_2 $\sim$ 0.040 kPa) and hypercapnia (seawater PCO_2 $\sim$ 0.112 kPa) at 10 °C

Parameter	Normocapnia	Hypercapnia
RMR		
P_eO_2 [kPa]	6.52 $\pm$ 1.13	7.95 $\pm$ 2.47
P_eCO_2 [kPa]	0.13 $\pm$ 0.02	0.26 $\pm$ 0.06[*]
pH_e (NBS scale)	7.67 $\pm$ 0.06	7.42 $\pm$ 0.09[*]
C_eCO_2 [mM]	1.87 $\pm$ 0.15	2.11 $\pm$ 0.08[*]
$[HCO_3^-]_e$ [mM]	1.81 $\pm$ 0.15	1.98 $\pm$ 0.06[*]
MMR		
P_eO_2 [kPa]	3.71 $\pm$ 1.06[+]	4.05 $\pm$ 0.58[+]
P_eCO_2 [kPa]	0.20 $\pm$ 0.05[+]	0.43 $\pm$ 0.10[*, +]
pH_e (NBS scale)	7.54 $\pm$ 0.10[+]	7.32 $\pm$ 0.09[*, +]
C_eCO_2 [mM]	2.10 $\pm$ 0.09[+]	2.45 $\pm$ 0.16[*, +]
$[HCO_3^-]_e$ [mM]	1.96 $\pm$ 0.05	2.25 $\pm$ 0.13[*, +]

Data are mean $\pm$ SD with $N = 13$–15 (RMR) and $N = 4$–5 (MMR)

RMR resting metabolic rate, *MMR* maximal metabolic rate, P_eO_2/P_eCO_2 extracellular partial pressure of O_2/CO_2, pH_e extracellular pH, *NBS* National Bureau of Standards, C_eCO_2 extracellular total dissolved inorganic carbon, $[HCO_3^-]_e$ extracellular bicarbonate concentration

[*] Significant differences between normocapnic and hypercapnic data at same metabolic rate

[+] Significant differences between RMR and MMR at same CO_2 levels

fatigued compared with resting animals in both normocapnia and hypercapnia groups (Table 2).

Clapping performance and metabolic rate

OA exposure at 10 °C had no impact on clapping numbers ($F_{13,11} = 2.512$, $t_{1,24} = 0.0683$, $p = 0.9461$), but a strong effect on force production resulting in significantly lowered total force, mean phasic force and tonic force values (F_{total}: $F_{12,13} = 2.788$, $t_{1,25} = 4.776$, $p < 0.0001$; $F_{mean\ phasic}$: $F_{11,11} = 1.626$, $t_{1,22} = 3.976$, $p = 0.0006$; F_{tonic}: $F_{12,13} = 2.818$, $t_{1,25} = 4.758$, $p < 0.0001$) (Fig. 3). Recovery period and the time until scallops were fatigued were more or less similar in normocapnic and hypercapnic animals.

OA exposure at 10 °C had no effect on resting metabolic rate (RMR) with medians of 5.10 µmol O_2 h^{-1} gDW^{-1} (normocapnia) and 5.27 µmol O_2 h^{-1} gDW^{-1} (hypercapnia) (Fig. 4a). After exercise maximal metabolic rate (MMR) was significantly increased above that of the resting animals in both normocapnia- and hypercapnia-exposed scallops ($F_{1,40} = 145.503$, $p < 0.001$; Fig. 4a). However, the exercise-induced increase was lower in the hypercapnia group resulting in a significantly lower MMR ($F_{1,40} = 4.396$, $p < 0.05$) and net aerobic scope (NAS, Fig. 4b) in hypercapnia- than in normocapnia-exposed animals ($F_{8,9} = 1.937$, $t_{1,17} = 2.359$, $p = 0.0305$).

Discussion

Mortality

In contrast to incubation experiments at 10 °C, we observed a high mortality among scallops exposed to 4 °C (55 % under normocapnia, 90 % under hypercapnia) (see Fig. 2). This was unexpected as animals had been reared at their winter environmental temperatures of 3–5 °C (see "Materials and methods"). As water quality (e.g. ammonium/nitrite levels) was similar between incubations, we assume that the high mortality at 4 °C is related to a time-dependent effect: By keeping the animals continually at 4 °C, "physiological wintertime" may have been over-extended resulting in enhanced mortality. Against the background of the OCLTT concept, these animals may have been at the lower end of their thermal window too long. Factors reflecting insufficient functional capacity that might have decreased fitness and survival rate in the cold include insufficient food uptake and digestion capacities in the cold as enzymes operate below the thermal optimum (Brock et al. 1986), and/or ciliate beat frequency may be insufficient (Riisgård and Larsen 2007). However, we observed no difference in condition or muscle indices between 4 °C- and 10 °C-exposed scallops, and our overall means of condition index (11.48 ± 1.31, $N = 46$) and muscle index (3.54 ± 0.48, $N = 46$) are comparable to literature data of *P. maximus* showing CIs of 6–10 and MIs of 3–6 in positively growing specimens (Pazos et al. 1997, CI was calculated from reported tissue and shell weights). Similar CI values between 10 and 25 are reported for juvenile bay scallops *Argopecten irradians* (Shriver et al. 2002). Specific reasons causing enhanced mortality and involving OCLTT capacity limitation (e.g. circulatory limitation) thus remain to be identified. In line with earlier findings on the warm side of the thermal tolerance window (see "Introduction"), our study indicates that OA exposure may have shifted the animals from pejus further to the critical range at the cold side of the thermal tolerance window.

Fig. 3 Data for clapping performance of *P. maximus* after long-term incubation under normocapnia (seawater $PCO_2 \sim 0.040$ kPa) and hypercapnia (seawater $PCO_2 \sim 0.112$ kPa) at 10 °C. **a** Total number of claps until fatigue ($N = 12$–14). **b** Total force ($N = 13$–14). **c** Mean phasic force ($N = 12$). **d** Tonic force ($N = 13$–14). Data are depicted in *boxplots*; *asterisk* significant differences between normocapnic and hypercapnic data
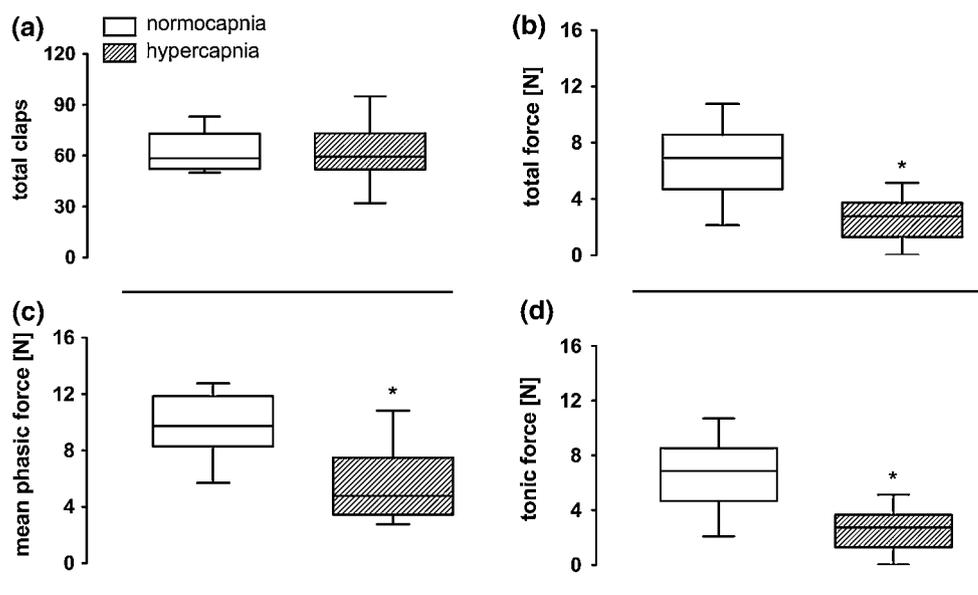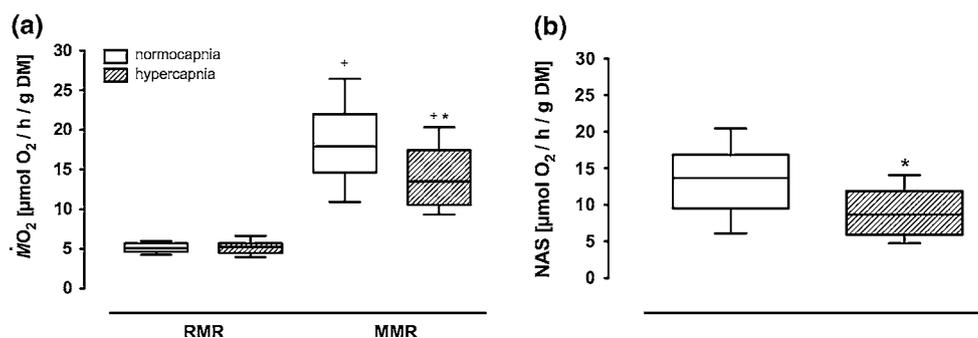
Fig. 4 Oxygen consumption ($\dot{M}_{O2}$) of *P. maximus* after long-term incubation under normocapnia (seawater $PCO_2 \sim 0.040$ kPa) and hypercapnia (seawater $PCO_2 \sim 0.112$ kPa) at 10 °C. **a** Oxygen consumption at rest (RMR) and after exercise (MMR) ($N = 9–13$). **b** Net aerobic scope (NAS; $N = 9$–10). Data are depicted in *boxplots*; *asterisks* significant differences between normocapnic and hypercapnic data. [+]significant differences between RMR and MMR

The hypothesis of cold limited tolerance is further supported by observations by Strand and Brynjeldsen (2003) who reported an extraordinarily high mortality rate (52–100 %) among juvenile *P. maximus* along the coast of Norway during an abnormally cold winter (1995/6) at temperatures between 2 and 4 °C. The normal temperature profile experienced by scallops from the Stavanger region since 2000 usually yielded monthly means of 5 °C at a depth of around 20 m, and during that whole period, there was only 1 month with a mean below 5 °C (Institute of Marine Research, Norway 2012). Furthermore, scallops survived well for more than 10 months in our aquarium system at 5 °C supporting our hypothesis that *P. maximus* may have reached its lower thermal limit at around 4 °C leading to an increase in mortality.

Haemolymph acid–base parameters

Scallops under hypercapnia had a lower pH_e, a higher P_eCO_2, bicarbonate and C_eCO_2 level than normocapnic animals, indicating that *P. maximus* did not compensate for the extracellular acidosis under long-term OA exposure. As already shown in other studies (e.g. Lindinger et al. 1984; Walsh et al. 1984; Michaelidis et al. 2005; Melzner 2009), the capacity for extracellular pH regulation is low in bivalves, including scallops. Similar to oysters (Lannig et al. 2010), scallops showed a significant, albeit small elevation in bicarbonate concentrations under hypercapnia. This indicates no or only a small degree of compensation of the acid–base disturbance in the haemolymph. Passive compensation depends on the level of non-bicarbonate buffer value that was not determined. Other bivalves, for example, *Mytilus edulis*, have haemolymph non-bicarbonate buffer lines ($\beta_{NB} = 0.4$ mmol L^{-1} pH^{-1}, Booth et al. 1984) similar to seawater (0.3 mmol L^{-1} pH^{-1}). It seems that in bivalves in general, a CO_2 induced acidosis remains largely uncompensated, due to low buffering and limited capacity of proton equivalent ion exchange.

Exhaustive exercise at 10 °C significantly affected *P. maximus* haemolymph parameters (see Table 2). Under both normocapnic and hypercapnic conditions, values of pH_e and P_eO_2 of the fatigued scallops decreased, while P_eCO_2, C_eCO_2 and bicarbonate levels increased compared with findings in resting scallops. The lack of respiratory pigments, the poor perfusion of the adductor muscle and its low mitochondrial density reflect insufficient supply and use of oxygen by the phasic adductor muscle that largely operates anaerobically during swimming (de Zwaan et al. 1980; Thompson et al. 1980). Exercising scallops mainly catabolize phospho-L-arginine and then glycogen stored in their adductor muscle (e.g. *Argopecten irradians* can use about 23–25 % of the glycogen stored in the adductor muscle, Epp et al. 1988). Glycolysis leads to octopine formation, largely during recovery after swimming (Grieshaber and Gäde 1977; Gäde et al. 1978; Chih and Ellington 1983); succinate formation may result from oxygen deficiency at mitochondrial level. In fact, P_eO_2 remains low during recovery, such that scallops initially recover under hypoxic conditions, associated with a rise in P_eCO_2 due to insufficient ventilation (MacDonald et al. 2006). An acidosis would thus result from respiratory CO_2 accumulation and non-respiratory proton release during anaerobic end product formation in excess of the proton consumption by phospho-L-arginine degradation (Pörtner 1987). The rise in metabolic rate after exhaustive exercise in scallops (see Fig. 4) is due to increased energy demands during glycogen resynthesis and involves the oxidative degradation of anaerobic end products like D-octopine (MacDonald et al. 2006).

Clapping performance and metabolic rate

Present data of around 62 claps until fatigue (independent of CO_2 level) fit very well with the 57 claps obtained by Bailey et al. (2003) for *P. maximus* at 12 °C. As shown by the same study, great differences in clapping performance

exist between scallop species, regardless of temperature. The authors compared the number of claps until exhaustion of three species, the Antarctic scallop, *Adamussium colbecki,* and two temperate species, *Aequipecten opercularis* and *P. maximus*. Each species was measured at its respective habitat temperature and the results varied between 24 claps (*A. opercularis*, 12 °C), 48 claps (*A. colbecki*, 0 °C) and the mentioned 57 claps (*P. maximus*, 12 °C). Fleury et al. (2005) elicited lower values of around 19 claps in the scallop *Placopecten magellanicus* at 9.5 °C, upon stimulation with starfish for 200 s. However, animals from that study were not taken to fatigue likely leading to an underestimation of the maximum possible clap numbers. Furthermore, the time of collection (season) seems to affect maximal clap numbers as shown by Guderley et al. (2009) where total clap numbers of *P. magellanicus* varied between 23 claps (spring) and 40 claps (autumn), both measured at 12 °C (close to habitat temperatures).

Our results on clapping performance and aerobic scope indicate an energetic trade-off under OA conditions at the expense of the scope of escape response. Although the number of claps was similar between normocapnic and hypercapnic animals at 10 °C, reduced force capacities in hypercapnic scallops revealed a significantly negative effect of OA exposure (see Fig. 3). The diminished activation of muscle fibres following OA exposure may indicate that ATP-consuming processes were slowed and energy demand reduced, which resulted in an weakened escape response. This effect may be mediated through the lowering of extracellular pH. In muscle tissues of marine invertebrates, extracellular acidosis slows ion exchange and acid–base regulation (Pörtner et al. 2000). The extracellular acidosis thereby mediates a slowing of myosin ATPase and the development of contractile force in muscle tissue (cf. Pörtner 2008). While oxygen consumption during rest (RMR) did not differ between normocapnia- and hypercapnia-exposed scallops at 10 °C, oxygen consumption following exhaustive exercise (MMR) was reduced in hypercapnic compared with normocapnic animals resulting in a significantly reduced net aerobic scope (NAS) by a factor of 1.49 in OA-exposed scallops (see Fig. 4).

The increase in oxygen consumption during exercise indicates enhanced aerobic energy provision on top of anaerobic metabolism. In sessile bivalves, feeding led to the highest oxygen consumption rates (Tremblay et al. 1998). Mackay and Shumway (1980) showed for the pectinid *Chlamys delicatula* that exercise (escape response) resulted in an even higher postexercise oxygen consumption rate than the rate seen during feeding. Therefore, net aerobic scope (NAS) calculated as the difference between oxygen consumption at rest and after exhaustive exercise can be assumed as the maximal NAS for scallops.

Limitations in functional capacity may be reached when cellular energy levels fall. According to Pörtner et al. (2004), OA-exposed animals would need to invest more energy into acid–base regulation. Our findings of reduced net aerobic scope indicate that OA-exposed animals at 10 °C reallocated available energy to, for example, ion regulation but at the expense of other processes, for example, activity. In the study of Wood et al. (2008), calcification rates and respiration rates of the brittlestar *Amphiura filiformis* exposed to hypercapnia were increased, but muscle mass was reduced instead. This "muscle wastage" was seen as a fast and time limited trade-off between structure (morphological integrity) and function (arm movement). In salmon and oysters, exposure to low pH or elevated PCO_2 led to a partial depletion of tissue energy reserves such as glycogen and lipids (Haya et al. 1985; Lannig et al. 2010; Dickinson et al. 2012).

Conclusion

Our study revealed that ocean acidification narrows the scope for exercise performance of the active calcifier, *Pecten maximus*. At elevated CO_2 levels, clapping force was reduced indicating that this species might become vulnerable to predators as their escape response is weakened following exposure to predicted OA scenarios. Our results seen together with those of other studies indicate that OA-induced energetic trade-offs exist, reducing the energy available for fitness-related processes such as locomotion, growth and/or stress resistance. The increased mortality among scallops exposed to 4 °C and elevated CO_2 levels implies an OA-induced exacerbation of cold stress, in line with a narrowing of the thermal tolerance range at the cold side. Further investigations at the cellular level are necessary to examine the allocation of metabolic power to different processes and to fully unravel the picture of OA-induced impacts on energy metabolism and associated energy reallocations.

References

Ansell A, Dao JC, Manson J (1991) Three European scallops: *Pecten maximus, Chlamys (Aequipecten) opercularis* and *C. (Chlamys) varia*. In: Shumway SE (ed) Scallops: biology, ecology and aquaculture, 1st edn. Elsevier, Amsterdam, pp 715–752

Bailey DM, Peck LS, Bock C, Pörtner HO (2003) High-energy phosphate metabolism during exercise and recovery in temperate and Antarctic scallops: an in vivo ^{31}P-NMR study. Physiol Biochem Zool 76(5):622–633. doi:10.1086/376920

Bailey DM, Johnston IA, Peck LS (2005) Invertebrate muscle performance at high latitude: swimming activity in the Antarctic scallop, *Adamussium colbecki*. Polar Biol 28:464–469. doi:10.1007/s00300-004-0699-9

Beniash E, Ivanina A, Lieb NS, Kurochkin I, Sokolova IM (2010) Elevated levels of carbon dioxide affect metabolism and shell formation in oysters *Crassostrea virginica*. Mar Ecol Prog Ser 419:95–108

Booth CE, McDonald DG, Walsh PJ (1984) Acid-base balance in the sea mussel, *Mytilus edulis*. I. Effects of hypoxia and air-exposure on hemolymph acid-base status. Mar Biol Lett 5:347–358

Brand AR (2006) Scallop ecology: distributions and behaviour. In: Shumway SE, Parson GJ (eds) Scallops: biology ecology and aquaculture, 1st edn. Elsevier, Amsterdam, pp 651–744. doi:10.1016/S0167-9309(06)80034-7

Brock V, Kennedy VS, Brock A (1986) Temperature dependency of carbohydrase activity in the hepatopancreas of thirteen estuarine and coastal bivalve species from the North American east coast. J Exp Mar Biol Ecol 103:87–101

Caldeira K, Wickett ME (2003) Anthropogenic carbon and ocean pH. Nature 425:365

Chih CP, Ellington WR (1983) Energy metabolism during contractile activity and environmental hypoxia in the adductor muscle of the Bay Scallop *Argopecten irradians concentricus*. Physiol Zool 56(4):623–631

de Zwaan A, Thompson RJ, Livingston DR (1980) Physiological and biochemical aspects of the valve snap and valve closure responses in the giant scallop *Placopecten magellanicus* II. Biochemistry. J Comp Physiol B 137:105–114

Denny M, Miller L (2006) Jet propulsion in the cold: mechanics of swimming in the Antarctic scallop *Adamussium colbecki*. J Exp Biol 209:4503–4514. doi:10.1242/jeb.02538

Dickinson GH, Ivanina AV, Matoo OB, Pörtner HO, Lannig G, Bock C, Beniash E, Sokolova IM (2012) Interactive effects of salinity and elevated CO_2 levels on juvenile eastern oysters, *Crassostrea virginica*. J Exp Biol 215:29–43. doi:10.1242/jeb.061481

Dickson AG, Millero FJ (1987) A comparison of the equilibrium constants for the dissociation of carbonic acid in seawater media. Deep-Sea Res 34(111):1733–1743

Doney SC, Fabry VJ, Feely RA, Kleypas JA (2009) Ocean acidification: the other CO_2 problem. Annu Rev Mar Sci 1:169–192

Epp J, Bricelj VM, Malouf RE (1988) Seasonal partitioning and utilization of energy reserves in two age classes of the bay scallop *Argopecten irradians irradians* (Lamarck). J Exp Mar Biol Ecol 121:113–136

Fabry VJ, Seibel BA, Feely RA, Orr JC (2008) Impacts of ocean acidification on marine fauna and ecosystem processes. ICES J Mar Sci 65:414–432

Findlay HS, Kendall MA, Spicer JI, Widdicombe S (2010) Relative influence of ocean acidification and temperature on intertidal post-larvae at the northern edge of their geographic distribution. Estuar Coast Shelf Sci 86:675–682

Fleury P-G, Janssoone X, Nadeau M, Guderley H (2005) Force production during escape responses: sequential recruitment of the phasic and tonic portions of the adductor muscle in juvenile sea scallop, *Placopecten magellanicus* (Gmelin). J Shellfish Res 24(4):905–911. doi:10.2983/0730-8000(2005)24[905:FPDERS]2.0.CO;2

Fry FE (1947) Effects of the environment on animal activity. Univ Toronto biol Ser 55. Pub Ont Fish Res Lab 68:1–62

Gäde G, Weeda E, Gabbott PA (1978) Changes in the level of octopine during the escape responses of the scallop, *Pecten maximus* (L.). J Comp Physiol 124:121–127

Grieshaber M, Gäde G (1977) Energy supply and the formation of octopine in the adductor muscle of the scallop, *Pecten jabobaeus* (Lamarck). Comp Biochem Physiol B 58:249–252

Gruffydd LD (1976) Swimming in *Chlamys islandica* in relation to current speed and an investigation of hydrodynamic lift in this and other scallops. Nor J Zool 24:365–378

Guderley H, Pörtner HO (2010) Metabolic power budgeting and adaptive strategies in zoology: examples from scallops and fish. Can J Zool 88:753–763

Guderley H, Labbé-Giguere S, Janssoone X, Bourgeois M, Pérez HM, Tremblay I (2009) Thermal sensitivity of escape response performance by the scallop *Placopecten magellanicus*: impact of environmental history. J Exp Mar Biol Ecol 377:113–119

Haya K, Waiwood BA, van Eeckhaute L (1985) Disruption of energy metabolism and smoltification during exposure of juvenile Atlantic salmon (*Salmo salar*) to low pH. Comp Biochem Physiol C 82(2):323–329

Heilmayer O, Brey T (2003) Saving by freezing? Metabolic rates of *Adamussium colbecki* in a latitudinal context. Mar Biol 143:477–484. doi:10.1007/s00227-003-1079-7

IPCC (2007) Climate Change 2007: the physical science basis. Summary for policymakers. Contribution of working group I to the fourth assessment report. The intergovernmental panel on climate change. www.ipcc.ch/SPM2feb07.pdf

Kroeker KJ, Kordas RL, Crim RN, Singh GG (2010) Meta-analysis reveals negative yet variable effects of ocean acidification on marine organisms. Ecol Lett 13:1419–1434

Langenbuch M, Pörtner HO (2003) Energy budget of hepatocytes from Antarctic fish (*Pachycara brachycephalum* and *Lepidonotothen kempi*) as a function of ambient CO_2: pH-dependent limitations of cellular protein biosynthesis? J Exp Biol 206:3895–3903

Langenbuch M, Pörtner HO (2004) High sensitivity to chronically elevated CO_2 levels in a eurybathic marine sipunculid. Aquat Toxicol 70:55–61. doi:10.1016/j.aquatox.2004.07.006

Lannig G, Eilers S, Pörtner HO, Sokolova IM, Bock C (2010) Impact of ocean acidification on energy metabolism of oyster, *Crassostrea gigas*—changes in metabolic pathways and thermal response. Mar Drugs 8:2318–2339. doi:10.3390/md8082318

Lewis E, Wallace DWR (1998) CO2SYS-Program developed for the CO_2 system calculations. Carbon dioxide information analysis center; Report ORNL/CDIAC-105, Oak Ridge, Tenn, USA

Lindinger MI, Lawren DJ, McDonald DG (1984) Acid–base balance in the sea mussel *Mytilus edulis*. Effects of environmental hypercapnia on intra and extracellular acid–base balance. Mar Biol Lett 5:371–381

MacDonald BA, Bricelj VM, Shumway SE (2006) Physiologie: energy acquisition and utilisation. In: Shumway SE, Parson GJ (eds) Scallops: biology, ecology and aquaculture, 1st edn. Elsevier, Amsterdam, pp 417–492. doi:10.1016/S0167-9309(06)80034-7

Mackay J, Shumway SE (1980) Factors affecting oxygen consumption in the scallop *Chlamys deliculata* (Hutton). Ophelia 19:19–26

Mehrbach C, Culberson CH, Hawley JE, Pytkowicz RM (1973) Measurement of the apparent dissociation constants of carbonic

acid in seawater at atmospheric pressure. Limnol Oceanogr 18(6):897–907

Melatunan S, Calosi P, Rundle SD, Moody AJ, Widdicombe S (2011) Exposure to elevated temperature and PCO_2 reduces respiration rate and energy status in the Periwinkle *Littorina littorea*. Physiol Biochem Zool 84(6):583–594. doi:10.1086/662680

Melzner F, Gutowska MA, Langenbruch M, Dupont S, Lucassen M, Thorndyke MC, Bleich M, Pörtner HO (2009) Physiological basis for high CO_2 tolerance in marine ectothermic animals: pre-adaptation through lifestyle and ontogeny? Biogeosciences 6:2313–2331

Melzner F, Stange P, Trübenbach K, Thomsen J, Casties I, Panknin U, Gorb SN, Gutowska A (2011) Food supply and seawater pCO_2 impact calcification and internal shell dissolution in the blue mussel *Mytilus edulis*. PLoS ONE 6(9):e24223. doi:10.1371/journal.pone.0024223

Metzger R, Sartoris F, Langenbuch M, Pörtner HO (2007) Influence of elevated CO_2 concentrations on thermal tolerance of the edible crab *Cancer pagurus*. J Therm Biol 32(3):144–151. doi:10.1016/j.jtherbio.2007.01.010

Michaelidis B, Ouzounis C, Paleras A, Pörtner HO (2005) Effects of long-term moderate hypercapnia on acid–base balance and growth rate in marine mussels *Mytilus galloprovincialis*. Mar Ecol Prog Ser 293:109–118

Orr JC (2011) Recent and future changes in ocean carbonate chemistry. In: Gattuso J-P, Hansson L (eds) Ocean acidification. Oxford University Press, Oxford, pp 41–66

Parker LM, Ross PM, O′Connor WA (2009) The effect of ocean acidification and temperature on the fertilization and embryonic development of the Sydney rock oyster *Saccostrea glomerata* (Gould 1850). Glob Change Biol 15:2123–2136. doi:10.1111/j.1365-2486.2009.01895.x

Pazos AJ, Román G, Acosta CP, Abad M, Sánchez JL (1997) Seasonal changes in condition and biochemical composition of the scallop Pecten maximus L. from suspended culture in the Ria de Arousa (Galicia, N.W., Spain) in relation to environmental conditions. J Exp Mar Biol Ecol 211:169–193

Pfeil B, Olsen A, Bakker DC et al. (2012) A uniform, quality controlled, Surface Ocean CO2 Atlas (SOCAT). Earth system science data (in preparation). http://www.socat.info/. Accessed 29 Mar 2012

Philipp EE, Schmidt M, Gsottbauer C, Sänger AM, Abele D (2008) Size- and age-dependent changes in adductor muscle swimming physiology of the scallop *Aequipecten opercularis*. Mar Ecol Prog Ser 389:193–202. doi:10.3354/meps08141

Pörtner HO (1987) Contributions of anaerobic metabolism to pH regulation in animal tissues: theory. J Exp Biol 131:69–87

Pörtner HO (2002) Environmental and functional limits to muscular exercise and body size in marine invertebrate athletes. Comp Biochem Physiol A 133:303–321

Pörtner HO (2008) Ecosystem effects of ocean acidification in times of ocean warming: a physiologist's view. Mar Ecol Prog Ser 373:203–217. doi:10.3354/meps07768

Pörtner HO (2010) Oxygen- and capacity-limitation of thermal tolerance: a matrix for integrating climate-related stressor effects in marine ecosystems. J Exp Biol 213:881–893. doi:10.1242/jeb.037523

Pörtner HO, Bock C (2000) A contribution of acid-base regulation to metabolic depression in marine ectotherms. In: Heldmaier G, Klingenspor M (eds) Life in the cold, 1st edn. Springer, Berlin, pp 443–458

Pörtner HO, Farrell AP (2008) Physiology and climate change. Science 322:690–692

Pörtner HO, Reipschläger A, Heisler N (1998) Metabolism and acid-base regulation in *Sipunculus nudus* as a function of ambient carbon dioxide. J Exp Biol 201:43–55

Pörtner HO, Bock C, Reipschläger A (2000) Modulation of the cost of pH_i regulation during metabolic depression: a ^{31}P-NMR study in invertebrate (*Sipunculus nudus*) isolated muscle. J Exp Biol 203:2417–2428

Pörtner HO, Langenbuch M, Reipschläger A (2004) Biological impact of elevated ocean CO_2 concentrations: lessons from animal physiology and earth history. J Oceanogr 60:705–718

Riisgård HU, Larsen PS (2007) Viscosity of seawater controls beat frequency of water-pumping cilia and filtration rate of mussels *Mytilus edulis*. Mar Ecol Prog Ser 343:141–150. doi:10.3354/meps06930

Scheibling RE, Hatcher BG, Taylor L, Barbeau MA (1995) Seeding trial of the giant scallop (*Placopecten magellanicus*) in Nova Scotia. In: Lubet P, Barret J, Dao J-C (eds) Fisheries, biology and aquaculture of Pectinids. 8th International Pectinid Workshop, Cherbourg, France, 22nd–29th May, 1991, IFREMER, Actes de Colloques 17:123–129

Shriver AC, Carmichael RH, Valiela I (2002) Growth, condition, reproductive potential, and mortality of bay scallops, *Argopecten irradians*, in response to eutrophic-driven changes in food resources. J Exp Mar Biol Ecol 279:21–40

Sokolova IM, Frederich F, Bagwe R, Lannig G, Sukhotin AA (2012) Energy homeostasis as an integrative tool for assessing limits of environmental stress tolerance in aquatic invertebrates. Mar Environ Res 79:1–15. doi:10.1016/j.marenvres.2012.04.003

Strand Ø, Brynjeldsen E (2003) On the relationship between low winter temperatures and mortality of juvenile scallops, *Pecten maximus* L., cultured in western Norway. Aquacult Res 34:1417–1422

Strand Ø, Nylund A (1991) The reproductive cycle of the scallop *Pecten maximus* (L.) from two populations in Western-Norway, 60 N and 64 N. In: Shumway SE (ed) An international compendium of scallop biology and culture. Special Publication, World Aquaculture Society, Baton Rouge, pp 95–105

Stumpp M, Wren J, Melzner F, Thorndyke MC, Dupont S (2011) CO_2 induced acidification impacts sea urchin larval development I: elevated metabolic rates decrease scope for growth and induce developmental delay. Comp Biochem Physiol A 160:331–340. doi:10.1016/j.cbpa.2011.06.022

Thompson RJ, Livingstone DR, de Zwaan A (1980) Physiological and biochemical aspects of the valve snap and valve closure responses in the giant scallop *Placopecten magellanicus* I. Physiology. J Comp Physiol 137:97–104

Tremblay R, Myrand B, Guderley H (1998) Thermal sensitivity of organismal and mitochondrial oxygen consumption in relation to susceptibility of blue mussels, *Mytilus edulis* (L.), to summer mortality. J Shellfish Res 17:141–152

Tremblay I, Guderley HE, Fréchette M (2006) Swimming performance, metabolic rates, and their correlates in the Iceland scallop *Chlamys islandica*. Physiol Biochem Zool 79(6):1046–1057

Walsh PJ, McDonald G, Booth CE (1984) Acid-base balance in the sea mussel, *Mytilus edulis*. II. Effects of hypoxia and air-exposure on the intracellular acid-base status. Mar Biol Lett 5:359–369

Walther K, Sartoris FJ, Bock C, Pörtner HO (2009) Impact of anthropogenic ocean acidification on thermal tolerance of the spider crab *Hyas araneus*. Biogeosciences 6:2207–2215

Weiss RF (1974) Carbon dioxide in water and seawater: the solubility of a non-ideal gas. Mar Chem 2:203–215

Wiborg KF (1963) Some observations on the Iceland scallop *Chlamys islandica* (Müller) in Norwegian waters. Fiskeridirecktoratets Skrifter. Serie Havundersøkelser 13:38–53

Wieser W, Medgyesy N (1990) Cost and efficiency of growth in the larvae of two species of fish with widely differing metabolic rates. Proc Biol Sci 242(1303):51–56

Wilkens LA (2006) Neurobiology and behaviour of the scallop. In: Shumway SE, Parson GJ (eds) Scallops: biology, ecology and

aquaculture, 1st edn. Elsevier, Amsterdam, pp 317–356. doi:10.1016/S0167-9309(06)80034-7

Winter MA, Hamilton PV (1985) Factors influencing swimming in Bay Scallops, *Argopecten irradians* (Lamarck, 1819). J Exp Mar Biol Ecol 88:227–242

Wood H, Spicer JI, Widdicombe S (2008) Ocean acidification may increase calcification rates, but at a cost. Proc R Soc Lond B 275:1767–1773

Zittier ZM, Hirse T, Pörtner HO (2012) The synergistic effects of increasing temperature and CO_2 levels on activity capacity and acid-base balance in the spider crab, *Hyas araneus*. Mar Biol. doi:10.1007/s00227-012-2073-8

S2

ORIGINAL ARTICLE

Morphological and genetic analyses of xeniid soft coral diversity (Octocorallia; Alcyonacea)

Kristina Stemmer · Ingo Burghardt · Christoph Mayer · Götz B. Reinicke · Heike Wägele · Ralph Tollrian · Florian Leese

Abstract Studies on the biodiversity and evolution of octocorals are hindered by the incomplete knowledge of their taxonomy, which is due to few reliable morphological characters. Therefore, assessment of true species diversity within abundant and ecologically important families such as Xeniidae is difficult. Mitochondrial genes provide a reliable solution to this problem for a wide range of taxa. However, low mutation rates of the mitochondrial DNA in octocorals result in insufficient variability for species discrimination. We compared the variation of a fragment of the Signal Recognition Particle 54 gene (SRP54, proposed for octocorals) and the mitochondrial ND6/ND3 marker among members of the xeniid genera *Ovabunda*, *Xenia*, *Heteroxenia* and *Bayerxenia*. The mean uncorrected pairwise sequence divergence was 39 % for SRP54 compared to 2 % for ND6/ND3. Morphological assignments were not always supported by genetics: Species diversity was underestimated (one case) or overestimated, probably reflecting intraspecific polymorphisms or hinting at recent speciations. ND6/ND3 is informative for some species-level assignments, whereas SRP54 shows the variability needed for species delimitations within this understudied taxon. Our results on both genes show their potential for evolutionary and biodiversity studies in Xeniidae.

Keywords Xeniidae · SRP54 · ND6/ND3 · Molecular marker · Systematics · Phylogeny

Kristina Stemmer and Florian Leese contributed equally to this study.

K. Stemmer · C. Mayer · R. Tollrian · F. Leese
Department of Animal Ecology, Evolution and Biodiversity,
Ruhr University Bochum, Bochum, Germany

C. Mayer · H. Wägele
Zoologisches Forschungsmuseum Alexander Koenig,
Bonn, Germany

K. Stemmer (✉)
Functional Ecology, Alfred Wegener Institute for Polar and Marine Research, Bremerhaven, Germany
e-mail: kristina.stemmer@awi.de

G. B. Reinicke
Deutsches Meeresmuseum, Stralsund, Germany

I. Burghardt
Leibniz-Center for Tropical Marine Ecology, Bremen, Germany

Introduction

Species within the alcyonacean soft coral family Xeniidae, in particular the genera *Ovabunda*, Alderslade (2001), *Xenia*, Lamarck (1816), *Bayerxenia*, Alderslade (2001) and *Heteroxenia*, Kölliker (1874), are essential members of tropical reef communities throughout the Indo-West-Pacific and the Red Sea. They play an important role in recolonising destroyed reef areas even before algae can grow (Reinicke 1995). Furthermore, their natural products are of interest to biochemists (Affeld et al. 2009; Anta et al. 2002). Since xeniid soft corals have a mutualistic symbiotic relationship with the dinoflagellate *Symbiodinium*, ecologists are concerned that they may be affected severely by climate change (Strychar et al. 2005). Xeniids are also an important food source for stenophagous nudibranchs, especially the genus *Phyllodesmium* (Burghardt and Waegele 2004; Burghardt et al. 2008a), and a radiation of the genus on this enigmatic soft coral family has been discussed recently (Waegele et al. 2010).

The main problem in soft coral research is the identification of most corals to species level due to few reliable

morphological characters in this understudied taxon (Reinicke 1995; Alderslade 2001; Berntson et al. 2001; McFadden et al. 2006). Hence, species identification prior to any phylogenetic or ecological studies is challenging, and using genetic markers additional to morphological characters becomes very important (Hebert et al. 2003a, b). In most eukaryotic organisms, mitochondrial DNA (mtDNA), in particular a fragment of the cytochrome c oxidase subunit I (COI), has been established as a barcode marker because of its relatively high mutation rate (Hebert et al. 2003b, 2004; Ward et al. 2005) and has been used successfully in phylogenetic analyses on the genus and family level (e.g. Hülsken et al. 2011). Unfortunately, COI is less variable in Cnidaria (Anthozoa and Medusozoa) than in most other taxa (Huang et al. 2008). Particularly, the substitution rate in the mitochondrial genome of the anthozoans has been reported to be about 100 times slower than in other metazoan taxa (France and Hoover 2001, 2002; Shearer et al. 2002). Therefore, the discrimination power of mitochondrial markers is limited within anthozoans (Hellberg 2006; McFadden et al. 2010a, b; Park et al. 2012; Shearer and Coffroth 2008).

In recent studies, even the fastest evolving mitochondrial regions lacked the resolution necessary to distinguish soft coral species within genera (McFadden and Hutchinson 2004; McFadden et al. 2006). For example, McFadden et al. (2006) used different mitochondrial markers (e.g. ND2, msh1) for phylogenetic analysis of octocorals, which unfortunately showed insufficient intrageneric resolution within the Xeniidae. COI and the extended mitochondrial DNA barcode COI+igr1+msh1, recently analysed by McFadden et al. (2010b), could not distinguish *Xenia* and *Heteroxenia*. In contrast, the nuclear DNA of anthozoans appears to accumulate mutations at the same rate or even faster as compared to other animal groups (Hellberg 2006; Chen et al. 2008). Consequently, most molecular coral research currently focuses on nuclear DNA markers for species-level studies. Several nuclear intron markers have been investigated for this purpose in scleractinian corals (Hatta et al. 1999; van Oppen et al. 2000, 2001, 2004), with limited success in only few taxa. The multi-copy marker ITS-1 (Internal Transcribed Spacer) has been used to reconstruct species-level relationships in some octocoral and scleractinian genera (Fukami et al. 2004; McFadden et al. 2001; McFadden and Hutchinson 2004; van Oppen et al. 2000, 2002; Forsmann et al. 2010; Flot et al. 2011) but the marker is not always reliable for species-level phylogeny (Vollmer and Palumbi 2004; Wei et al. 2006). Recently, Concepcion et al. (2008) introduced a hypervariable, single-copy nuclear marker that can be used for phylogenetic investigation of closely related soft coral taxa: the 54-kDa subunit of the Signal Recognition Particle (SRP54). Their results revealed a great number of differences between sequences even

between closely related taxa. Pairwise sequence divergences within octocorals were 8–13 times greater for SRP54 than for mtDNA. Among scleractinian corals, within the same genus, even up to 2.8 % pairwise sequence divergence was found for the SRP54 fragment, whereas no variation was found for the mtDNA markers at all. Concepcion et al. (2008) sequenced eight individuals of xeniids and reported up to 17 % pairwise sequence divergence among specimens based on a 129-bp SRP54 alignment.

Due to the reported high variability, we applied this promising and highly variable nuclear marker to analyse species-level assignments and phylogenetic relationships between species of the xeniid genera *Ovabunda, Xenia*, *Heteroxenia* and *Bayerxenia*. We also analysed the slow evolving ND6/ND3 gene fragment for assessing and comparing its suitability for biodiversity studies on xeniid soft corals. Furthermore, we tested and discussed species assignments based upon morphological characters with the SRP54 and ND6/ND3 markers. Finally, we discussed the potential use of these genes as possible barcode markers.

Methods

Sampling

Specimens were collected from selected sites in the Indo-Pacific and the Red Sea by SCUBA diving or snorkelling (Table 1; Supplementary material). Samples were initially preserved in either absolute ethanol for further DNA analysis or in 7 % formalin in seawater for morphological investigation. All samples were transferred again into absolute ethanol and stored at 4 °C. Alternatively, when no suitable ethanol for preservation was available, a high percentage spirit such as gin was used for specimen preservation.

Species determination and morphological analyses

Taxonomic identification to the genus and, when possible, species level was performed by applying character analysis according to Reinicke (1995, 1997) and the systematic revisions from Alderslade (2001).

Morphology was investigated under a stereomicroscope. For investigation of sclerites, whole tissue material was dissolved in 10 % NaClO. The sclerites were then washed in distilled water, centrifuged, mounted and finally spattered with gold. Electron microscope images were taken with a scanning electron microscope (ZEISS DSM 950, Fig. 2).

DNA analysis

The DNeasy® Mini Kit (Qiagen, Valencia, CA) was used to extract octocoral genomic DNA according to the animal

Table 1 Species, GenBank accession numbers (Gbn #) from SRP54 and ND6/ND3, collection site and date for the xeniid specimens analyzed. The column "clade" refers to the genetically defined phylogenetic lineage based on the SRP54 alignment

Species	SRP Gbn #	ND6/ND3 Gbn #	Clade	Collection date	Collection site
Ovabunda faraunensis_04	KC341803	KC341874	1	2008.04.25	Dahab: Housereef
Ovabunda faraunensis_06	KC341805	KC341875	1	2008.04.25	Dahab: Housereef
Ovabunda faraunensis_09	KC341813	KC341876	1	2008.04.26	Dahab: Three pools
Ovabunda faraunensis_12	KC341804	KC341877	1	2008.04.28	Dahab: Moray eel garden
Ovabunda faraunensis_13	KC341808	KC341878	1	2008.04.30	Dahab: Three pools
Ovabunda faraunensis_17	KC341806	KC341879	1	2008.04.30	Dahab: Three pools
Ovabunda faraunensis_22	KC341815	KC341880	1	2008.05.05	Dahab: Lagoon
Ovabunda macrospiculata_02	KC341807	KC341881	1	2008.04.27	Dahab: Moray eel garden
Ovabunda macrospiculata_03	KC341814	KC341882	1	2008.05.05	Dahab: Lagoon
Ovabunda macrospiculata_06	KC341818	KC341883	1	2008.05.05	Dahab: Lagoon
Ovabunda macrospiculata_07	KC341819	KC341884	1	2008.05.05	Dahab: Lagoon
Ovabunda macrospiculata_08	KC341812	KC341885	1	2008.05.05	Dahab: Lagoon
Ovabunda macrospiculata_09	KC341816	KC341886	1	2008.05.13	Dahab: Lagoon
Ovabunda macrospiculata_10	KC341809	KC341887	1	2008.05.13	Dahab: Lagoon
Ovabunda macrospiculata_11	KC341810	KC341888	1	2008.05.13	Dahab: Lagoon
Ovabunda macrospiculata_12	KC341811	KC341889	1	2008.05.13	Dahab: Lagoon
Ovabunda macrospiculata_13	KC341817	KC341890	1	2008.05.13	Dahab: Lagoon
Xenia sp.*1_01*	KC341820	KC341891	2	2007.07.13	Palawan: Dimakya
Xenia sp.*2_01*	KC341821	KC341892	2	2007.07.15	Palawan: Dimakya
Xenia sp.*3_03*		KC341893			
Xenia sp.*3_04*	KC341822	KC341894	3	2007.06.28	Lizard Island: on pipe
Xenia sp.*3_05*	KC341823	KC341895	3	2007.06.29	Lizard Island: on pipe
Xenia sp.*3_06*	KC341824	KC341896	3	2007.06.29	Lizard Island: on pipe
Xenia sp.*3_08*	KC341825	KC341897	3	2007.07.01	Lizard Island: Loomis beach
Xenia sp.*3_09*	KC341831	KC341898	3	2007.07.01	Lizard Island: Loomis beach
Xenia sp.*3_10*	KC341832	KC341899	3	2007.07.01	Lizard Island: Loomis beach
Xenia sp.*3_11*	KC341826	KC341900	3	2007.07.01	Lizard Island: Loomis beach
Xenia sp.*3_12*	KC341827	KC341901	3	2007.07.01	Lizard Island: Loomis beach
Xenia sp.*3_13*	KC341828	KC341902	3	2007.07.01	Lizard Island: Loomis beach
Xenia sp.*4_02*	KC341829	KC341903	4	2007.06.29	Lizard Island: on pipe
Xenia sp.*4_03*	KC341830	KC341904	4	2007.07.02	Lizard Island: on pipe
Xenia sp.*5_01*	KC341773	KC341905	5	2007.07.01	Lizard Island: Loomis beach
Xenia sp.*6_01(a/b)*	KC341774/75	KC341906	7	2007.07.13	Palawan: Dimakya
Heteroxenia ghardaqensis_02	KC341794	KC341865	4	2008.04.28	Dahab: Moray eel garden
Heteroxenia ghardaqensis_03	KC341795	KC341866	4	2008.04.28	Dahab: Moray eel garden
Heteroxenia ghardaqensis_04	KC341796	KC341867	4	2008.04.28	Dahab: Moray eel garden
Heteroxenia ghardaqensis_05	KC341797	KC341868	4	2008.04.28	Dahab: Moray eel garden
Heteroxenia ghardaqensis_06	KC341798	KC341869	4	2008.04.28	Dahab: Moray eel garden
Heteroxenia ghardaqensis_07	KC341799	KC341870	4	2008.05.05	Dahab: Lagoon
Heteroxenia ghardaqensis_08	KC341800	KC341871	4	2008.05.05	Dahab: Lagoon
Heteroxenia ghardaqensis_09	KC341801	KC341872	4	2008.05.05	Dahab: Lagoon
Heteroxenia guardaqensis_10	KC341802	KC341873	4	2008.05.05	Dahab: Lagoon
Bayerxenia sp.*1_01*	KC341757	KC341833	5	2007.08	Bali: Uthamuda
Bayerxenia sp.*1_02*	KC341758	KC341834	5	2007.08	Bali: Uthamuda
Bayerxenia sp.*1_03*	KC341759	KC341835	5	2007.08	Bali: Uthamuda
Bayerxenia sp.*1_04*	KC341760	KC341836	5	2007.08	Bali: Uthamuda
Bayerxenia sp.*1_05*	KC341761	KC341837	5	2007.08	Bali: Uthamuda
Bayerxenia sp.*1_06*	KC341762	KC341838	5	2007.08	Bali: Tempokchantik

Table 1 (continued)

Species	SRP Gbn #	ND6/ND3 Gbn #	Clade	Collection date	Collection site
Bayerxenia sp.*1_07*	KC341763		5	2007.08	Bali: Tempokchantik
Bayerxenia sp.*1_09*	KC341764	KC341839	5	2007.08	Bali: Tempokchantik
Bayerxenia sp.*1_10*	KC341765		5	2007.08	Bali: Tempokchantik
Bayerxenia sp.*1_11*	KC341766	KC341840	5	2007.08	Bali: Tempokchantik
Bayerxenia sp.*2_01*	KC341767	KC341841	5	2007.06.22	Lizard Island: Casuarina beach
Bayerxenia sp.*2_03*	KC341768	KC341842	5	2007.06.28	Lizard Island: Loomis beach
Bayerxenia sp.*2_05*	KC341769	KC341843	5	2007.06.28	Lizard Island: Loomis beach
Bayerxenia sp.*2_06*	KC341770	KC341844	5	2007.06.29	Lizard Island: on pipe
Bayerxenia sp.*2_09*	KC341771	KC341846	5	2007.06.29	Lizard Island: on pipe
Bayerxenia sp.*2_04*	KC341789	KC341850	6	2007.06.29	Lizard Island: on pipe
Bayerxenia sp.*2_08*	KC341790	KC341845	6	2007.07.01	Lizard Island: Loomis beach
Bayerxenia sp.*2_10*	KC341791	KC341847	6	2007.07.01	Lizard Island: Loomis beach
Bayerxenia sp.*2_11*	KC341792	KC341851	6	2007.07.02	Lizard Island: on pipe
Bayerxenia sp.*2_12*	KC341793	KC341848	6	2007.06.25	Lizard Island: Loomis beach
Bayerxenia sp.*3_01*	KC341772	KC341849	5	2007.06.22	Lizard Island: Vicky's Reef
Heteroxenia fuscescens_01	KC341777	KC341853	8	2008.04.28	Dahab: Moray eel garden
Heteroxenia fuscescens_02	KC341778	KC341854	8	2008.04.28	Dahab: Moray eel garden
Heteroxenia fuscescens_03	KC341779	KC341859	8	2008.04.28	Dahab: Moray eel garden
Heteroxenia fuscescens_04	KC341780	KC341860	8	2008.04.29	Dahab: Front of Sinai Divers
Heteroxenia fuscescens_05	KC341781	KC341855	8	2008.04.29	Dahab: Front of Sinai Divers
Heteroxenia fuscescens_06	KC341782	KC341856	8	2008.04.29	Dahab: Front of Sinai Divers
Heteroxenia fuscescens_07	KC341783	KC341857	8	2008.05.05	Dahab: Lagoon
Heteroxenia fuscescens_08	KC341784	KC341861	8	2008.05.07	Dahab: Nabaq
Heteroxenia fuscescens_10	KC341785	KC341862	8	2008.05.07	Dahab: Nabaq
Heteroxenia fuscescens_11	KC341776	KC341863	8	2008.05.07	Dahab: Nabaq
Heteroxenia fuscescens_12	KC341786	KC341864	8	2008.05.07	Dahab: Nabaq
Heteroxenia fuscescens_13	KC341787	KC341852	8	2008.05.13	Dahab: Lagoon
Heteroxenia fuscescens_14	KC341788	KC341858	8	2008.05.13	Dahab: Lagoon

tissue protocol. Approximately 2 mg of tissue was cut from a polyp of each sample with sterilised scissors and dried on a sterile paper. Instead of 2×200 µl AE-buffer as outlined in the protocol, only 2×100 µl was added to the spin column and incubated for 5 min before elution. Protocols for amplifying the fragment of the mitochondrial NADH subunit 6 and NADH subunit 3 (ND6 and ND3) were adapted from McFadden et al. (2004). For the amplification of SRP54, three different primer pairs were tested: one primer pair published by Concepcion et al. (2008) and two newly designed pairs (Table 2). The new primers were designed using sequence alignment information of xeniid sequences from GenBank (Concepcion et al. 2008). Due to the great variability, several wobble bases were introduced to the primers (Table 2). The optimal annealing temperature was assessed using a gradient PCR. A concentration of 0.03 U/µl of EuroTaq polymerase (Biocat) and a final concentration of 1.5 mM $MgCl_2$ were used for the PCR. Thermal cycling conditions were: an initial denaturation at 94 °C for 2 min followed by 35 cycles, each with

94 °C for 20 s, annealing at the species-specific temperature for 30 s and an extension at 72 °C for 25 s, followed by a final 5-min extension step. Using an annealing temperature of 45 °C for samples identified as *Heteroxenia* and *Bayerxenia* produced the most distinct bands, whereas the best results were achieved at a higher temperature of 56 °C for samples identified as *Xenia* and *Ovabunda*. For the elimination of residual oligonucleotides and dNTPs from the PCR mixes, 3 µl of shrimp alkaline phosphatase (SAP, 1 U/µl) and 0.75 µl exonuclease I (Exo, 1 U/µl) were added to 16.25 µl of the PCR products, following an incubation at 37 °C for 15 min and an inactivation step at 80 °C for 15 min. The purified products were sent to the commercial sequencing companies Macrogen, Inc. (Seoul, Korea) and GATC-Biotech (Konstanz, Germany).

Phylogenetic analysis

DNA sequences were assembled, corrected and edited using the GENEIOUS 5.5 (Drummond et al. 2012).

Table 2 Primers developed for amplification of a SRP54 fragment in xeniids. Only primers SRP54-f2/r1 amplified successfully for xeniid specimens in this study

Primer name	Sequence
CrSRP54f	5′-CGAACTAAAATTAGAAGAAAACGAAG-3′
CrSRP54r	5′-TCATACATGTCTCTCAGCGTAAAC-3′
SRP54-f1	5′-GAAGGACTGATNGATAAAGTC-3′
SRP54-f2	5′-GAAGGACTGATNGATAAAGTCA-3′
SRP54-r1	5′-CAAWGTRAAYTGYCCTGAAGT-3′
SRP54-r2	5′-TGGAATTGNTCATACATGTC-3′

Multiple sequence alignment was performed using MAFFT v6.240 (Katho et al. 2002). *Asterospicularia* sp. (EU006867 for SRP54 and AF530513 for ND6/ND3) (Alderslade 2001), a member of the clearly distinct genus within the Xeniidae, was selected from GenBank as an additional member of the ingroup. Representatives of the genera *Muricea* (*M. purpurea*, GQ293342), *Alaskagorgia* sp. (GQ293337) and *Alcyonium* (*A. digitatum*, AF530498) were chosen as outgroup taxa for the ND6/ND3 analysis and *Sympodium caeruleum* (EU006855) for the SRP54 analysis. Maximum likelihood (ML) bootstrap trees with 10,000 replicates were computed with RAxML, version 7.3.0, using the GTRCAT model (Stamatakis 2006) with four rate categories. Bayesian tree reconstructions were performed using MrBayes v3.1.2 (Huelsenbeck 2001) by computing 10,000,000 generations in two runs, with four chains each. Trees were sampled every 100th generation. A burn-in was determined (1) by requiring that split frequencies were <0.01 and (2) by inspecting the time series of log posterior probabilities to ensure convergence. Appropriate DNA substitution models were determined using the Akaike information criterion (AIC) implemented in jModeltest (Posada 2008) (Table 3).

Results

Morphological analysis and taxonomy

In total, six different morphospecies of *Xenia*, two of the genus *Ovabunda*, two different morphospecies of *Heteroxenia* and three of the genus *Bayerxenia* could be identified. The four genera were distinguished on the basis of presence or absence of polyp dimorphism (Fig. 1) as well as the size and structure of sclerites (Fig. 2, Table 4) (see Alderslade 2001). Species assignment was based on colony morphology (general shape, size and organisation) and polyp morphology (especially pinnules and sclerite structure). All characters are listed in Table 4. Picture tables of all morphospecies are provided as an online resource and will be further referred to as "Figure (S1–6)". Voucher specimens have been deposited in the Museum of Stralsund (Germany) if not entirely used for DNA or sclerite analyses. Voucher numbers are also listed in Table 4.

Presence of distinct siphonozooids in analysed specimens led to an assignment to the genera *Heteroxenia* and *Bayerxenia* (Fig. 1a). Thirteen colonies studied from Dahab (Egypt, Red Sea) with unbranched single syndete growth forms but variable colours were referred to *Heteroxenia fuscescens* (Ehrenberg 1834) (Table 4). Analysis of the sclerite structure revealed a surface appearance similar to the sclerites of the genus *Xenia* (Fig. 2k, l). The corpusculars were more of rodlet shape rather than triangular (comparison with *Bayerxenia* in Fig. 2i and j). The colonies of *H. fuscescens* were the only ones associated with the nudibranch *Phyllodesmium hyalinum*, Ehrenberg (1831) (Figure S6 B). Nine colonies from two locations at Dahab were of brownish colour and distinctly branched with pulsating polyps (autozooids) arising from the terminal dome-shaped capitula, with siphonozooids present and sclerites lacking (Table 4, Figure S6 C, D). These characters allow assigning the specimens to *Heteroxenia ghardaqensis*, Gohar (1940), described from Hurghada and the Gulf of Aqaba (Red Sea) (Gohar 1940; Reinicke 1997). The colonies collected from Uthamuda (*n*=5) and Tempokchantik (*n*=5, all Bali, Indonesia, here named *Bayerxenia* sp. 1) as well as those from Lizard Island (Great Barrier Reef, Australia, *Bayerxenia* sp. 2) revealed very similar sclerite surface structures with prominently triangular-shaped corpusculars as described by Alderslade 2001 (Fig. 2i, j). The long and stretched anthocodiae of *Bayerxenia* sp. 1 were also very similar to those of the *H. fuscescens* colonies found in the Dahab Lagoon (Figure S4 A, Figure S5 C, respectively).

All other specimens without siphonozooids were assigned to the genera *Ovabunda* Alderslade 2001, and *Xenia* Lamarck 1816. One specimen exhibited distinct triangles in the sclerites (Fig. 2h) and was therefore also assigned to the genus *Bayerxenia* (sp. 3), despite the lack of siphonozooids. *Ovabunda* is characterised by sclerites with round corpuscular-shaped microsclerites (Aharonovich and Benayahu 2011). Seven colonies from different sites at Dahab (Egypt, Red Sea) were identified as *Ovabunda faraunensis* (Verseveldt and Cohen 1971) and ten colonies as *Ovabunda macrospiculata* (Gohar 1940) (Figure S1). Both have rather large sclerites, which in addition show species-specific spherical corpusculars (Fig. 2a–c).

About six species of *Xenia* were collected from various locations in the Philippines, Indonesia and Australia. Their taxonomic affiliation to the genus is based on the lack of siphonozooids and rodlet-form corpusculars of the sclerites (Fig. 2d–g), but an assignment to specific species was not possible because of the lack of appropriate descriptions and revisions for the Indo-Pacific region. *Xenia* sp. 1 lacked sclerites.

Table 3 Pairwise genetic distances (uncorrected) of the SRP54 (below diagonal) and the ND6/ND3 gene fragments (above diagonal) of selected taxa. For clades with several identical taxa one representative has been chosen. Shading indicates intraspecific comparisons. For *Xenia* sp. 6 we distinguish the two SRP54 alleles *Xenia* sp. *6_a* and *Xenia* sp. *6_b*. ND6/ND3 has just one allele denoted as *Xenia* sp. *6_a* and the missing values of Xenia sp. 6_b are indicated by "-" symbols

|		1	2	3	4	5	6	7	8	9	10	11	12	13	14	15	16	17	18	19	20	21	22	23	24	25	26
1	*Ovabunda faraunensis _13*	*	0.0000	0.0000	0.0020	0.0000	0.0000	0.0000	0.0020	0.0000	0.0000	0.0000	0.0000	0.0000	0.0130	0.0190	0.0150	0.0150	0.0220	0.0220	-	0.0240	0.0220	0.0240	0.0240	0.0230	0.0240
2	*Ovabunda faraunensis_22*	0.0496	*	0.0000	0.0020	0.0000	0.0000	0.0000	0.0020	0.0000	0.0000	0.0000	0.0000	0.0000	0.0130	0.0190	0.0150	0.0150	0.0220	0.0220	-	0.0240	0.0220	0.0240	0.0240	0.0230	0.0240
3	*Ovabunda faraunensis_17*	0.0455	0.0121	*	0.0020	0.0000	0.0000	0.0000	0.0020	0.0000	0.0000	0.0000	0.0000	0.0000	0.0130	0.0190	0.0150	0.0150	0.0220	0.0220	-	0.0240	0.0220	0.0240	0.0240	0.0230	0.0240
4	*Ovabunda faraunensis_12*	0.0413	0.0161	0.0124	*	0.0020	0.0020	0.0020	0.0000	0.0020	0.0020	0.0020	0.0020	0.0000	0.0130	0.0220	0.0170	0.0170	0.0240	0.0240	-	0.0260	0.0240	0.0260	0.0260	0.0250	0.0260
5	*Ovabunda faraunensis_04*	0.0372	0.0199	0.0163	0.0121	*	0.0000	0.0000	0.0020	0.0000	0.0000	0.0000	0.0000	0.0000	0.0130	0.0190	0.0150	0.0150	0.0220	0.0220	-	0.0240	0.0220	0.0240	0.0240	0.0230	0.0240
6	*Ovabunda faraunensis_09*	0.0496	0.0202	0.0081	0.0207	0.0204	*	0.0000	0.0020	0.0000	0.0000	0.0000	0.0000	0.0000	0.0130	0.0190	0.0150	0.0150	0.0220	0.0220	-	0.0240	0.0220	0.0240	0.0240	0.0230	0.0240
7	*Ovabunda faraunensis_06*	0.0537	0.0276	0.0242	0.0202	0.0159	0.0323	*	0.0020	0.0000	0.0000	0.0000	0.0000	0.0000	0.0130	0.0190	0.0150	0.0150	0.0220	0.0220	-	0.0240	0.0220	0.0240	0.0240	0.0230	0.0240
8	*Ovabunda macrospiculata_03*	0.0413	0.0315	0.0202	0.0161	0.0279	0.0282	0.0354	*	0.0020	0.0020	0.0020	0.0020	0.0000	0.0130	0.0220	0.0170	0.0170	0.0240	0.0240	-	0.0260	0.0240	0.0260	0.0260	0.0250	0.0260
9	*Ovabunda macrospiculata_09*	0.0537	0.0197	0.0081	0.0202	0.0239	0.0161	0.0315	0.0276	*	0.0000	0.0000	0.0000	0.0000	0.0130	0.0190	0.0150	0.0150	0.0220	0.0220	-	0.0240	0.0220	0.0240	0.0240	0.0230	0.0240
10	*Ovabunda macrospiculata_10*	0.0537	0.0202	0.0161	0.0207	0.0245	0.0242	0.0323	0.0363	0.0242	*	0.0000	0.0000	0.0000	0.0130	0.0190	0.0150	0.0150	0.0220	0.0220	-	0.0240	0.0220	0.0240	0.0240	0.0230	0.0240
11	*Ovabunda macrospiculata_13*	0.0455	0.0282	0.0161	0.0207	0.0245	0.0242	0.0323	0.0202	0.0242	0.0323	*	0.0000	0.0000	0.0130	0.0190	0.0150	0.0150	0.0220	0.0220	-	0.0240	0.0220	0.0240	0.0240	0.0230	0.0240
12	*Ovabunda macrospiculata_06*	0.0413	0.0161	0.0040	0.0083	0.0122	0.0121	0.0202	0.0161	0.0121	0.0202	0.0121	*	0.0000	0.0130	0.0190	0.0150	0.0150	0.0220	0.0220	-	0.0240	0.0220	0.0240	0.0240	0.0230	0.0240
13	*Ovabunda macrospiculata_08*	0.0455	0.0204	0.0082	0.0124	0.0082	0.0163	0.0163	0.0204	0.0163	0.0245	0.0163	0.0041	*	0.0140	0.0200	0.0150	0.0150	0.0210	0.0210	-	0.0230	0.0210	0.0230	0.0230	0.0230	0.0260
14	*Xenia sp. 1_01*	0.3077	0.3038	0.2996	0.3034	0.2869	0.3038	0.2996	0.3080	0.3038	0.2911	0.3080	0.2996	0.2954	*	0.0000	0.0100	0.0100	0.0240	0.0240	-	0.0210	0.0240	0.0260	0.0260	0.0250	0.0260
15	*Xenia sp. 2_01*	0.3034	0.2996	0.2954	0.2991	0.2827	0.2996	0.2954	0.3038	0.2996	0.2869	0.3038	0.2954	0.2911	0.0032	*	0.0150	0.0150	0.0280	0.0280	-	0.0280	0.0280	0.0300	0.0300	0.0290	0.0300
16	*Xenia sp. 3_09*	0.2275	0.2322	0.2275	0.2275	0.2133	0.2322	0.2275	0.2417	0.2322	0.2227	0.2417	0.2275	0.2227	0.2169	0.2129	*	0.0000	0.0220	0.0220	-	0.0240	0.0220	0.0240	0.0240	0.0230	0.0240
17	*Xenia sp. 4_04*	0.2275	0.2322	0.2275	0.2275	0.2133	0.2322	0.2275	0.2417	0.2322	0.2227	0.2417	0.2275	0.2227	0.2169	0.2129	0.0277	*	0.0220	0.0220	-	0.0240	0.0220	0.0240	0.0240	0.0230	0.0240
18	*Xenia sp. 5_01*	0.2675	0.2771	0.2771	0.2719	0.2641	0.2814	0.2771	0.2814	0.2771	0.2771	0.2771	0.2727	0.2727	0.3333	0.3370	0.2686	0.2769	*		-	0.0090	0.0220	0.0020	0.0020	0.0020	0.0020
19	*Xenia sp. 6_a*	0.2763	0.2857	0.2857	0.2807	0.2727	0.2900	0.2857	0.2900	0.2944	0.2857	0.2900	0.2814	0.2814	0.3370	0.3407	0.2727	0.2810	0.0534	*	-	0.0090	0.0000	0.0020	0.0020	0.0020	0.0020
20	*Xenia sp. 6_b*	0.2675	0.2814	0.2814	0.2719	0.2684	0.2857	0.2814	0.2857	0.2900	0.2814	0.2857	0.2771	0.3297	0.3333	0.2603	0.2686	0.0463	0.0214	*	-	-	-	-	-	-	
21	*Heteroxenia ghardaqensis_10*	0.2981	0.3146	0.3146	0.3077	0.2986	0.3192	0.3099	0.3146	0.3239	0.3146	0.3192	0.3099	0.3081	0.3411	0.3372	0.2431	0.2523	0.2262	0.2024	0.2024	*	0.0090	0.0110	0.0110	0.0110	0.0110
22	*Heteroxenia fuscescens_01*	0.2711	0.2622	0.2622	0.2578	0.2578	0.2711	0.2622	0.2667	0.2711	0.2622	0.2667	0.2578	0.2578	0.3221	0.3258	0.2645	0.2727	0.1018	0.0982	0.0873	0.2439	*	0.0020	0.0020	0.0020	0.0020
23	*Bayerxenia sp. 1_01*	0.2675	0.2771	0.2771	0.2719	0.2641	0.2814	0.2771	0.2814	0.2771	0.2771	0.2771	0.2727	0.2727	0.3333	0.3370	0.2686	0.2769	0.0071	0.0534	0.0463	0.2262	0.1018	*	0.0000	0.0000	0.0000
24	*Bayerxenia sp. 2_01*	0.2675	0.2771	0.2771	0.2719	0.2641	0.2814	0.2771	0.2900	0.2944	0.2857	0.2900	0.2814	0.2814	0.3333	0.3370	0.2686	0.2769	0.0036	0.0498	0.0427	0.2222	0.1018	0.0036	*	0.0000	0.0000
25	*Bayerxenia sp. 2_04*	0.2585	0.2627	0.2627	0.2585	0.2500	0.2669	0.2627	0.2627	0.2627	0.2627	0.2669	0.2585	0.2585	0.3525	0.3561	0.2727	0.2810	0.0866	0.1011	0.0903	0.2205	0.1091	0.0866	0.0830	*	0.0000
26	*Asterospicularia sp.*	0.2573	0.2500	0.2459	0.2448	0.2336	0.2500	0.2459	0.2500	0.2541	0.2500	0.2459	0.2418	0.2418	0.3368	0.3333	0.2390	0.2470	0.2384	0.2491	0.2384	0.2711	0.2545	0.2349	0.2349	0.2500	*
		1	2	3	4	5	6	7	8	9	10	11	12	13	14	15	16	17	18	19	20	21	22	23	24	25	26

Genetics

SRP54

Amplification of the partial SRP54 gene with the *Carijoa*-specific primers CrSRP54f and CrSRP54r failed completely for the samples analysed (Table 2). Of the newly developed primer pairs (SRP54-f1/SRP54-r1/SRP54-f2/SRP54-r2) only the combination SRP54_f2 with SRP54_r1 resulted in a successful amplification (Table 2). Similar to the study of Concepcion et al. (2008), the PCR success rate for SRP54 varied depending on the taxon. A total of 75 xeniid specimens were sequenced, resulting in 25 distinct haplotypes identified from a 453-bp alignment. Fragment sizes ranged from 214 bp to 338 bp (GenBank accession numbers; Table 1). The alignment of the 79 sequences, which also included two NCBI sequences and the second allele of *Xenia* sp. 6, consisted of 37.3 % gap sites. Not considering the gaps, 213 sites were variable and 173 parsimony-informative. The best substitution model suggested by the AIC for this data set was the GTR+I model.

The Bayesian phylogenetic tree is shown in Fig. 3 (left side). The ML bootstrap tree (not shown) is less resolved

Fig. 1 Colony morphology of Xeniidae: **a** *Heteroxenia* and *Bayerxenia* (here *Bayerxenia* sp.1). Siphonozooids are seen as white rings between the polyps. **b** *Ovabunda* and *Xenia* (here *Xenia* sp. 5). These genera lack siphonozooids
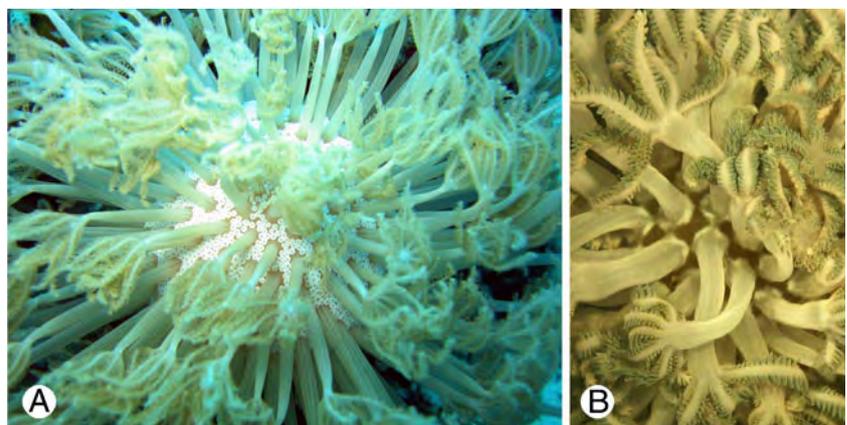
and has no conflicts with the Bayesian tree. The phylogenetic analyses reveal eight well-supported clades and the *Asterospicularia* sp. specimen in the ingroup. All clades differ from each other by more than 6 % pairwise distances with the highest divergence of up to 35.6 % (Fig. 3, Table 3). The uncorrected pairwise distances between the 25 different haplotypes are listed in Table 3 (lower panel). Divergences within clades are less than 6 %. In the well-supported clade 1, the two morphospecies of the genus *Ovabunda* (*O. macrospiculata* and *O. faraunensis*) cluster together in a comb-like structure. Thus, the two morphologically well-characterised species are not recovered by the SRP54 gene, although sequences within the *Ovabunda* clade show up to 5.4 % sequence divergence. Clade 2 and clade 3 encompass four morphospecies of the genus *Xenia* (here labelled as *Xenia* sp. 1, 2, 3 and 4*)*. The morphologically distinct *Xenia* sp. 1 and *Xenia* sp. 2 (clade 2) show no differences in their SRP54 gene. Similarly, in clade 3 two distinct morphospecies (*Xenia* sp. 3 and *Xenia* sp. 4 from Lizard Island) cluster together. Although there are two well-supported subclades within clade 3, they do not correspond to the morphologically described species boundaries (Fig. 3).

In this analysis, clade 1, 2 and 3, represented by *Xenia* and *Ovabunda* specimens, form a monophyletic group supported with a posterior probability of 0.99 and a ML bootstrap of 93 %. Clades 4 to 8 contain *Heteroxenia* and *Bayerxenia* specimens. Both dimorphic genera are supported with a posterior probability of 1 and a ML bootstrap support of 95 %. However, two specimens with monomorphic polyps, determined as *Xenia* sp., cluster within the dimorphic clade (Fig. 3: *Xenia* sp. 5_01 and the two alleles of the specimen *Xenia* sp. 6, 6a and 6b). Clade 4 hosts all individuals identified as *H. ghardaqensis* whereas all clade 8 animals are identified as *H. fuscescens*. Within clade 5, all specimens of *Bayerxenia* sp. 1, which form a weakly supported monophyletic taxon, group together with one *Heteroxenia* sequence from GenBank (accession no. EU006856), some sequences of *Bayerxenia* sp. 2, the one sequence of *Bayerxenia* sp. 3 and one morphologically determined *Xenia* species (sp. 5). The sister group to clade 5 is *Xenia* sp. 6 (clade 6). Individuals 04, 08, 10, 11 and 12 from Australia, morphologically assigned to *Bayerxenia* sp. 2, form a strongly supported separate clade (clade 7). According to SRP54, neither *Heteroxenia* nor *Bayerxenia* are resolved as monophyletic but specimens of both of these genera form one group. The single sequence of *Asterospicularia* sp. grouped as sister taxon to the dimorphic clade.

For the whole SRP54 data set, seven individuals were found to have heterozygous genotypes. Thus, for all specimens analysed, 9.3 % could not be sequenced directly because of heterozygous genotypes. For *Xenia* sp. 6, both

alleles could be identified from the electropherograms because of phase differences in the fluorescence peaks of the second allele, which had only a limited number of differences (3 %).

ND6/ ND3

A partial fragment of the ND6 and ND3 gene could be obtained for 76 xeniid specimens using the primers of McFadden et al. (2004), resulting in 12 distinct haplotypes (and three outgroup taxa) identified from a 545-bp MAFFT alignment (GenBank accession numbers; sequences will be submitted to GenBank before publication). The alignment of the 80 sequences also included one species of the genus *Asterospicularia* (AF530513) and three outgroup species. Sequences of nine specimens contained "Ns". Sixty-three positions in the alignment were variable (11.56 %), 50 of which were parsimony-informative. While the AIC suggested the HKY+I model of sequence evolution as most adequate for this data set, we computed Bayesian phylogenetic trees for the HKY+I as well as the GTR+I model. The GTR+I model was used because of the general advice (see MrBayes manual) that posterior probabilities are more realistic if more model parameters are varied during the analysis. The two trees show no conflicts. The tree computed with the GTR model is slightly more resolved and has marginally higher posterior probabilities. Only this tree is shown in Fig. 3 (right side). Branch labels indicate posterior probabilities and ML bootstrap values. The phylogenetic analyses reveal five well-supported clades that differ from each other by a maximum of 3 % uncorrected pairwise distances, which is only about one tenth of the divergence found within the SRP54 gene fragment (see scale bar in Fig. 3). The uncorrected pairwise distances between the different haplotypes are listed in Table 3 (upper diagonal).

Similar to the results from the SRP54 analysis, the *Ovabunda* species, *O. macrospiculata* and *O. faraunensis,* clustered in a well-supported clade (posterior probability of 1, ML bootstrap of 100) and formed the sister taxon to the monophyletic genus *Xenia* (Fig. 3, posterior probability 1, ML bootstrap 100). *Xenia* sp. 1 and *Xenia* sp. 2, as well as *Xenia* sp. 3 and *Xenia* sp. 4, have identical ND6/ND3 gene fragments (see Table 3, Fig. 3).

All *Heteroxenia* and *Bayerxenia* sequences (and sequences of *Xenia* sp. 5 and sp. 6, as well as the GenBank sequence *Xenia* sp. AF530512 and *Asterospicularia* AF530513) cluster in one major clade, with the exception of *H. ghardaqensis*. Among the morphospecies, only *H. ghardaqensis* (clade 4) forms a distinct monophyletic group that is consistent with the morphological determination and the SRP54 results. All other morphologically distinct species (*H. fuscescens*, *Bayerxenia* sp. 1, sp. 2 and sp. 3) cluster in an internally unresolved clade. Similar to the SRP54
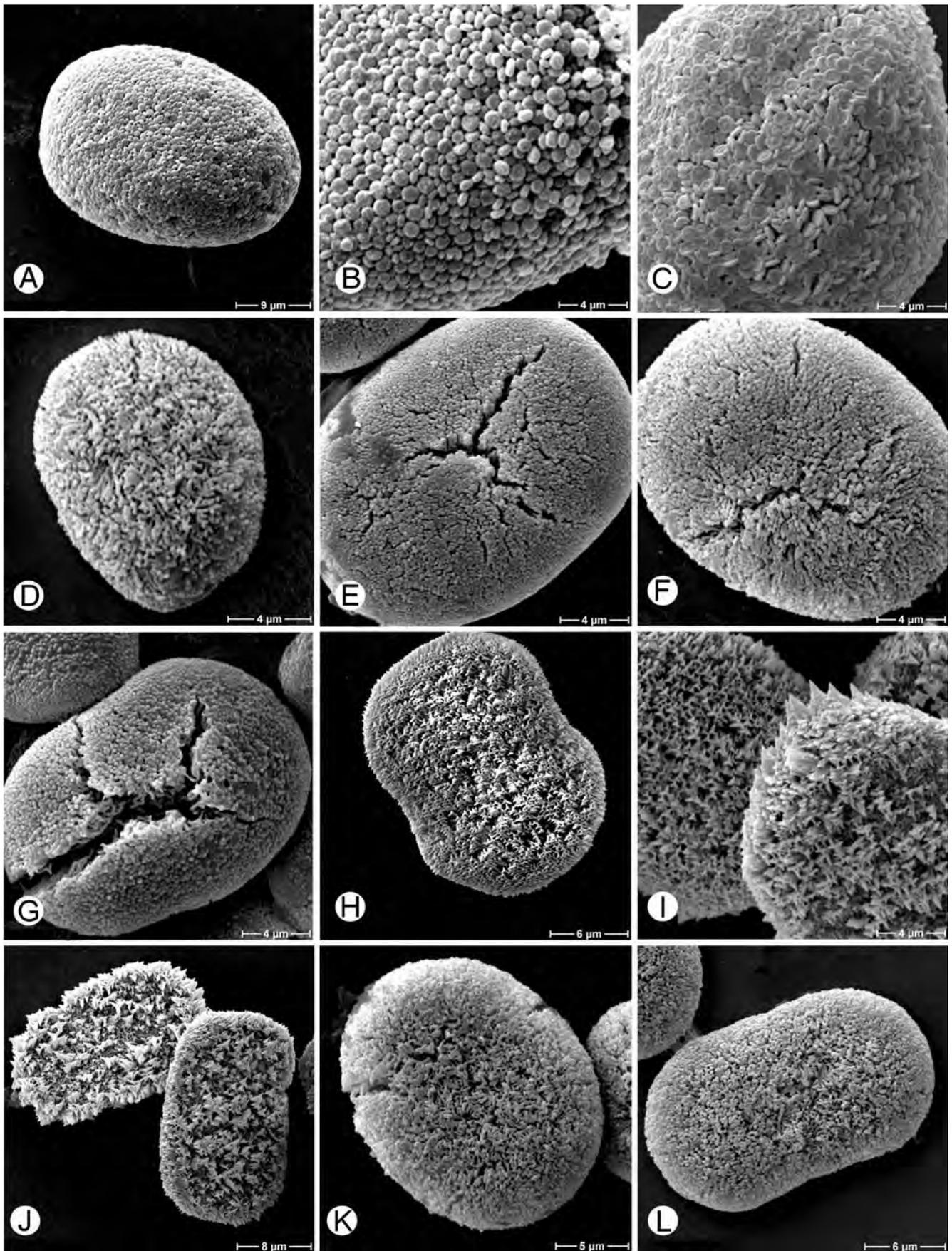
Fig. 2 Sclerites. **a** *Ovabunda faraunensis*_03; **b** *Ovabunda faraunensis*_03; **c** *Ovabunda macrospiculata*_04; **d** *Xenia* sp.1_01; **e** *Xenia* sp.3_05; **f** *Xenia* sp.4_02; **g** *Xenia* sp.5_01; **h** *Bayerxenia* sp.3_01; **i** *Bayerxenia* sp.1_10; **j** *Bayerxenia* sp.2_09; **k** *Heteroxenia fuscescens*_14; **l** *Heteroxenia fuscescens*_13

analyses the two specimens morphologically assigned to the genus *Xenia* (Xenia sp. 5, and sp. 6) as well as the GenBank sequence *Xenia* sp. AF530512 cluster within this last clade.

The GenBank sequence of *Asterospicularia* sp. AF530513 is again part of the Xeniidae, but in contrast to the SRP54 analysis, its position is not resolved.

Discussion

Species and/or genus assignment based on morphological characters is supported by the nuclear and mitochondrial gene fragments for some of the taxa investigated here. These include the genus *Ovabunda* and the species *Heteroxenia ghardaqensis*. Conflicting results are obtained especially for the dimorphic clade with regard to the species *Bayerxenia* sp. 1, sp. 2 and sp. 3 as well as two species morphologically determined as members of the genus *Xenia*, and *Heteroxenia fuscescens*.

The two genes investigated differ in the resolution within the dimorphic clade with *Heteroxenia* and *Bayerxenia*, whereas results are very similar with regard to the two *Ovabunda* species and the position of the *Xenia* species. *Asterospicularia* is part of the ingroup in both gene analyses. Whereas *Xenia* clusters with *Ovabunda* in the SRP54 analysis, it is a sister group to the clade *Heteroxenia*/ *Bayerxenia* in the ND6/ND3 gene fragment analysis.

Comparing the nucleotide alignments, almost half of the alignment sites are variable for the SRP54 gene fragment and only about 10 % of the positions are variable in the 545-bp alignment of the mitochondrial ND6/3 gene fragment. Both genes, however, are sufficiently variable to distinguish the genera *Ovabunda, Asterospicularia* and *Xenia* as well as the group of *Bayerxenia* and *Heteroxenia* (under the premises that *Xenia* sp. 5 and sp. 6 are misidentified members of one of the genera *Heteroxenia* and *Bayerxenia*; see below). Furthermore, it is possible to distinguish several clades within these genera: With the SRP54 marker, nine genetically distinct clades with deep phylogenetic breaks between the clades, indicative of separate species, are obtained, whereas only six can be distinguished with the mitochondrial marker (two of which are weakly supported). The SRP54 gene also concurs with morphological results found in the main clades.

Ovabunda

The two identified morphospecies of the genus *Ovabunda*, (*O. faraunensis* and *O. macrospiculata*) form one well-

supported monophyletic group (clade 1) in both genes analysed. However, the two morphospecies are not recovered. This is interesting, since both taxa could be well distinguished according to the morphological descriptions in Reinicke (1995) and Alderslade (2001): *O. faraunensis* appeared in big branching upright colonies connected by stolons. Each clavate colony was only up to 2 cm high and polyps showed a random arrangement on the upper surface of the coenenchyme. The monomorphic polyps were not pulsating and showed only one or two rows of pinnules (Figure S1 A, B). *O. macrospiculata* could be distinguished from *O. faraunensis* by the pulsating and feathery polyps. The specimens were also found in aggregations, often in the vicinity of *O. faraunensis* (Figure S1 E). Instead of the grey-white colour exhibited by *O. faraunensis*, the colonies of *O. macrospiculata* were characterised by a more yellowish appearance and a noticeably dense sclerite aggregation around the oral opening of the autozooids forming a white star around the mouth of the autozooid (Figure S1 C, D). The sclerites of both morphospecies had the same size of about 30×20 µm and showed "closely packed, round and flattened corpusculars" (Benayahu 1990) at the surface (Fig. 2a–c). The form of these corpusculars also distinguished the two species. *O. macrospiculata* exhibited deep pits in these corpusculars, whereas *O. faraunensis* showed spherically shaped corpusculars without these pits. The incongruence between morphology and both independent genetic markers may be due to a very recent divergence of *O. faraunensis* and *O. macrospiculata* that has not been manifested in the two markers yet (incomplete lineage sorting and the presence of ancestral polymorphisms). We consider the range of morphological characters that distinguish these two species as sufficiently distinctive and do not doubt their validity at the moment.

Xenia

The sister taxon relationship of *Xenia* sp. 1 and *Xenia* sp. 2 (clade 2 in Fig. 3) is characterised by an extremely low sequence divergence for both molecular markers (0.3 % and 0 % for SRP54 and ND6/ND3, respectively). This is in contrast to morphological data indicating two distinct species: *Xenia* sp. 1 lacked sclerites and the polyps exhibited a very low number of pinnules at the outer row of the tentacles (Figure S2 A, B). In *Xenia* sp. 2, sclerites were present. Since the same preservatives were used, it seems very unlikely that the absence of sclerites in *Xenia* sp. 1 is an artefact due to preservation. But possibly this colony was very young and sclerites have not yet been formed. As a consequence, the presence or absence of sclerites, as a species-specific character, has to be considered carefully (see below).

The morphospecies *Xenia* sp. 3 was distinguished from *Xenia* sp. 4 with the aid of size differences in the syndete

Table 4 List of different taxon characters sorted according to geographic and systematic criteria. (Loc. = location: Red Sea, Philippines, Indonesia, Great Barrier Reef; S = siphonozooids; P = pulsating polyps)

Species[a]	Voucher no.	Loc.	S	No. of rows of pinnules	No. of pinnules (outer) Row	Max. sclerites ø [μ]	Colony size ø [cm]	Colony morphology	P	Colour	Depth [m]	SRP54 clade/ monophyletic?	ND6/3 clade/ monophyletic?
Ovabunda faraunensis	DMM II-C/3701	RS		1 to 2	16 to 20	30×20	2	Aggregation, branched syndetes connected by stolons		Grey white	5 to 18	1/no	1/no
Ovabunda macrospiculata	DMM II-C/3702	RS		2 to 3	12 to 16	30×20	2	Aggregation, short branched syndetes	x	White, yellow	8 to 13	1/no	1/no
Heteroxenia ghardaqensis	DMM II-C/3703	RS	x	2 to 3	20	-	5	Branched, terminated with domed polyp bearing capitulum	x	Brown	4 to 9	4/yes	4/yes
Heteroxenia fuscescens		RS—moray eel garden	x	4 to 5	26 to 30	22×12	7	Short syndete with convex capitulum	x	White brown	5	8/yes	5/no
Heteroxenia fuscescens	DMM II-C/3704	RS—lagoon	x	4	30	22×12	7	Short syndete with convex capitulum	x	Light brownish	12	8/yes	5/no
Heteroxenia fuscescens	DMM II-C/3705	RS—Nabaq	x	4	20	22×12	4	Aggregation, short syndete	x	Orange brown	1	8/yes	5/no
Heteroxenia fuscescens		RS—Sinai front	x	4	20	22×12	4	Short syndete with convex capitulum	x	Orange brown	8	8/yes	5/no
Xenia sp. 1		Philip.		2 to 3	7	-	2	Short syndete with polyp bearing region		Light yellow	2	2/no	2/no
Xenia sp. 2		Philip.		3	20	15×13	3	Short syndete with polyp bearing region		Light brownish	6	2/no	2/no
Xenia sp. 6		Philip.		2 to 3	16 to18	22×16	7	Short syndete with convex capitulum	x	Light brownish	11	7/yes	5/no
Xenia sp. 5	DMM II-C/3706	Indon.		3 to 4	30	20×17	7	Short syndete with convex capitulum, fleshy tentacles		Creamy white	1 to 2	5/no	5/no
Bayerxenia sp.1		Indon.	x	2 to 3	30	22×15	6	Short syndete with convex capitulum	x	Light brownish	13 to 22	5/no	5/no
Xenia sp. 3	DMM II-C/3707	GBR		3	29	19×14	6	Aggregation, with fleshy short syndete		Light blue	1 to 2	3/no	3/no
Xenia sp. 4	DMM II-C/3708	GBR		2 to 3	18	15×13	2	Short syndete with polyp bearing region		Light yellow	1	3/no	3/no
Bayerxenia sp.3	DMM II-C/3709	GBR		3 to 4	20	24×16	4	Short syndete with convex capitulum	x	Light brownish	6	5/no	5/no
Bayerxenia sp.2	DMM II-C/3710	GBR	x	3 to 4	25	20×17	4	Short syndete with convex capitulum	x	Red brown	1 to 2	6/yes	5/no

[a] Picture tables of all morphotypes are provided in the "Supplementary material"
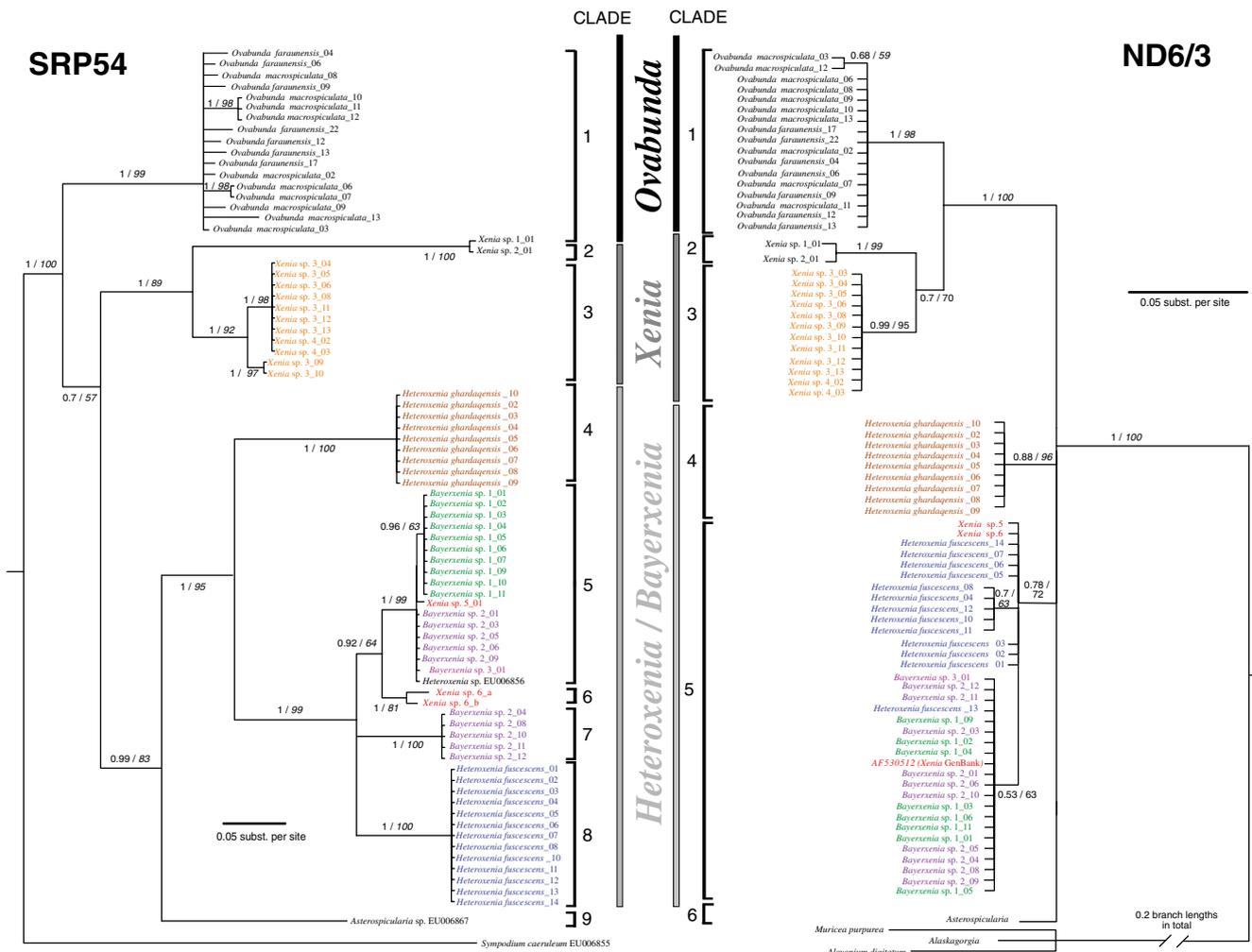
Fig. 3 Bayesian phylogenetic tree of *Ovabunda*, *Xenia*, *Bayerxenia* and *Heteroxenia*. *Node labels* indicate Bayesian posterior probabilities and maximum likelihood bootstrap support values (*in italics*) based on 10,000 replications. The non-vanishing terminal branch lengths in multifurcations of identical sequences are an artefact of the Bayesian inference as well as due to the occurrence of Ns in the alignment

(6 cm versus 2 cm, respectively). No differences between the two species were observed in the mitochondrial gene fragment, except that the sequence reads of *Xenia* sp. 3 were shorter than those from *Xenia* sp. 4 and terminal Ns had to be added. In the SRP54 gene two distinct subclades are found (Fig. 3): one subclade encompassing specimens of *Xenia* sp. 3 and *Xenia* sp. 4 and the other containing only two *Xenia* sp. 3 specimens. Distinction of these two species is mainly based on the size of the sclerites and the syndete. Both species (some specimens of *Xenia* sp. 3 and both specimens of *Xenia* sp. 4) were collected at exactly the same locality, i.e. the water pipeline of the Lizard Island Research station. Following the results of the genetic analyses, it seems unlikely that *Xenia* sp. 3 and 4 represent two distinct species. Morphological differences may be a consequence of daily exposure to air, wave action or other ecological factors. Nevertheless, a recent speciation process might have resulted in the two *Xenia* sp. 3 specimens (*Xenia* sp. 3_09 and *Xenia* sp. 3_10) with

morphologically similar but genetically distinct features from all other specimens of clade 3.

All other specimens assigned to the genus *Xenia* based on the absence of siphonozooids (Xenia sp. 5, sp. 6a and 6b) cluster within the dimorphic genera *Heteroxenia* and *Bayerxenia*.

Heteroxenia

Heteroxenia ghardaqensis is supported as a monophyletic species by both genes. The species can be distinguished easily from all other samples by the dark brown colour of the clearly branched colonies and by the lack of sclerites (Reinicke 1995). Interestingly, not all colonies showed polyp dimorphism, reflecting Gohar's (1940) statement that siphonozooids appear during the reproductive season in spring. Thus, the use of this trait as a diagnostic character is limited.

All 13 specimens identified *a priori* as *Heteroxenia fuscescens* have the same haplotype of the SRP54 gene and form a monophyletic group supported by a posterior probability value of 1 and ML bootstrap value of 100 in the analysis. This result is not supported by the analysis of the mitochondrial gene fragment, where *H. fuscescens* is paraphyletic, clustering with other members of the genera *Heteroxenia* and *Bayerxenia*. All 13 investigated specimens had siphonozooids, the same number of rows of pinnules (4) and a large number of pinnules at the outer row. Additionally, the sclerites exhibited a uniform diameter in all specimens (22×12 μm). Noticeable is a variable growth form, which seems to be related to their locality (Figure S5 and S6): The specimens collected at a depth of 8 m ("moray eel garden") formed single cylindrical colonies (<7 cm) with a convex capitulum and dense, feathery and pulsating polyps (Figure S5 A, B). At the lagoon of Dahab, similar specimens were collected at a depth of 12 m with much longer and thinner anthocodiae (Figure S5 C, D), similar to specimens of the genus *Bayerxenia* within clade 5. Compared to the latter, specimens from "Sinai front" (3 m depth) (Figure S5 E, F) and "Nabaq" (1 m depth) (Figure S6 A, B) had a much smaller colony size of 4 cm, very short anthocodiae and did not appear as cylindrical as the first two morphs. These latter *Heteroxenia* specimens, preliminarily assigned to *H. fuscescens*, had a similar growth form as those described as *Heteroxenia elisabethae* by Reinicke (1995). But this species distinction is not supported by our genetic data. Specimens collected in "Nabaq" appeared in aggregations slightly underneath the surface. On two morphospecies the nudibranch *Phyllodesmium hyalinum*, Ehrenberg (1831) was found in a pouch between the siphonozooids (Figure S6 B). No evaluation of the morphological characters was possible for *Heteroxenia* sp. EU 006856 (clade 5) from GenBank. Since it groups together in clade 5 with *Bayerxenia* specimens, it may possible be a misidentified specimen.

Bayerxenia

Bayerxenia sp. 2, identified as a distinct and well-defined species on the basis of various morphological characters, is paraphyletic in the SRP54 analysis with two distinct and strongly supported groups, but remains unresolved in the ND6/ND3 analysis. Specimens of *Bayerxenia* sp. 2 occurred in dense aggregations of distinguishable and sometimes fused colonies and were collected from three different locations along the same beach on Lizard Island (Figure S6 E). The red-brownish colonies had a size of about 4 cm and the autozooids were pulsating. Siphonozooids were visible between the dense, feathery autozooids. At the same locality, also colonies of *Xenia* sp. 3 were found. Both species formed huge and dense intermingling colonies (Figure S6 F). Only

Bayerxenia sp. 2 was colonised by the slug *Phyllodesmium lizardensis*, Burghardt et al. (2008b) (Figure S4 C). Affeld et al. (2009) showed that two new secondary metabolites (sesquiterpenes) were only present in the dimorphic xeniid and the associated slug, but not in the sympatric species *Xenia* sp. 3. In their study, the dimorphic xeniid was still assigned to the genus *Heteroxenia* because the sclerite structure of their material was not analysed until now in this study.

It is astonishing that in the SRP54 gene analysis some of the specimens identified as *Bayerxenia* sp. 2 from Lizard Island group together with a morphotype classified as *Bayerxenia* sp. 1 from Bali (SRP54 clade 5). Differences between these *Bayerxenia* sp. 2 specimens are 8.3 % uncorrected pairwise distances for SRP54. Specimens assigned to *Bayerxenia* sp. 1 can be distinguished from *Bayerxenia* sp. 2 by larger sclerites, longer anthocodiae and a smaller number of pinnule rows with similarities to *Heteroxenia pinnata*, described for the Philippine Sea by Roxas (1933). This discrepancy can potentially be explained by ancestral polymorphisms together with incomplete lineage sorting. Alternatively, members of *Bayerxenia* sp. 2 may belong to two different species (clade 5 and clade 7 in SRP54, Fig. 3), and the morphological characters used for the delimitation of species may be phenotypically plastic and thus of limited use. However, both morphospecies can be assigned unambiguously to the genus *Bayerxenia* because of the distinct sclerite surface structures with triangular corpusculars as described by Alderslade (2001). This also applies to *Bayerxenia* sp. 3, which we initially determined as a *Xenia* species based on the lack of siphonozooids. The analysis of the sclerites revealed the typical triangular corpusculars of *Bayerxenia* (Fig. 2h), and both genetic analyses confirmed its assignment to this genus. Achituv and Benayahu (1990) have shown that siphonozooids are not present throughout the whole life cycle in dimorphic xeniid species. This clearly shows that the absence of siphonozooids is an ambiguous character and ontogenetic variability has to be taken into consideration in the process of species identification. Similar results were obtained for two further specimens identified preliminarily as members of the genus *Xenia* because of the absence of siphonozooids (*Xenia* sp. 5 and sp. 6). They clearly group within the dimorphic clade (*Heteroxenia/Bayerxenia*, Fig. 3), but the two genetic analyses are not congruent in the assignment to a certain genus. Whereas SRP54 indicates a closer relationship of these two species to one of the *Bayerxenia* clades (clade 5), the ND3/ND6 analysis shows no resolution. We assume that the *Xenia* sequence taken from GenBank (AF530512) also represents a misidentification.

In this study, *Asterospicularia* is resolved as the sister group to the dimorphic clade in the SRP54 analysis but shows no particular affiliation to any xeniid genus in the less resolved tree of the ND6/ND3 analysis. Its grouping

within the Xeniidae analysed in this study confirms the rejection of the monotypic family Asterospiculariidae and the placement of the monogeneric *Asterospicularia* within the family Xeniidae (Alderslade 2001).

In summary, resolution was much higher for the fast-evolving nuclear marker SRP54 compared to the mitochondrial gene fragment ND6/ND3. Furthermore, several incongruencies have been found between morphological and genetic characters: On the one hand, the molecular genetic data cannot confirm the validity of some distinct morphospecies, whereas, on the other hand, the morphologically identical specimens of *Xenia* sp. 3 revealed high sequence divergence in the fast-evolving SRP54 gene, indicative of overlooked or cryptic species. A reasonable explanation for these incongruencies between genetic markers and morphological characters could lie in the properties of the very fast-evolving gene SRP54 and its heterozygote nature. But they could also be the result of the usage of polymorphic morphological characters as diagnostic features, which hence are of limited use for species classification. Similar observations were made by Concepcion et al. (2008) for the octocoral genus *Carijoa*. Furthermore, sampling of differing ontogenetic stages may lead to a misidentification. We need more information on the ontogeny, life cycle and environmentally induced changes in the morphology of Xeniidae to re-evaluate diagnostic characters used for discriminating species of the family Xeniidae and also other phenotypic plastic octocorals. So far, it cannot be determined whether the genetically distinct clades in this study represent cryptic species that have not been recognised previously or whether they represent other, already described species whose morphs are difficult to distinguish or have been synonymised (McFadden et al. 2006). At this point it is also interesting to note that the specimens within each of the eight clades always originated from the same sampling site (Table 1), indicating a clear genetic differentiation with respect to geographic location.

Our results give evidence that SRP54 is a suitable marker for phylogenetic analyses on the generic and species levels within Xeniidae, whereas ND6/ND3 probably will contribute more to the generic and higher taxa levels. It is also evident that SRP54 is a good marker for discriminating several xeniid species, whereas morphological characters showed limitations and therefore have to be re-evaluated. Even though ND6/ND3 is less variable than SRP54, it was sufficiently variable for genus and even species delimitation in some cases.

The mitochondrial gene msh1 (MutS homolog 1) has been in the focus with regard to octocoral phylogenies (McFadden et al. 2006). But according to McFadden et al. (2006), this marker shows a low genetic divergence among xeniid species. For the octocoral *Narella*, Baco and Cairns (2012) showed that 83 % of the species within this group could be resolved by a combination of COI and msh1 along with the ND2 marker. Future studies should focus on comparing existing and finding additional markers for studying biodiversity and evolution in the xeniid genera.

Amplification and sequencing problems

The main advantage of SRP54, i.e. its high variability, but it also has major drawback compared to the mitochondrial genes, which can be amplified without problems. The primers used by Concepcion et al. (2008) failed in the present analysis and new primers with several wobble bases had to be designed. Also for these primers, several DNA samples could not be amplified. So far, no primers have been found that work well for a wider range of alcyonarian species. Most likely, this is the effect of variability at the 3′ terminus of the priming sites, a problem already recognised by Concepcion et al. (2008). Baco and Cairns (2012) also mention difficulties in sequencing SRP54 across diverse octocoral taxa. Another drawback of the SRP54 gene is that several heterozygous specimens were found for the SRP54 region. These heterozygous specimens were excluded from the data set and will be analysed in subsequent studies by sequencing the clones of different allelic variants. It should be mentioned that the high variability of this marker and the high genetic distances found between sequence fragments (Table 3) are partly the result of regions of low complexity. In these, mutations can quickly introduce a long insertion or deletion in one single event. Flot and coworkers (2011) realised that despite the drawbacks of sequencing problems, di-allelic nuclear markers were superior to haploid mt-markers on the species-level.

Benefits and limitation of SRP54

Nuclear gene fragments can pose a problem when analysing di- or even polyploid species with heterozygous genotypes. They require more intensive analyses and are therefore regarded to be inappropriate as a barcode marker (Hebert et al. 2003a). However, since the haploid mtDNA evolves too slowly to resolve species relationships in some cases, sufficiently variable nuclear markers must be considered. In soft corals, but also several other taxa, multicopy markers such as the ITS-1 have been investigated (Pillay et al. 2006; Wei et al. 2006). For soft corals, however, the ITS analyses were of limited success (Aguilar and Sanchez 2007; Dorado and Sanchez 2009). The results of our study using the single-copy nuclear SRP54 marker introduced by Concepcion et al. (2008) showed that (at least) 9.3 % of the genotypes analysed were heterozygous and had to be analysed separately or excluded from the analysis. Within eight of nine individuals screened, differences between alleles were below 3 %. However, for one heterozygous

Ovabunda specimen we found two alleles that differed by 6.4 % uncorrected pairwise distance. Hence, using nuclear markers such as SRP54 has the downside that analyses cannot be performed as convenient as for haploid mitochondrial markers of other animal taxa (Hebert et al. 2004). But, in the case where useful haploid molecular markers such as ND6/ND3 do not have the necessary variability, SRP54 seems to be a good marker that is worth testing in other octocoral families. To avoid time-consuming and laboratory-intensive cloning methods, other techniques could be used that allow the discrimination of heterozygous genotypes by confirming the presence of one of a set of known alleles, such as single-strand conformation polymorphism (SSCP) or denaturing gradient gel electrophoresis (DGGE).

Conclusions

The short SRP54 gene fragment amplified with the primers established in this study is highly variable and provides sufficient resolution to distinguish the genera *Ovabunda*, *Xenia, Bayerxenia, Heteroxenia* and *Asterospicularia*, as well as several clades therein. High bootstrap support values also indicate good resolution concerning intergeneric relationships, thus promoting this gene as a valuable marker for broader phylogenetic analyses including more xeniid genera. The gene has an about 10× higher variation than the mitochondrial ND6/ND3 gene, although the variation of ND6/ND3 was sufficiently high for genus and even species delimitation in several cases. Therefore, ND6/ND3 should not be completely discarded for future phylogenetic analyses in combined data sets and when including further xeniid genera or other octocoral taxa. Comparing genetic and morphological analyses revealed one likely case of overlooked species diversity but several cases of polymorphic species: Only nine distinct clades were found in the SRP54 and six in the mitochondrial ND6/ND3 analysis, whereas 14 morphospecies have been identified (*Asterospicularia* included). Both of these problems, i.e. overlooking species and splitting of morphologically variable species, can systematically bias biodiversity estimates and should be avoided. Since molecular and morphological analyses provide different and partly contradicting pictures, the morphological characters used in the past for species and even genus discrimination have to be re-evaluated carefully by taking into account variation that may be due to differences in the life cycle as well as geographic variations. Additionally, life history traits influenced by environmental factors (symbiotic relationship with zooxanthellae including depth and exposure to irradiance, hydrodynamics and seasonality) may influence the growth form. These effects are hardly known at all. But also the different allelic variants of SRP54 need to be investigated further for a full picture of the discriminating power of this marker.

Our study shows that SRP54 constitutes a promising candidate marker for evolutionary studies within octocoral families and even suggests its potential use as barcode marker. We recommend that future studies with a similar broad sampling should also include the msh1 marker and the extended COI+igr1+msh1 barcode for comparison.

Our analyses on the Xeniidae represent an important step toward resolving and understanding the systematics and evolution of this difficult and poorly known group.

References

Achituv, Y., & Benayahu, Y. (1990). Polyp dimorphism and functional, sequential hermaphroditism in the soft coral *Heteroxenia fuscescens* (Octocorallia). *Marine Ecology Progress Series, 64*, 263–269.

Affeld, S., Kehraus, S., Waegele, H., & Koenig, G. (2009). Dietary derived sesquiterpenes from *Phyllodesmium lizardensis* Burghardt, Schrödl & Wägele (Opisthobranchia, Nudibranchia, Aeolidoidea). *Journal of Natural Products, 72*, 298–300.

Aguilar, C., & Sanchez, J. A. (2007). Phylogenetic hypotheses of gorgoniid octocorals according to ITS2 and their predicted RNA secondary structures. *Molecular Phylogenetics and Evolution, 43*, 774–786.

Aharonovich, D., & Benayahu, Y. (2011). Microstructure of octocoral sclerites for diagnosis of taxonomic features. *Marine Biodiversity.* doi:10.1007/s12526-011-0102-3.

Alderslade, P. (2001). Six new genera and six new species of soft coral, and some proposed familial and subfamilial changes within the Alcyonacea (Coelenterata, Octocorallia). *Bulletin of the Biological Society of Washington, 10*, 15–65.

Anta, C., González, N., Santafé, G., Rodríguez, J., & Jiménez, C. (2002). New *Xenia* diterpenoids from the Indonesian soft coral *Xenia* sp. *Journal of Natural Products, 65*, 766–768.

Baco, A. R., & Cairns, S. D. (2012). Comparing molecular variation to morphological species designations in the deep-sea coral *Narella* reveals new insights into seamount coral ranges. *PLoS One, 7*(9), e45555. doi:10.1371/journal.pone.0045555.

Benayahu, Y. (1990). Xeniidae (Cniadaria: Octocorallia) from the Red Sea, with the description of a new species. *Zoologische Medelingen Leiden, 64*, 113–120.

Berntson, E. A., Bayer, F. M., McArthur, A. G., & France, S. C. (2001). Phylogenetic relationships within the Octocorallia (Cnidaria: Anthozoa) based on nuclear 18S rRNA sequences. *Marine Biology, 138*, 235–246.

Burghardt, I., & Waegele, H. (2004). A new solar powered species of the genus *Phyllodesmium* Ehrenberg, 1831 (Mollusca: Nudibranchia: Aeolidoidea) from Indonesia with analysis of its photosynthetic activity and notes on biology. *Zootaxa, 596*, 1–18.

Burghardt, I., Stemmer, K., & Waegele, H. (2008). Symbiosis between *Symbiodinium* (Dinophyceae) and different taxa of Nudibranchia (Mollusca: Gastropoda) with analyses of longterm retention. *Organisms, Diversity and Evolution, 8*, 66–76.

Burghardt, I., Schroedl, M., & Waegele, H. (2008). Three new solar-powered species of the genus Phyllodesmium Ehrenberg, 1831 (Mollusca:Nudibranchia:Aeolidioidea) from the tropical Indo-Pacific, with analysis of their photosynthetic activity and notes on biology. *Journal of Molluscan Studies, 74*, 277–292.

Chen, I. P., Tang, C. Y., Chiou, C. Y., Hsu, J. H., Wei, N. V., Wallace, C. C., et al. (2008). Comparative analyses of coding and non-coding DNA regions indicate that Acropora (Anthozoa: Scleractinia) possesses a similar evolutionary tempo of nuclear vs. mitochondrial genomes as in plants. *Marine Biotechnology, 11*, 141–152.

Concepcion, G. T., Crepeau, M. W., Wagner, D., Kahng, S. E., & Toonen, R. J. (2008). An alternative to ITS, a hypervariable, single-copy nuclear intron in corals, and its use in detecting cryptic species within the octocoral genus *Carijoa*. *Coral Reefs, 27*, 323–336.

Dorado, D., & Sanchez, J. A. (2009). Internal Transcribed Spacer 2 (ITS2) variation in the Gorgonian Coral *Pseudopterogorgia bipinnata* in Belize and Panama. *Smithsonian Contributions to the Marine Sciences, 38*, 173–179.

Drummond, A. J., Ashton, B., Buxton, S., Cheung, M., Cooper, A., Duran, C., et al. (2012). Geneious v5.6. http://www.geneious.com.

Ehrenberg, G. G. (1831). Symbolae Physicae seu icones est descriptiones animalium evertebratorum sepositis insectis quae ex itinere per Agricam Borealem et Asiam Occidentalem. Decas 1 Moll.

Ehrenberg, C. G. (1834). Beiträge zur Kenntnis der Corallenthiere im allgemeinen, und besonderen des Rothen Meeres, nebst einem Versuche zur physiologischen Systematik derselben. *Abhandlungen der Königlichen Akademie der Wissenschaft Berlin (1832), 1*, 225–380.

Flot, J.-F., Blanchot, J., Charpy, L., Cruaud, C., Licuanan, W. Y., Nakano, Y., et al. (2011). Incongruence between morphotypes and genetically delimited species in the coral genus *Stylophora*: phenotypic plasticity, morphological convergence, morphological stasis or interspecific hybridization? *BMC Ecology, 11*, 22.

Forsmann, Z. H., Concepcion, G. T., Haverkort, R. D., Shaw, R. W., Maragos, J. E., & Toonen, R. J. (2010). Ecomorph or endangered coral? DNA and microstructure reveal Hawaiian species complexes: *Montipora dilatata/ flabellata/turgescens* & *M. patula/ verrilli*. *Plos One, 5*, 12.

France, S., & Hoover, L. (2001). Analysis of variation in mitochondrial DNA sequences (ND3, ND4L, MSH) among Octocorallia (Alcyonaria) (Cnidaria: Anthozoa). *Bulletin of the Biological Society of Washington, 10*, 110–118.

France, S., & Hoover, L. (2002). DNA sequences of the mitochondrial *COI* gene have low levels of divergence among deep-sea octocorals (Cnidaria: Anthozoa). *Hydrobiologia, 471*, 1–3.

Fukami, H., Budd, H. F., Levitan, D. R., Jara, J., Kersanach, R., & Knowlton, N. (2004). Geographic differences in species boundaries among members of the *Montastraea annularis* complex based on molecular and morphological markers. *Evolution, 58*, 324–337.

Gohar, H. A. F. (1940). Studies on the Xeniidae of the Red Sea. Their ecology, physiology, taxonomy and phylogeny. *Publications of the Marine Biological Station, Al Ghardaqa, Egypt, 2*, 25–118.

Hatta, M., Fukami, H., Wang, W., Omori, M., Schimoike, K., Hayashibara, T., et al. (1999). Reproductive and genetic evidence for a reticulate evolutionary history of mass-spawning corals. *Molecular Biology and Evolution, 16*, 1607–1613.

Hebert, P. D. N., Cywinska, A., Ball, S. L., & deWaard, J. R. (2003). Biological identifications through DNA barcodes. *Proceedings of the Royal Society of London B, 270*, 313–321.

Hebert, P. D. N., Ratnasingham, S., & de Waard, J. R. (2003). Barcoding animal life: cytochrom C oxidase subunit 1 divergences among closely related species. *Proceedings of the Royal Society of London B, 270*, 596–599.

Hebert, P. D. N., Stoeckle, M. Y., Zemlak, T. S., & Francis, C. M. (2004). Identification of birds through DNA barcodes. *PLoS Biology*. doi:10.1371/journal.pbio.0020312.

Hellberg, M. E. (2006). No variation and low synonymous substitution rates in coral mtDNA despite high nuclear variation. *BMC Evolutionary Biology, 6*, 24.

Huang, D., Meier, R., Todd, P. A., & Ming Chou, L. (2008). Slow mitochondrial COI sequence evolution at the base of the metazoan tree and its implications for DNA barcoding. *Journal of Molecular Evolution, 66*, 167–174.

Huelsenbeck, J. P. (2001). MrBayes: A program for the Bayesian inference of phylogeny. Manual.

Huelsken, T., Waegele, H., Peters, B., Mather, A., & Hollmann, M. (2011). Molecular analysis of adults and egg masses reveals two independent lineages within the infaunal gastropod *Naticarius onca* (Röding, 1798) (Caenogastropoda: Naticidae). *Molluscan Research, 3*, 141–151.

Katho, K., Misawa, K., Kuma, K., & Miyata, T. (2002). Mafft: a novel method for rapid multiple alignment based on fast Furier transform. *Nucleic Acids Research, 30*, 3059–3066.

Koelliker, A. (1874). Die Pennatulidae *Umbellula* und zwei neue Typen der Alcyonarien. Festschrift zur Feier des 25-jährigen Bestehens der Physikalisch-Medizinischen Gesellschaft 5–23.

Lamarck, J. B. P. A. (1816). Polypes tubiferes. In *Histoire naturelle des animeaux sans vertebres*. IV + 568 pp. Paris, Verdiere

McFadden, C. S., & Hutchinson, M. B. (2004). Molecular evidence for the hybrid origin of species in the soft coral genus *Alcyonium* (Cnidaria: Anthozoa: Octocorallia). *Molecular Ecology, 13*, 1495–1505.

McFadden, C. S., Donahue, R., Hadland, B. K., & Weston, R. (2001). A molecular phylogenetic analysis of reproductive trait evolution in the soft coral genus *Alcyonium*. *Evolution, 55*, 54–67.

McFadden, C. S., Tullis, I. D., Hutchinson, M. B., Winner, K., & Sohm, J. A. (2004). Variation in coding (NADH Dehydrogenase Subunits 2, 3 and 6) and noncoding intergenetic spacer regions of the mitochondrial genome in Octocorallia (Cnidaria: Anthozoa). *Marine Biotechnology, 6*, 516–526.

McFadden, C. S., France, S. C., Sánchez, J. A., & Alderslade, P. (2006). A molecular phylogenetic analysis of the Octocorallia (Cnidaria: Anthozoa) based on mitochondrial protein-coding sequences. *Molecular Phylogenetics and Evolution, 41*, 513–527.

McFadden, C. S., Sanchez, J., & France, S. (2010a). Molecular phylogenetic insights into the evolution of Octocorallia: a review. *Integr Comp Biol*, 1–22.

McFadden, C. S., Benayahu, Y., Pante, E., Thoma, J. N., Nevarez, A., & France, S. (2010). Limitations of mitochondrial gene barcoding in Octocorallia. *Molecular Ecology Resources*. doi:10.1111/j.1755-0998.2010.02875.x.

Park, E., Hwang, D. S., Lee, J. S., Song, J. I., Seo, T. K., & Won, Y. J. (2012). Estimation of divergence times in cnidarian evolution based on mitochondrial protein-coding genes and the fossil record. *Molecular Phylogenetics and Evolution, 62*, 329–345.

Pillay, K. R. M., Asahida, T., Chen, C. A., Terashima, H., & Ida, H. (2006). ITS ribosomal DNA distinctions and the genetic structures of populations of two sympatric species of *Pavona* (Cnidaria; Scleractinia) from Mauritius. *Zoological Studies, 45*, 132–144.

Posada, D. (2008). jModelTest: phylogenetic model averaging. *Molecular Biology and Evolution, 25*, 1253–1256.

Reinicke, G. B. (1995). Xeniidae des Roten Meeres (Octocorallia, Alcyonacea)—Beiträge zur Systematik und Ökologie. *Essener Ökologische Schriften, 6*, 1–168.

Reinicke, G. B. (1997). Xeniidae (Coelenterata, Octocorallia) of the Red Sea, with descriptions of six new species of *Xenia*. *Fauna of Saudi Arabia, 16*, 5–62.

Roxas, H. A. (1933). The Philippine Alcyonaria. The families Cornulariidae and Xeniidae. *Philippine Journal of Science, 50*, 49–110.

Shearer, T. L., & Coffroth, M. A. (2008). Barcoding corals: limited by interspecific divergence, not intraspecific variation. *Molecular Ecology Resources, 8*, 247–255.

Shearer, T. L., vanOppen, M. J. H., Romano, S. L., & Woerheide, G. (2002). Slow mitochondrial DNA sequence evolution in the Anthozoa (Cnidaria). *Molecular Ecology, 11*, 2475–2487.

Stamatakis, A. (2006). RAxML-VI-HPC: maximum likelihood-based phylogenetic analyses with thousands of taxa and mixed models. *Bioinformatics, 22*, 2688–2690.

Strychar, K. B., Coates, M., Sammarco, P. W., Piva, T. J., & Scott, P. T. (2005). Loss of *Symbiodinium* from bleached soft corals *Sarcophyton ehrenbergi*, *Sinularia* sp. and *Xenia* sp. *Journal of Experimental Marine Biology and Ecology, 320*, 159–177.

Van Oppen, M. J. H., Willis, B. L., Van Vugt, H., & Miller, D. J. (2000). Examination of species boundaries in the *Acropora cervicornis* group (Scleractinia, Cnidaria) using nuclear DNA sequence analyses. *Molecular Ecology, 9*, 1363–1373.

Van Oppen, M. J. H., McDonald, B. J., Willis, B., & Miller, D. J. (2001). The evolutionary history of the coral genus *Acropora* (Scleractinia, Cnidaria) based on a mitochondrial and a nuclear marker: reticulation, incomplete lineage sorting, or morphological convergence? *Molecular Biology and Evolution, 18*, 1315–1329.

Van Oppen, M. J. H., Willis, B. L., Van Rheede, T., & Miller, D. J. (2002). Spawning times, reproductive compatibilities and genetic structuring in the *Acropora aspera* group: evidence for natural hybridization and semi-permeable species boundaries in corals. *Molecular Ecology, 11*, 1363–1376.

Van Oppen, M. J. H., Koolmees, E. M., & Veron, J. E. N. (2004). Patterns of evolution in the scleractinian coral genus *Montipora* (Acroporidae). *Marine Biology, 144*, 9–18.

Verseveldt, J., & Cohen, J. (1971). Some new species of Octocorallia from the Gulf of Elat (Red Sea). *Israel Journal of Zoology, 20*, 53–67.

Vollmer, S. V., & Palumbi, S. R. (2004). Testing the utility of internally transcribed spacer sequences in coral phylogenetics. *Molecular Ecology, 13*, 2763–2772.

Waegele, H., Raupach, M. J., Haendeler, K., & Burghardt, I. (2010). Solar powered seaslugs: Incorporation of photosynthetic units—a key character enhancing radiation? In M. Glaubrecht & H. Schneider (Eds.), *Evolution in action—adaptive radiations and the origins of biodiversity* (pp. 263–282). Berlin: Springer.

Ward, R. D., Zemlak, T. S., Innes, B. H., Last, P. R., & Hebert, P. D. N. (2005). DNA barcoding Australia's fish species. *Philosophical Transactions of the Royal Society B, 360*, 1847–1857.

Wei, N. V., Wallace, C. C., Dai, C. F., Pillay, K. R. M., & Chen, C. A. (2006). Analyses of the ribosomal internal transcribed spacers (ITS) and the 5.8S gene indicate that extremely high rDNA heterogeneity is a unique feature in the scleractinian coral genus *Acropora* (Scleractinia; Acroporidae). *Zoological Studies, 45*, 404–418.

→ meinem Dreamteam in der finalen Päpa-fabrik: Anna B. und Duygu! Ohne unseren gemeinsamen wissenschaftlichen Wahnsinn wäre dieses Ende nur halb so schön! Vielen Dank für all die Stunden, Minuten und Sekunden in denen wir so sein durften wie wir sind: Wild, weise, wissbegierig und wahnsinnig!

→ Duygu Sevilgen. All die Nachtschichten, Wochenenden, den stetigen Austausch und Deine Unterstützung in jeglicher Hinsicht, dass werden ich vermissen. Dies war eine sehr intensive Zeit und ich bin sehr froh, dass Du da warst!

Zum guten Abschluss möchte ich mich bei meinen Freunden und meiner Familie bedanken ohne deren Unterstützung, festen Glauben und Verständnis diese Arbeit nicht möglich gewesen wäre. Worte können meinen Dank wohl nicht beschreiben!

Maria und Martha, für Euch!
Liebste Grüße an den Colourgatestoneway!
Lieben Dank an Familiy Rau für die Powerpakete!
Danke meinem Bro, Anna und Frida!

Mi Jones, Du hast mich mit durchgepuscht! Danke für alles! 2013 wird super!

Meine Eldies: Ihr seid einfach die Besten!

Und alle weiteren Menschen die ich hier vergessen habe zu erwähnen!

Danke!

Name: Kristina Stemmer
Anschrift: Buntentorsteinweg 170, 28201 Bremen

Erklärung

Hiermit erkläre ich, dass ich die Arbeit mit dem Titel

"Shell formation and microstructure of the ocean quahog *Arctica islandica*: Does ocean acidification matter?"

selbstständig verfasst und geschrieben habe und außer den angegebenen Quellen keine weiteren Hilfsmittel verwendet habe.

_____

Kristina Stemmer